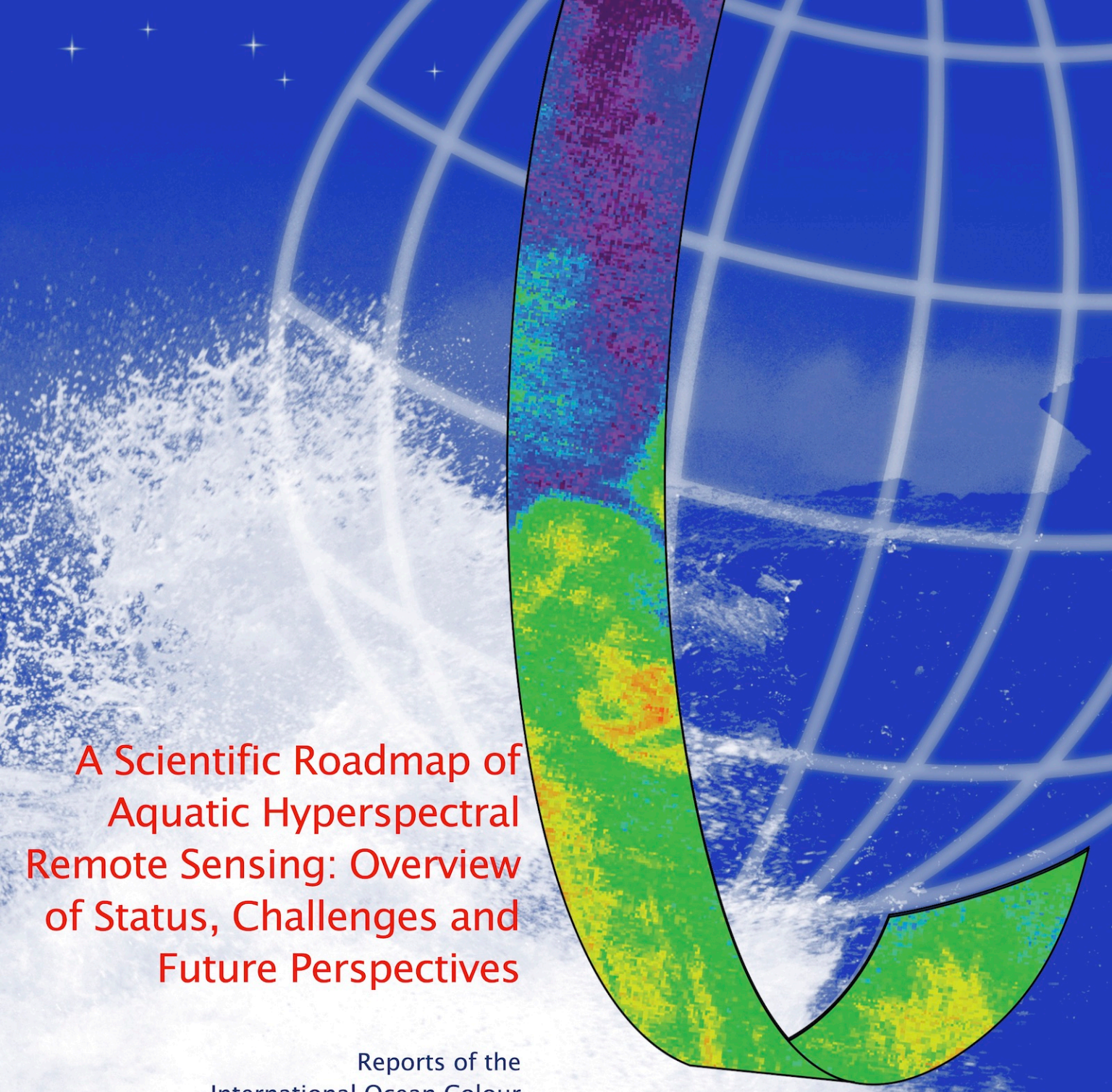

A Scientific Roadmap of Aquatic Hyperspectral Remote Sensing: Overview of Status, Challenges and Future Perspectives

Reports of the
International Ocean Colour
Coordinating Group

REPORT NUMBER 22

IOCCG

An Affiliated Program of SCOR
An Associate Member of CEOS

In the IOCCG Report Series:

1. *Minimum Requirements for an Operational Ocean-Colour Sensor for the Open Ocean (1998)*
2. *Status and Plans for Satellite Ocean-Colour Missions: Considerations for Complementary Missions (1999)*
3. *Remote Sensing of Ocean Colour in Coastal, and Other Optically-Complex, Waters (2000)*
4. *Guide to the Creation and Use of Ocean-Colour, Level-3, Binned Data Products (2004)*
5. *Remote Sensing of Inherent Optical Properties: Fundamentals, Tests of Algorithms, and Applications (2006)*
6. *Ocean-Colour Data Merging (2007)*
7. *Why Ocean Colour? The Societal Benefits of Ocean-Colour Technology (2008)*
8. *Remote Sensing in Fisheries and Aquaculture (2009)*
9. *Partition of the Ocean into Ecological Provinces: Role of Ocean-Colour Radiometry (2009)*
10. *Atmospheric Correction for Remotely-Sensed Ocean-Colour Products (2010)*
11. *Bio-Optical Sensors on Argo Floats (2011)*
12. *Ocean-Colour Observations from a Geostationary Orbit (2012)*
13. *Mission Requirements for Future Ocean-Colour Sensors (2012)*
14. *In-flight Calibration of Satellite Ocean-Colour Sensors (2013)*
15. *Phytoplankton Functional Types from Space (2014)*
16. *Ocean Colour Remote Sensing in Polar Seas (2015)*
17. *Earth Observations in Support of Global Water Quality Monitoring (2018)*
18. *Uncertainties in Ocean Colour Remote Sensing (2019)*
19. *Synergy between Ocean Colour and Biogeochemical/Ecosystem Models (2020)*
20. *Observation of Harmful Algal Blooms with Ocean Colour Radiometry (2021)*
21. *Evaluation of Atmospheric Correction Algorithms over Turbid Waters (2025)*
22. *A Scientific Roadmap of Aquatic Hyperspectral Remote Sensing: Overview of Status, Challenges and Future Perspectives (this volume)*

Reports and Monographs of the International Ocean Colour Coordinating Group

An Affiliated Program of the Scientific Committee on Oceanic Research (SCOR)
An Associated Member of the Committee on Earth Observation Satellites (CEOS)

IOCCG Report Number 22, v1.0, 2026

A Scientific Roadmap of Aquatic Hyperspectral Remote Sensing: Overview of Status, Challenges and Future Perspectives

Edited by:
Astrid Bracher, Ana I. Dogliotti, and Jeremy Werdell

Report of an IOCCG task force chaired by Astrid Bracher, Ana Dogliotti, and Jeremy Werdell and based on contributions from (in alphabetical order):

Astrid Bracher	Alfred-Wegener-Institute Helmholtz Centre for Polar and Marine Research (AWI), Germany
Malik Chami	Sorbonne Université, France
Maycira Costa	University of Victoria, Canada
Heidi Dierssen	University of Connecticut, USA
Ana I. Dogliotti	Instituto de Astronomía y Física del Espacio (IAFE), CONICET/UBA, Argentina
Claudia Giardino	National Research Council of Italy (CNR), Institute for Electromagnetic Sensing of the Environment (IREA), Italy
Toru Hirawake	National Institute of Polar Research, Japan
Chuanmin Hu	University of South Florida, USA
Amir Ibrahim	National Aeronautics and Space Administration (NASA) Goddard Space Flight Center (GSFC), USA
Wonkook Kim	Pusan National University, Korea
Emanuele Organelli	National Research Council of Italy (CNR), Institute of Marine Sciences (ISMAR), Italy
Shaoling Shang	Xiamen University, China
Fang Shen	East China Normal University, China
Jeremy Werdell	National Aeronautics and Space Administration (NASA) Goddard Space Flight Center (GSFC), USA

Series Editor: Raisha Lovindeer

Correct citation for this publication:

IOCCG (2026). A Scientific Roadmap of Aquatic Hyperspectral Remote Sensing: Overview of Status, Challenges and Future Perspectives. Bracher, A., Dogliotti, A., Werdell, J. (eds.), IOCCG Report Series, No. 22, Version 1.0, International Ocean Colour Coordinating Group, Dartmouth, Canada.

The International Ocean Colour Coordinating Group (IOCCG) is an international group of experts promoting the application of remotely-sensed ocean-colour and inland water radiometric data across all aquatic environments, acting as a liaison and communication channel between users, managers and agencies in the ocean colour arena.

The IOCCG is sponsored by the Centre National d'Etudes Spatiales (CNES, France), Canadian Space Agency (CSA, Canada), Commonwealth Scientific and Industrial Research Organisation (CSIRO, Australia), Department of Fisheries and Oceans (Bedford Institute of Oceanography, Canada), European Commission/Copernicus Programme, European Organisation for the Exploitation of Meteorological Satellites (EUMETSAT), European Space Agency (ESA), Indian Space Research Organisation (ISRO), Japan Aerospace Exploration Agency (JAXA), Joint Research Centre (JRC, EC), Korea Institute of Ocean Science and Technology (KIOST), National Aeronautics and Space Administration (NASA, USA), National Oceanic and Atmospheric Administration (NOAA, USA), Scientific Committee on Oceanic Research (SCOR), and the State Key Laboratory of Satellite Ocean Environment Dynamics (Second Institute of Oceanography, Ministry of Natural Resources, China)

http://www.ioccg.org

Published by the International Ocean Colour Coordinating Group,
P.O. Box 1006, Dartmouth, Nova Scotia, B2Y 4A2, Canada.

ISSN: 1098-6030
ISBN:

Contents

Chapter 1

Introduction

Jeremy Werdell, Astrid Bracher, Ana Dogliotti

1.1 Background

Understanding how the aquatic system (open ocean, coastal and inland waters) responds to global-scale climate change and regional-scale localized environmental forcing is essential for studying global environmental systems. The aquatic system plays a major role in the Earth's carbon cycle, which links land, the ocean, and the atmosphere. It also supports marine and inland water ecosystems that are sensitive to natural hazards and environmental stressors. Coastal and inland aquatic ecosystems, including wetlands, for example, are of fundamental interest to society and the economy given their tight link to urbanization and economic value creation. These ecosystems, which are continuously impacted by natural processes and human activities, also play a significant role in the carbon cycle and comprise critical habitats for biodiversity. Systematic, high-quality and global observations, such as those provided by satellite remote sensing techniques, are key to understanding the intertwined and complex aquatic system. Remote sensing of aquatic ecosystems provides an essential tool for assembling such datasets. Satellites equipped with optical sensors to sense the ocean surface gather information over broad spatial areas and long time periods, something that traditional field methods onboard ships or aircrafts cannot equivalently achieve. As such, the geophysical records derived from these satellite sensor measurements, called *ocean colour*, are critical for monitoring water quality and carbon storage; understanding shifts in phytoplankton communities; assessing primary productivity; and tracking long-term environmental trends in key regions of the aquatic system, including sinks for atmospheric carbon, drinking water reservoirs, and fishing grounds. In the context of climate change and human impacts, satellite-based aquatic monitoring therefore remains an essential tool for both basic research and applied science and policy.

The continuous global data record from polar orbiting optical satellites in low Earth orbit now spans nearly thirty years and has focused on sensing the global oceans. Heritage ocean colour satellite instruments measure the spectral radiance emanating from the top of the atmosphere at several visible, near-infrared, and sometimes, short-wave infrared bands. Atmospheric correction algorithms are typically applied to remove the contribution of the atmosphere from the top-of-atmosphere (TOA, all abbreviations are listed in the section Acronyms) radiances which can exceed 90% of the total signal, and produce estimates of spectral water-leaving radiance, which is the light exiting the water that describes the *colour* of the water body. Bio-optical algorithms are then applied to the water-leaving signal to produce estimates of geophysical and optical quantities, such as the near-surface concentration of the phytoplankton pigment chlorophyll-a (CHL), and spectral inherent optical properties, among many others. In turn, these quantities can be used to infer higher order geophysical factors (for

example, metrics of phytoplankton community composition) that contain critical ecological information of interest as described above.

Most heritage satellite ocean colour instruments collect(ed) data within a limited number of broad wavelength bands in the visible (approximate band resolution of 10–20 nm) and near-infrared (NIR) to shortwave infrared (SWIR; approximate band resolution of 20–40 nm) regions of the spectrum. The visible bands are used to determine key oceanic properties, while the NIR and SWIR bands facilitate atmospheric correction. Generally, the number of visible spectral bands increased progressively from the proof-of-concept National Aeronautics and Space Administration (NASA) Coastal Zone Color Sensor (CZCS; 1978 to 1986), to the most recent missions, e.g., NASA Moderate Resolution Imaging Spectroradiometer (MODIS; 1999, 2002) and the European Space Agency (ESA) Sentinel-3 (S3) Ocean and Land Colour Imager (OLCI; 2016, 2018) sensors with 7.5 to 10 nm band resolution and 7 and 10 bands, respectively, for aquatic remote sensing applications. S3-OLCI, with two missions flying in tandem, has also improved global full resolution datasets at 300 m (daily global coverage) which significantly advanced the monitoring of coastal and inland waters. Over the same period, however, the range and sophistication of scientific applications using ocean colour data expanded dramatically. Following the launch of the NASA Sea-viewing Wide Field-of-view Sensor (SeaWiFS; 1997), the community began to recognize a growing gap between scientific demands and the capabilities of existing instruments. In response, the aquatic radiometry community initiated activities to define the observational requirements for future satellite missions that could meet emerging scientific and environmental monitoring needs. These evolving goals ultimately led to the development of missions such as the NASA Plankton, Aerosol, Cloud, ocean Ecosystem (PACE) observatory, Copernicus Hyperspectral Imaging Mission for the Environment (CHIME), and Sentinel-3 Next Generation Optical (S3NGO) Advanced OLCI (AOLCI), all of which are designed to provide advanced spectral and radiometric capabilities for studying the Earth's ocean and inland waters.

Additionally, several missions not targeted originally for ocean colour applications have been exploited for aquatic ecosystem monitoring. Atmospheric optical sensors, such as the Scanning Imaging Absorption Spectrometer for Atmospheric Chartography (SCIAMACHY, operation 2002-2012) and the TROPOspheric Monitoring Instrument (TROPOMI, Sentinel-5 Precursor, S5P, since 2018) have been used to derive innovative products for the global oceans. These sensors have high spectral resolution and high sensitivity over dark waters, but with large ground-pixel sizes (see Chapter 2). Conversely, imaging spectroscopy satellite sensors, often designed primarily for terrestrial applications, provide high spatial resolution data ($<$100 m), which offers the opportunity, despite their low temporal coverage, to explore applications for coastal and inland waters, e.g., Deutsches Zentrum für Luft- und Raumfahr (DLR, German Aerospace Center) Earth Sensing Imaging Spectrometer (DESIS, since 2018), Agenzia Spaziale Italiana (ASI, Italian Space Agency) PRecursore IperSpettrale della Missione Applicativa (PRISMA; since 2019) or the Copernicus Expansion Mission, CHIME (launch expected 2028). For details on all hyperspectral sensors see Chapter 2.

The primary advancement realized by the latter missions remains the move from multispectral to hyperspectral radiometry, which we define here as the continuous measurement of light in incremental steps ($<$10 nm) across the ultraviolet-to-near-infrared spectrum. Heritage multispectral instruments were designed to measure the bulk optical and geophysical properties that modulated spectral water-leaving radiances (e.g., CHL and diffuse downwelling attenuation coefficients). Traditional algorithms often estimated these properties by relating blue-to-green radiance ratios to specific water properties. Spectral matching approaches ap-

plied to multispectral radiometry retrieved more detailed optical parameters, such as spectral phytoplankton absorption, metrics of coloured dissolved organic matter (CDOM), and particle backscattering. These more advanced techniques require higher spectral resolution than band ratio algorithms, but are still limited by the number of wavelengths available from heritage instrumentation. As a result, most modern and emerging geophysical retrievals benefit from hyperspectral radiometry with resolutions finer than 5-nm. This increased visible spectral sampling improves detection of pigment absorption and particulate backscattering, leading to more accurate estimates of phytoplankton diversity, net primary production (NPP), and carbon stocks. Additionally, as discussed in Chapter 3, precise measurements across the CHL fluorescence region provide key information on phytoplankton nutrient stress and pigment composition in complex waters.

1.2 Scope of the report

This scientific roadmap (version 1) serves to document the state-of-the-art in hyperspectral remote sensing of the aquatic environment. It aims to:

- define the benefits of hyperspectral remote sensing techniques relative to retrievals from heritage multispectral sensors, with a focus on improved aquatic geophysical retrieval capabilities;
- identify new and emerging basic research and applied science questions to be addressed through future improved capabilities from aquatic hyperspectral retrievals; and,
- highlight gaps and challenges that remain to be addressed.

The primary audiences are:

- agencies and institutions that can facilitate addressing gaps and challenges and improving retrieval capabilities (e.g., via funding or other support); and,
- the scientific research and applied communities that can progress towards remediating gaps and challenges and developing new and advanced retrieval approaches.

In other words, this document serves as a baseline so that the aquatic radiometry community can prepare more efficiently to take action on pursuing and remediating the identified gaps.

The guiding questions to be addressed within this report are:

- What are the pressing science questions globally and regionally, for which hyperspectral remote sensing may allow progress for aquatic applications where multispectral remote sensing has reached its limit?
- What are the constraints on hyperspectral remote sensing in addressing these questions? (This includes limitations in terms of spatial and temporal resolution, signal-to-noise, calibration/validation (Cal/Val) of hyperspectral data and so on).

More specifically, these chapters aim to answer the following science questions (SQ):

SQ1. Which current products are derived from hyperspectral data and what are the associated challenges?

SQ2. What additional science and applications can hyperspectral enable, not being addressed by multispectral remote sensing?

SQ3. What is the current status and limitations of aircraft and satellite hyperspectral remote sensing?

SQ4. What is the current status of in situ data and radiative transfer modelling for Cal/Val and algorithm development? What are the current gaps?

SQ5. What advances in atmospheric corrections have we made using hyperspectral data? How can we further improve the corrections?

SQ6. How will radiometric and product uncertainty quantification be addressed [for harmonization of international missions]?

SQ7. What new methodologies can improve hyperspectral Level-1 and Level-2 products and enhance their application?

Chapters 2 to 4 answer the above-mentioned scientific questions and focus on hyperspectral satellite sensors, the methodologies to retrieve products for aquatic applications, and the calibration and validation of water leaving reflectance products. Specifically, Chapter 2 provides an overview of the current status of satellite sensors and states their limitations (SQ3). Chapter 3 includes subsections on specific geophysical retrievals from ocean colour remote sensing across geographic scales and domains. Each subsection describes the societal applications and user needs and provides an overview on the status of existing methodologies and their limitations (SQ1, SQ6). In addition, each subsection states the primary current ecological/applied science questions in the field and emphasizes the improved or new applications enabled by hyperspectral radiometry in comparison to multispectral remote sensing (SQ2). Chapter 4 concentrates on the status and challenges of methodologies used for system vicarious calibration (SQ6), atmospheric correction (SQ4, SQ5), product validation (SQ4), and sensor performance assessment (SQ6). The concluding chapter, Chapter 5, provides overall perspectives on how to improve sensor technology, algorithms, and data harmonization, and even create new products in order to enhance their societal application and better meet user needs (SQ7). This chapter ends with core recommendations for actions to be taken concerning satellite missions and associated research.

Chapter 2

Overview of Air- and Space-borne Sensors

Claudia Giardino, Astrid Bracher, Malik Chami

Imaging spectrometry of aquatic ecosystems has been in development since the late 1980s when the first airborne hyperspectral sensors were deployed mostly over lakes. As the space-borne and airborne hyperspectral sensors become increasingly available and appropriate for aquatic ecosystem detection, monitoring, and assessment, new studies are possible. Satellite instruments, with very high spectral resolution (1 nm and better), originally designed for atmospheric applications, have shown to provide additional opportunities for applications of retrieving information on optical properties of the open ocean. However, science-based applications will need to be further developed to an operational level.

In such a frame we aim to provide a summary of the current status and limitations of airborne and satellite hyperspectral remote sensing for water applications. For the purposes of this report, we consider the term *imaging spectroscopy* as acquisition of images in hundreds of contiguous, registered, spectral bands, such that for each pixel a radiance spectrum can be derived.

2.1 Status

2.1.1 Airborne imaging spectroscopy

Since the early 1980s, airborne observations have been used to demonstrate the capabilities that hyperspectral remote sensing brings to understanding environment, atmosphere components, and terrestrial and aquatic ecosystems, as summarized in Table 2.1. In this context, high-resolution airborne hyperspectral sensors (Table 2.1) have been providing enhanced mapping tools (e.g., Dekker et al., 2011; Hunter et al., 2010). The Airborne Prism EXperiment (APEX) has also been used to define and validate algorithms for mapping primary producers in eutrophic lake waters (Bolpagni et al., 2014), or to assess atmospheric correction procedures over small eutrophic lakes using the Flexible Experimental Imaging Spectrometer (FENIX) sensor (Markelin et al., 2016).

2.1.2 Spaceborne imaging spectroscopy

Several reviews (e.g., Giardino et al., 2019) have been recently published on hyperspectral remote sensing for aquatic ecosystems. Particularly, Dierssen et al., 2021 provided an analysis on science, resources, and an outlook of the state-of-the-art in the field. A figure from that review, originally presented in Hestir et al., 2015, nicely illustrated the spectral, temporal and spatial characteristics of the majority of the present and future spaceborne hyperspectral sensors commonly used for freshwater ecosystem measurements. We extended the review

Table 2.1 Main features of some typical airborne hyperspectral imaging systems, including spectral range, spectral sampling interval (SSI), number of channels, field of view (FOV) and instantaneous field of view (IFOV) (adapted from Taramelli et al., 2020). See Acronyms for full sensor names.

Mission/ Sensor (Country)	Spectral range (nm)	SSI (nm)	Number of bands	FOV (deg)	IFOV (mrad)	Features
AISA EAGLE (Finland)	400-970	1.25	488	37.7	1	Coastal monitoring, classification of vegetation
APEX (Europe)	380–970 940–2500	0.5–8.0 10.0–6.0	114 199	28	0.48	Pigments and CHL fluorescence in agriculture
AVIRIS-NG (USA)	380-2500	9.7-12	224	30	7.5	Ecology, agricultural and forest status, oceanography, geology, atmosphere, ice, snow, clouds
CASI (Canada)	400–2500	2.4/7.5	96/200	40	0.49/ 0.698	Oil/gas/mineral resource exploration and other fields such as agriculture, forestry, and coastal issues
AISA FENIX (Finland)	380-2500	3.37	620	32.3	17.453	Similar to AVIRIS
HyMap (Australia)	400–2500	10–20	128	61.3	2×2.5	Mineral exploration and environmental, agricultural and forest monitoring
Hyplant-DUAL (Germany-Finland)	380–970 970–2500 670–780	4.0 13.3 0.25	350 272 1024	32.3	0.0832	Agricultural and forest status, vegetation fluorescence
MIVIS (Italy)	433–833 1150–1550 2000–2500 8200–12700	20 50 8 400–500	20 8 64 10	70	2	Geology and environmental study

of Dierssen et al., 2021 by adding a few recently launched and planned spaceborne imaging spectroscopy missions (Fig. 2.1).

Details of most of the current and future hyperspectral missions are reported in Table 2.2. Table 2.2 additionally includes the following atmospheric satellite sensors which have been offering high spectral resolution (~0.25–1 nm) enabling innovative ocean applications on water constituents (Bracher et al., 2009) and the underwater light field (e.g., Oelker et al., 2022): SCIAMACHY (operation 2002-2012); Global Ozone Monitoring Experiment 2 (GOME-2, measuring since 2007); the Ozone Monitoring Instrument (OMI) sensor (measuring since 2004); S5P-TROPOMI (with data since 2018); and the ultraviolet, visible, near-infrared light spectrometer (UVN, launched 2025 on Sentinel-4 and Sentinel-5). For comparison we added an overview of multispectral ocean colour satellites (e.g., OLCI), which also provide high spectral resolution (~10 nm) at determined wavebands, and those with broad bands but a pixel size suitable for fine scale mapping of aquatic ecosystems (e.g., MultiSpectral Instrument (MSI)). The Fluorescence Imaging Spectrometer (FLORIS) on the FLuorescence EXplorer (FLEX) was

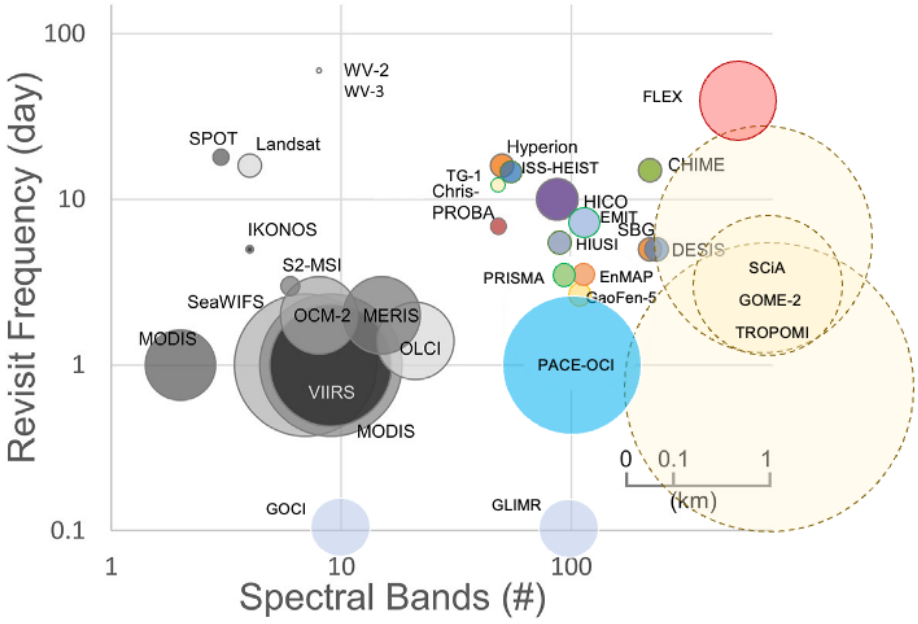

Figure 2.1 The spectral (x-axis, in nm), temporal (y-axis, in days), and spatial (size of the bubble, in km) characteristics of satellite sensors commonly used for freshwater ecosystem measurements. Note: sensors that provide different spatial resolutions are plotted separately, and sensors with overlapping resolution characteristics are slightly skewed for graphing purposes. Multispectral missions are in grey, and hyperspectral missions are coloured. All hyperspectral missions here considered have at least 60 bands within the visible-NIR spectral range. Atmospheric sensors are indicated in light yellow at 1000 spectral bands. Pixel size is indicated with dashed lines. SCIAMACHY is listed with 6-day coverage and 30 x 60 km spatial resolution, GOME-2 with 3-day and 40 x 40 km, and TROPOMI with daily coverage and 5.5 x 3.5 km. The FLuorescence EXplorer, FLEX, is listed for its potential use in water application (Gupana et al., 2021). These sensors are listed with the other hyperspectral sensors in Table 2.2.

also included. It does not cover the entire VIS-NIR, but, being in tandem with Sentinel-3, can complement OLCI observations.

Figure 2.2 shows an example of images collected from the last generation of spaceborne imaging spectroscopy missions. All images were collected on the same day (21 May 2025) over Lake Malawi, which is the ninth largest freshwater lake on Earth, located in the East African Rift. Pseudo true-colour composites were plotted alongside remote sensing reflectance (R_{rs}) data derived from Level-2 products over the area of water imaged by all sensors, in the northern part of the lake. The spectra derived from the five sensors were similar to those of deep blue lakes. EnMAP also provided fine-scale details of a coastal lagoon, which showed spectral signatures more typical of turbid, productive waters.

In addition to the missions described above, we note that the number of commercial hyperspectral satellite missions is continuously increasing in recent years. At the *3rd Workshop on International Cooperation In Spaceborne Imaging Spectroscopy*, held at ESA in November 2024, it was noted that approximately 78% of satellite imaging spectroscopy missions are for commercial initiatives, which reflects the rapid increase of the sector, particularly in the USA and China. These commercial missions are typically oriented to minisatellites with a ground sampling distance on the order of <10 m, and, usually, lower radiometric performance but increased ability to enable local to regional applications.

Table 2.2 Main features of some current and planned spaceborne hyperspectral imaging systems including current atmospheric sensors SCIAMACHY, OMI, TROPOMI, GOME-2, and UVN. BRDF is the Bidirectional Reflectance Distribution Function (adapted from Taramelli et al., 2020). For comparison, multispectral ocean and land sensors have been included.

Mission/ Sensor (Country)	Launch date	Spectral range (nm)	Spectral resolution (nm)	Number of bands	Spatial resolution (m)	Swath (km)	Features	Data portal
EO1-Hyperion (USA)	2000	450-2500	10	220	30	7.5	Technology validation/demonstration mission	data.nasa.gov
CHRIS-PROBA (Europe)	2001	400-1050	1.25 @400 nm; 11 @1050 nm	62 Mode 1; 18 Mode 2-5	36 Mode 1; 18 Mode 2-5	14	Technological demonstrator to collect BRDF data	earth.esa.int
SCIAMACHY (DE-NL-BE)	2002	240-2380	0.4 in UV-VIS	~1150 in UV-VIS	30000 by 60000	960	Atmospheric sensor also sensing open ocean	earth.esa.int
OMI (NL-USA)	2004	270-500	0.5 in VIS	~460	13000 by 24000	2600	Atmospheric sensor also sensing open ocean	earth-data.nasa.gov
GOME-2 (Europe)	2006	240-790	0.26-0.51	~1150 in UV-VIS	40000 by 40000	1920	Atmospheric sensor also sensing open ocean	data.eumetsat.int
ISS-HICO (USA)	2009	380-960	5.7	102	90	42-192	Observing coastal ocean	earth-data.nasa.gov
S5P-TROPOMI (Europe)	2017	270-495 675-775 2305-2385	0.55 0.55 0.25	410 182 320	3500 by 5500	2600	Atmospheric sensor also sensing open ocean (and coastal?)	mpc-vdaf.tropomi.eu
ISS-DESIS (Germany)	2018	402-1000	10, 2.5	60, 235	30	30	Applications relying to VIS-NIR and to use the BRDF	dlr.de
PRISMA (Italy)	2019	400-2500, 400-700	10, 300	239, 1	30, 5	30	Precursor of Application Mission for different applications	prisma.asi.it
ISS-HIUSI (Japan)	2019	440-2500	10-12.5	185	20 x 30	20	Oil/gas/mineral resource exploration and other fields such as agriculture, forestry, and coastal issues	eoportal.org

Gaofen-5-AHSI (China)	2021	400-2500	5-10	330	30	60	Ecological environment monitoring and natural resource exploration	space.skyrocket.de
EnMAP (Germany)	2022	420-2450	10	246	30	30	Scientific path finder mission for later operational services, for environmental monitoring, process understanding	planning.enmap.org
ISS-EMIT (USA)	2022	380-2500	≤7.5	285	60	77	Mineral Dust Source Measurements	earth.jpl.nasa.gov
PACE-OCI (USA)	2024	315-895; 940, 1038, 1249, 1378, 1618, 2130, 2258	1.25-2.5 UV-NIR	>200	1200 at nadir	2663	Global ocean biology, chemistry and ecology	earthdata.nasa.gov
S4-UVN (Europe)	2025	305-500 (750-775)	0.5 (0.12)	391 (209)	8000 by 8000	-	Open ocean and coast 16.6°W-8.8°E, 30°N to 65°N Geostationary, every hour	esa.int eumetsat.int
S5-UVN (Europe)	2025	300-500 685-710 743-773 1590-1675 2305-2385	0.5 0.25 0.25	400 101 121	7500 by 7500	2670	Atmospheric sensor also sensing open ocean (and coastal?)	esa.int eumetsat.int
FLEX-FLORIS (Europe)	2026	500-780	0.3-3		300	150	Quantitative global mapping of actual photosynthetic activity of terrestrial ecosystems, as a function of variable vegetation health status and environmental stress conditions	earth.esa.int

CHIME (Europe)	2028	400-2500	≤10	>200	20-30	130	World ecosystems, natural disasters	sentinels.copernicus.eu
GLIMR (USA)	2029	340-1040	1-15	250	300		Ocean biology, chemistry and ecology and coastal hazards from U.S. to Brazil	science.nasa.gov
SBG (USA)	2030	400-2500, TIR	8-12	>210	30	185	World ecosystems, natural disasters	sbg.jpl.nasa.gov
S3NGO-AOLCI (Europe)	2034	340-1040, TIR	1.25-5	408	150	1400	global ocean, coastal and most inland waters biology, chemistry and underwater radiation	
Multispectral Ocean colour satellites (SeaWiFS, MODIS, MERIS, OLCI)	since 1980s	400-900 (not continuous)	10	~20	>300	>1000	Oceans, coastal and inland waters	See space agencies data portal
Land Multispectral missions (e.g. Landsat, S2, S2NG, Landsat-Next)	since 1984	400-2500 (not continuous)	20-40	~10	10-30	>180	Land	See space agencies data portals

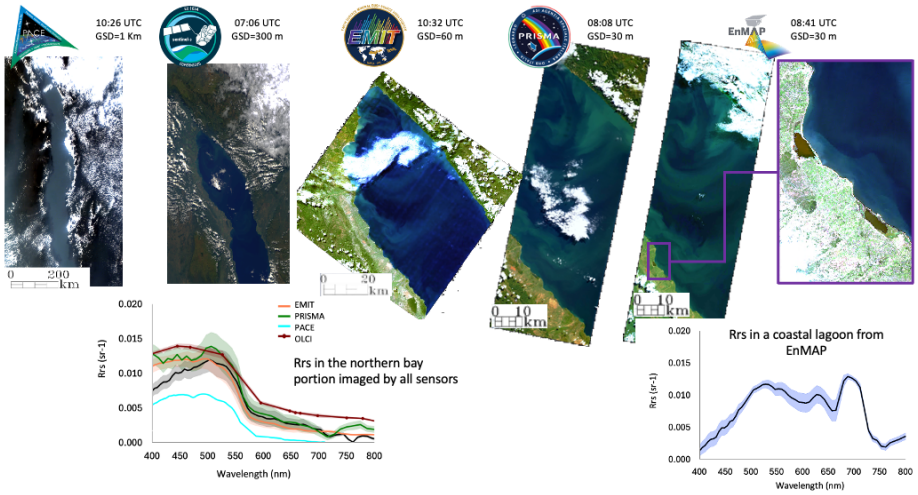

Figure 2.2 True-colour composite of the spaceborne hyperspectral images from PACE, EMIT, PRISMA and EnMAP, along with Sentinel-3 OLCI, all acquired on 21-05-2025 in Lake Malawi; bottom left: the R_{rs} spectra from Level-2 products covering a common portion of waters in the Northern part of the lake; bottom right: an R_{rs} spectrum from EnMAP over the coastal lagoon.

2.2 Limitations

2.2.1 Airborne

In addition to providing flexible fine scale and improved radiometry mapping and short-term changes (Zhang et al., 2018), airborne imaging spectroscopy offers unique data for testing satellite-based systems (e.g., PRISMA, EnMAP, Surface Biology and Geology, SBG) despite limitations of spatial and temporal coverage. For example, Giardino et al., 2005 and Cogliati et al., 2021 used airborne MIVIS and HyPlant images respectively, for simulating MERIS data on lakes and assessing PRISMA mission requirements during its commissioning phase.

Limitations of airborne imaging spectrometry include the larger cost of associated field work. Airborne campaigns can be expensive to organize as a result of the rental expenses of the plane. Another limitation is the technical challenge in processing airborne data, especially when accurate atmospheric correction is required for high-altitude flights, and when georeferencing becomes problematic without known ground control points over aquatic scenes (Zhang, Hu, et al., 2015).

2.2.2 Spaceborne

Despite the recognized success of spaceborne hyperspectral satellite observations, they may still present some inaccuracies in monitoring environments that are highly variable in space and time, such as inland and near coastal waters (Ozesmi and Bauer, 2002). Olmanson et al., 2015 observed that spatial resolution was one of the primary limiting factors in the application of satellite remote sensing to freshwater ecosystems. The signal-to-noise ratio (SNR) of the sensor is critical in making accurate measurements of water quality parameters (Gege and Dekker, 2020). Since water is inherently darker than the land surface, ocean colour sensors require much higher SNRs than those for measuring the land surface (Hu et al., 2012). Current hyperspectral, high spatial (100m) sensors provide SNR values typically lower than 400 which is convenient for land surfaces but does not meet the minimal requirements of measuring

the relatively dark ocean (Qi et al., 2017). An SNR value higher than 500 (ideally 800, Muller-Karger et al., 2018) is required to observe dark absorbing waters that are often encountered, for example, in a significant number of productive lakes at latitudes >40°N/S. Thus, high spatial and spectral resolution data are essential attributes to provide accurate retrieval of water quality in both optically deep and shallow waters. They are also essential in feasibility studies and proposals for an aquatic ecosystem Earth observing sensor (CEOS, 2018).

Another limitation of many spaceborne hyperspectral sensors is their narrow swath (<200 km) that is not necessarily appropriate for observing aquatic ecosystems at a global scale. These require a revisit time that is sufficient to characterize highly dynamic fine-scale processes such as river discharges, flooding events, and phytoplankton blooms (<2 days). Only the PACE hyperspectral mission is currently able to provide a global coverage of the Earth every two days, and this coverage is at the expense of reduced spatial resolution (1 km) that is usually not sufficient for inland and coastal water applications.

Since no single sensor can meet all requirements of high spatial, temporal, and spectral resolution with sufficient SNRs for aquatic applications, final recommendations for future directions in imaging spectrometry should also exploit using synergistically different sensor types (hyper- and multispectral, high spatial and high temporal resolution, VIS-NIR and other spectral domains), as e.g., described in Losa et al., 2017 or Guanter et al., 2019. Satellite instruments, with a very high spectral resolution (1 nm and better, originally designed for atmospheric applications), so far do not provide operational water-leaving radiance products. This has limited their exploitation for aquatic remote sensing applications. Algorithms designed for these sensors so far focus on retrieving information from the top of the atmosphere to define strong spectral features in the ocean (either caused by inelastic scattering effects or phytoplankton pigments) while simultaneously accounting for the strong absorption by trace gases and broad band absorption and scattering effects from the ocean and atmosphere (e.g., see PhytoDOAS method and products described in Chapters 3.1, 3.4, and 3.6). For SCIAMACHY and GOME-2 the major constraint is their large footprint (around 0.5° latitude / longitude), which limits assessing their retrieval accuracy with in situ point measurements, and also limits application of their products to the open ocean. These limitations have been improved by OMI (18 by 24 km footprint) and more so by TROPOMI for which the global coverage is reached nearly within one day on a much smaller footprint (~5.5 km). On the other hand, OMI and TROPOMI only deliver data from UV to blue (500 nm), while SCIAMACHY and GOME-2 cover the whole UV-VIS-NIR range. Since different atmospheric sensors have different configurations, producing consistent time series for specific ocean colour products is challenging (Oelker et al., 2019). In 2025, ESA and the European Organisation for the Exploitation of Meteorological Satellites (EUMETSAT) launched two successor missions to TROPOMI, UVN on Sentinel-4 and Sentinel-5, with a pixel size of 3.5 km x 7 km.

2.3 Perspectives

In order to improve future sensor capabilities for hyperspectral remote sensing applications, we envisaged the following perspectives:

1. Combining data from multiple satellite sensors (hyperspectral and multispectral) and Earth observation (EO) missions (land, ocean, and atmospheric satellite platforms) can overcome limitations of individual sensors and platforms through synergistic integration.

2. As the requirements for observing ecological and hydrological processes in inland and coastal waters are not fully met, priority should, for example, be given to developing imaging spectroscopy satellite sensors with a spatial resolution of around 20–30 m and enhanced technical specifications, such as higher SNRs.
3. It is crucial to transition current hyperspectral satellite research missions into operational platforms to ensure the routine and reliable monitoring of water quality.
4. Airborne hyperspectral remote sensing has provided valuable support in the field for the development and operation of satellite missions and applications, including fine-scale mapping and hazard identification. This support should be maintained and augmented as the role of drones increases.
5. Public and commercial operators are expected to provide high-quality airborne/drone hyperspectral data with appropriate geocoding and accurate atmospheric correction methods for water.

Chapter 3

Products and Applications

Astrid Bracher, Ana Dogliotti, Maycira Costa, Heidi Dierssen, Claudia Giardino, Toru Hirawake, Chuanmin Hu, Wonkook Kim, Emanuele Organelli, Shaoling Shang, Fang Shen, Jeremy Werdell

For over 40 years, the exploitation of high spectrally resolved sensor data has been pursued to develop and improve methods. In the last decade, these efforts have exponentially increased. This chapter provides a summary of such efforts for a range of critical products that can be resolved using ocean colour remote sensing. The chapter provides information on the current status of the methodologies to generate the retrievals, and the limitations and gaps associated with these derived products (see SQ2 in Chapter 1). The chapter outlines the progress gained by new technologies for hyperspectral remote sensing (SQ2) and current perspectives on potential new and improved science and applications that may be addressed by hyperspectral remote sensing retrievals in the future (SQ3 and SQ4, respectively).

3.1 Spectral Inherent and Apparent Optical Properties

3.1.1 Societal application and user needs

The interest in remote-sensing-relevant inherent optical properties (IOPs), namely spectral absorption ($a(\lambda)$; m^{-1}) and backscattering coefficients ($b_b(\lambda)$; m^{-1}), and their derivation from ocean colour radiometry stems from their role in the propagation of light in water, which in turn affects light-associated processes such as primary production, visibility, and phytoplankton diel vertical migration. IOPs are the main determinants of $R_{rs}(\lambda)$ (sr^{-1}) and thus play a critical role in the interpretation of UV-to-NIR remote-sensing data (Werdell and Bailey, 2005). The total IOPs (those that result from additive contributions of all water constituents with optical signatures) determine the propagation of light within an aquatic medium and, hence, the changes in the magnitude and spectral composition of the light field throughout the water column. The sensitivity of IOPs to the variability of optically significant components enables their use as proxies of various seawater dissolved and particulate constituents of biogeochemical significance. Specifically, the spectral variation of IOPs provides insight on the composition of specific optical water constituents (OWCs), particularly when presented as subcomponents of the bulk property, such as absorption by phytoplankton ($a_{ph}(\lambda)$; m^{-1}), non-algal particles ($a_{NAP}(\lambda)$; m^{-1}), chromophoric dissolved organic matter ($a_{CDOM}(\lambda)$; m^{-1}), the sum of the latter two ($a_{dg}(\lambda)=a_{NAP}(\lambda)+a_{CDOM}(\lambda)$), and backscattering by particles ($b_{bp}(\lambda)$; m^{-1}). These subcomponents have been shown to improve retrievals of many ocean colour products (e.g., CHL concentration (m^{-3}) and total suspended matter concentration (TSM; g m^{-3} g/L)) in complex waters. IOPs are also relevant for a proper bio-optical treatment of the light regime of the upper ocean mixed layer and the related heat budget (e.g., Morel and Antoine, 1994;

Ohlmann et al., 1996). This manifests in their ability to inform the availability of UV light and photosynthetic useable radiance (PUR), to provide estimates of primary production (PP) and phytoplankton functional types (PFTs), and to identify sources of CDOM and the nature of particulate inorganic and organic matter across all water types. Ultimately, IOPs are beneficial to answer many user needs related to aquatic ecosystem management, monitoring of water quality, and assessment of long-term changes in response to anthropogenic pressure, among others. In this subchapter, we focus on spectral IOPs, but partially exclude CDOM absorption, $a_{CDOM}(\lambda)$, which is covered thoroughly in subchapter 3.2.

More directly linked to the underwater light regime is the average attenuation coefficient for downwelling irradiance ($K_d(\lambda)$; m^{-1}), which is an apparent optical property (AOP), as is based on IOPs as well as the light environment driven by sun elevation, observation geometry, and sea state. $K_d(\lambda)$ describes how the wavelengths of sunlight dissipate as they travel downward into the ocean. These data are key for estimating PP through identifying the depths to which wavelengths in the range of photosynthetically active radiation (PAR) penetrate for use in photosynthesis. In addition, UV $K_d(\lambda)$ improves estimates of photodegradation processes and many other effects of this short-wave radiation on aquatic ecosystems and biogeochemical fluxes. $K_d(\lambda)$ also informswater clarity, which remains especially important for assessments of water quality in coastal and inland waters. Most common remotely-sensed $K_d(\lambda)$ retrievals refer to a bulk average attenuation within the first optical (e-folding) depth where approximately 90% of the photons within the euphotic depth are available. It is typically defined as the depth at which the downwelling irradiance has reduced to 1/e of its subsurface value (Gordon and McCluney, 1975). While $K_d(\lambda)$ is included in this chapter, other AOPs are addressed in Chapter 4.

3.1.2 Inventory of existing algorithms: innovations and improvements to multispectral methods

Many radiative transfer codes have been developed that compute $R_{rs}(\lambda)$ from user-input IOPs and other key environmental parameters (e.g., sea surface state, atmospheric transmittance, sky radiance distribution, solar geometry, viewing geometry, and water column depth). In parallel, considerable effort has focused on the development of analytical frameworks for deriving aquatic IOPs from sensor-observed $R_{rs}(\lambda)$, recognizing that these frameworks cannot be equivalently reduced to an analytical equation or expression (IOCCG, 2006; Werdell et al., 2018). Rather, deriving IOPs in this way requires the solution of an inverse problem, which is often mathematically ill-posed, since different combinations of IOPs can result similar $R_{rs}(\lambda)$ spectra in visible light (e.g., Defoin-Platel and Chami, 2007). This is particularly true when the number of independent observations (i.e., the number of sensor VIS bands) is small compared to the number of unknown IOP variables, or when the uncertainty in the observed $R_{rs}(\lambda)$ is high. Despite this difficulty, many IOP retrieval methods applied to multispectral $R_{rs}(\lambda)$ have yielded high quality data and operational products (e.g., as provided by NASA (McKinna and Werdell, 2024a), by ESA at oceancolor.org, and by the Copernicus Marine Service at data.marine.copernicus.eu).

3.1.2.1 Algorithm architectures to derive IOPs

The community has invested substantially in the development of methods to retrieve IOPs from ocean colour radiometry and numerous methods exist (see e.g., IOCCG, 2006; Werdell et al., 2018; and others for reviews on this topic). This section focuses on two distinct algorithm

architectures to derive IOPs. Each broadly represents multiple published approaches, and both are currently adopted for standard processing by an agency.

The Generalized Inherent Optical Property (GIOP) framework retrieves $a(\lambda)$, $b_b(\lambda)$, $a_{ph}(\lambda)$, $a_{dg}(\lambda)$ and $b_{bp}(\lambda)$ (Werdell et al., 2013) and represents a broad class of approaches that adopt spectral optimization. It has been implemented in standard NASA Level-2 ocean colour processing since 2013 in its default configuration (DC) and provides products for all multispectral sensors in their purview (e.g., SeaWIFS, MODIS-Aqua, MODIS-Terra, MERIS, S3A OLCI, S3B OLCI, VIIRS-SNPP, VIIRS-NOAA20) at their respective input wavelengths (access available at oceancolor.gsfc.nasa.gov/data). As for most semi-analytical (spectral matching) IOP approaches, GIOP-DC assigns constant spectral values for seawater absorption and backscattering ($a_w(\lambda)$ and $b_{bw}(\lambda)$, respectively; m^{-1}), assumes spectral shape functions of the remaining constituent absorption and scattering components, and retrieves the magnitudes of each remaining constituent required to match the spectral distribution of $R_{rs}(\lambda)$. The retrieved $a_{ph}(\lambda)$, $a_{dg}(\lambda)$ and $b_{bp}(\lambda)$ are then summed with the seawater IOPs to derive total IOPs (a bottom-up approach). Mechanically, GIOP-DC considers multi- and hyperspectral $R_{rs}(\lambda)$ identically. In fact, the first hyperspectral IOP products from PACE/OCI were recently released by NASA (Version 3 Reprocessing, Feb 2025, pace.oceansciences.org/data_table.htm). GIOP-DC adopts a fixed $a_{ph}(\lambda)$ spectrum normalized to CHL ($a_{ph}^*(\lambda)$, Bricaud et al., 1998), a fixed slope for a_{dg} (Sa_{dg}) of 0.018 nm^{-1}, a temperature to salinity dependent $b_{bw}(\lambda)$ (Zhang et al., 2009), a Raman scattering correction (McKinna et al., 2016), a dynamic slope for b_{bp} (Sb_{bp}, Lee et al., 2002), and Levenberg-Marquadt solution for least square minimization. However, the GIOP framework within NASA processing allows for user-defined reparameterization to use alternative spectral slopes for its eigenvectors, as well as alternative optimization scheme. NASA's GIOP-DC retrievals are provided with standard uncertainties, following McKinna et al., 2019.

The three-step semi-analytical algorithm (3SAA) retrieves $a(\lambda)$, $b_{bp}(\lambda)$, $a_{ph}(\lambda)$, $a_{dg}(\lambda)$ and $K_d(\lambda)$ (Jorge et al., 2021) and represents a broad class of approaches that adopt bulk inversion and spectral deconvolution. EUMETSAT derives its IOP and $K_d(\lambda)$ products for S3 OLCI using 3SAA at bands centered at 400, 412, 443, 490, 510, 560, 620, and 665 nm (see Fig. 1 in Bracher et al., 2025 as an overview). 3SAA was implemented in February 2024 into operational processing for S3-A and -B OLCI data (Data Store | EUMETSAT - User Portal; EUMETSAT, 2018). 3SAA is based on the Loisel-Stramski Version 2 (LS2) model (Loisel et al., 2018), which adopts statistical relationships between $R_{rs}(\lambda)$ and IOPs and makes no assumption about the spectral shape of $a(\lambda)$ and $b_b(\lambda)$ (a bottom-up approach). LS2 requires $R_{rs}(\lambda)$ and $K_d(\lambda)$ as inputs. The latter is estimated from $R_{rss}(\lambda)$ using a neural network from Jamet et al., 2012. An advantage of LS2 is that the spectral slope of $b_{bp}(\lambda)$ can be retrieved independently at several wavelengths (Loisel et al., 2006), which can then be used to assess information about particle size distribution (Kostadinov et al., 2009, 2010). From $a(\lambda)$, which can be estimated at each visible wavelength independently, the different sub-components $a_{ph}(\lambda)$ and $a_{dg}(\lambda)$ can be calculated using various models (Ciotti and Bricaud, 2006; Zhang, Huot, et al., 2015; Zheng and Stramski, 2013). The 3SAA algorithm extends the calculations of these sub-components by accounting for bio-optical specificity through the use of optical water type (OWT) classification based on Mélin and Vantrepotte, 2015.

3.1.2.2 Retrieving $K_d(\lambda)$

Unlike the most common approaches to derive IOPs, which typically adopt spectral matching techniques, most historical $K_d(\lambda)$ retrieval methods are based on empirical algorithms that

employ a band ratio of $R_{rs}(\lambda)$ (mostly blue to green) to statistically derive K_d at one waveband (typically at 490 nm) or for the entire PAR spectrum. Several inverse methods based on radiative transfer models, neural networks, or semi-analytical models exist, largely to explore expanding the solution space to spectral $K_d(\lambda)$. Recently, NASA, ESA, and EUMETSAT have implemented various algorithms to obtain operational products of spectral $K_d(\lambda)$, but the number of methods with direct application to hyperspectral satellite sensors are limited.

The method by Lee et al., 2005, further optimized in Lee et al., 2013, enables the retrieval of spectral $K_d(\lambda)$ based on a semi-analytical model where $K_d(\lambda)$ is derived as a function of $a(\lambda)$ and $b_b(\lambda)$, independent of the source of the latter. As for the GIOP-like approach described above, this method considers multi- and hyperspectral IOPs identically. The approach captures variability in $K_d(\lambda)$ due to changes in solar zenith angle and does not require extensive field data training datasets. It is sensitive to both absorption and backscattering and performs well for $K_d(412)$ and $K_d(490)$ at waters with very low OWC concentrations (Begouen Demeaux and Boss, 2022; Begouen Demeaux et al., 2024). This is opposed to the band ratio algorithms (e.g., Austin and Petzold, 1981), which have low sensitivity due to the ratio of R_{rs}(blue) to R_{rs}(green) reaching an asymptotic value and are also generally only sensitive to absorption. McKinna and Werdell, 2024b implemented the Lee et al. (2005, 2013) model for application to PACE OCI data retrieving $K_d(\lambda)$ at 17 wavebands (400, 413, 425, 442, 460, 470, 490, 510, 532, 555, 583, 618, 640, 655, 665, 678 and 711 nm). Uncertainties are provided with the products, which are sourced from standard uncertainty in $a(\lambda)$ and $b_b(\lambda)$, the internal model uncertainties due to assumptions and approximations, and within the pixel variability due to horizontal inhomogeneity. Standard uncertainties are estimated for all via analytical uncertainty propagation following the framework outlined by IOCCG, 2019; McKinna et al., 2019.

$K_d(\lambda)$ has been additionally retrieved by quantifying filling-in of Fraunhofer lines in various UV and short blue (<500 nm) wavelength regions. The retrieval developed by Vountas et al., 2007 and updated by Dinter et al., 2015 uses a radiative transfer-based pseudo-absorption spectrum of vibrational Raman scattering (VRS) that is fitted, together with other relevant absorbers from the atmosphere and ocean, in a specific wavelength region using differential optical absorption spectroscopy (DOAS). The VRS fit factors are converted to the responding emission wavelength region's $K_d(\lambda)$ value via radiative-transfer-built look-up tables (LUTs) using the coupled ocean-atmospheric Radiative Transfer Model (RTM) SCIATRAN (Rozanov et al., 2017), which also accounts for the solar zenith angle and observation geometry (Oelker et al., 2022). The method, so far, has only been shown to be applicable to highly spectrally resolved atmospheric satellite sensors within contiguous spectra, meeting a spectral resolution of at least 1 nm. Initially, $K_d(\lambda)$ was retrieved for the wavelength range λ = 390 to 423 nm from the atmospheric optical sensor SCIAMACHY on the Environmental Satellite (Envisat) by Dinter et al., 2015, for which a global dataset was compiled for the entire Envisat lifetime in Losa et al., 2017. Later, application of the retrieval was also shown for the currently operating MetOp/GOME-2 (since 2007) and Aura/OMI (since 2004) missions (Oelker et al., 2019). Recently, the retrieval was extended and applied to TROPOMI on S5P by Oelker et al., 2022 to retrieve $K_d(\lambda)$ in the UV-A (λ = 356.5 to 390 nm) and UV-A to UV-B (λ = 312.5 to 338.5 nm), and was validated for the Atlantic Ocean with $K_d(\lambda)$ data obtained from hyperspectral in situ radiometric measurements. The retrieval has recently been implemented into the ESA TROPOMI operational processing of innovative products at the Copernicus S5P Product Algorithm Laboratory (S5P-PAL: S5P-pal.com/). These data products are processed in near-real time and available at data-portal.S5P-pal.com/products/kd.html (the TROPOMI data series started in January 2018). The advantage of TROPOMI K_d-UV and short blue products is that they pro-

vide much higher temporal and spatial resolution when compared to the previous atmospheric sensor data from SCIAMACHY, GOME-2 and OMI. With the broad swath of TROPOMI, globally near-daily overpasses are possible, and pixel resolution (at 3.5 by 5.5 km) is comparable to the merged global operational products of Copernicus (data.marine.copernicus.eu, Globcolor, and OC-CCI).

Finally, several empirical methods allow the retrieval of $K_d(\lambda)$ in the UV at bands centered at 380 nm (Cao et al., 2014; Johannessen et al., 2003; Smyth, 2011) or at many more bands (between 350 to 400 nm, Morel and Maritorena, 2001; Vasilkov et al., 2001) using as input $R_{rs}(\lambda)$ data from the visible. These methods range from: algorithms using a simple band ratio (Johannessen et al., 2003); two-step band ratio including CHL from band ratios (Morel and Maritorena, 2001); principal component analysis of the multispectral visible water reflectance spectra used to obtain multivariate regression coefficients for predictions (Cao et al., 2014); a(443)-based empirical fit for different UV bands (Smyth, 2011); multi-step approach by Vasilkov et al., 2001 using Monte Carlo simulations accounting for the relationships of $a(\lambda)$ and $b_b(\lambda)$; to $K_{\mathrm{d}}(\lambda)$ following Gordon, 1998 and using CHL and K_d(490) retrieved from band ratio algorithm inputs. These retrievals were recently inter-compared, along with the method by Lee et al., 2005, 2013, in Wang et al., 2022. The algorithms were applied to VIIRS and validated with a global in situ $K_d(\lambda)$ dataset.

3.1.3 Limitations and challenges associated with current algorithms or applications

Evaluation of full spectrum IOPs and $K_d(\lambda)$ retrievals from space only truly became possible in 2024 with the launch of PACE. Previous hyperspectral satellite instruments were not designed for aquatic application. Previously launched hyperspectral, high spatial resolution sensors, including NASA Hyperion, ESA CHRIS/PROBA, DESIS and EnMAP, ASI PRISMA and JPL EMIT, have low sensitivity over dark waters that becomes worse in the blue spectral region relative to other visible regions. Moreover, these sensors are targeted mappers with narrow swaths and correspondingly low revisit times (>10 days) that acquire data over particular areas based on data acquisition requests. Similarly, HICO, onboard the International Space Station (ISS), which was designed for coastal ocean observations, only showed minor potential for exploitation (Mouw et al., 2015). Conversely, the high resolution atmospheric sensors SCIAMACHY and GOME-2 have very large footprints that only allow large mesoscale patterns in the open ocean to be resolved (>50 km), while TROPOMI (and the follow-on similar sensors UVN on S4 and S5) only provides continuous measurements from the UV (~280 nm) to the blue (<500 nm). The latter only allows submesoscale features (~5-7 km) to be resolved in the global oceans (Bracher, Bouman, et al., 2017). Despite their limitations, however, all of the above have proven to be good test beds for more suited aquatic sensors, such as PACE/OCI and S3NGO/AOLCI (to be launched ~2034) for the open ocean, as well as for future hyperspectral sensors designed for coastal and inland waters (e.g., Surface Biology and Geology (SBG) Earth mission, Cawse-Nicholson et al., 2021; or Global Assessment of Limnological, Estuarine and Neritic Ecosystems (GALENE), Chami et al., 2025).

Although in situ datasets of spectral IOPs have recently become increasingly available in common data repositories (e.g., NASA SeaWiFS Bio-optical Archive and Storage System (SeaBASS), Australian Ocean Data Network (AODN), and PANGAEA® Data Publisher) and through compilation of global datasets (e.g., Begouen Demeaux et al., 2023; Casey et al., 2020; Valente et al., 2022), the development of algorithms remains challenged by the low availability of hy-

perspectral $K_d(\lambda)$, $b_{bp}(\lambda)$, and to a lesser extent, absorption data, to enable a solid assessment of the accuracy of these methods. In addition, most $K_d(\lambda)$ in situ data only provide hyperspectral data with full width at half maximum of 10 nm, while current and future satellite data are often more finely resolved, and most field radiometers have either no measurements or only measurements with very high uncertainty in wavelength ranges below 350 nm.

Few satellite products include consistent uncertainty information. For example, current EUMETSAT IOP and $K_d(\lambda)$ product uncertainties are provided based on OWT-specific validation that addresses systematic errors while not accounting for random error sources. A more complete uncertainty assessment was provided in Oelker et al., 2022 and is followed by NASA for the PACE GIOP and $K_d(\lambda)$ products. An inter-comparison of these uncertainty assessments should be pursued. Furthermore, performance assessments and validation of the satellite retrievals remain spatially and temporally limited. For example, at the time of writing, validation for PACE $K_d(\lambda)$ and GIOP-DC products has yet to be presented. Methods for validation of uncertainty retrievals should also be pursued. Spectral optimization approaches to derive IOPs (and, thus, $K_d(\lambda)$) require a-priori assignment of spectral shape functions for the OWC specific IOPs. GIOP-DC currently adopts a fixed spectral slope for $a_{dg}(\lambda)$, a dynamically varying spectral slope for $b_{bp}(\lambda)$, and a dynamically varying shape $a_{ph}(\lambda)$. While the latter two vary from pixel to pixel, largely based on blue-to-green $R_{rs}(\lambda)$, all truly bear only limited information on the composition of the OWCs. Furthermore, within this bottom-up strategy, the inherent uncertainty associated with the $a(\lambda)$ or $b_b(\lambda)$ retrievals may be wrongly compensated when these two IOPs are simultaneously estimated during the optimization process, which also influences the downstream $K_d(\lambda)$ retrievals based on Lee et al., 2005. While bulk inversion approaches do not generally rely on assignment of spectral shapes, some assumptions about IOPs remain necessary within the training dataset used for developing the neural networks for each OWT to estimate $K_d(\lambda)$ from $R_{rs}(\lambda)$.

Currently, the EUMETSAT 3SAA implementation only produces operational OLCI products at one waveband (IOPs at 443 nm and K_d at 490 nm). Spectral IOP retrievals by Jorge et al., 2021 are possible using the SNAP toolbox. This software, which includes the C source code, is freely available under the terms of the GNU General Public License, version 3. Recent in situ validation of OLCI absorption products at eight spectral bands across all water types shows similarly good quality for the blue and green bands (Bracher et al., 2025). However, results also showed large uncertainty for absorption products at red wavebands. The quality of $K_d(\lambda)$ and $b_{bp}(\lambda)$ 3SAA products remains uncertain, as former validation efforts were obstructed by too few in situ spectral data, limited to the open ocean (Bracher et al., 2025; Jorge et al., 2021). Following a top-down strategy, 3SAA may be more sensitive to $R_{rs}(\lambda)$ noise propagation in contrast to bottom-up models that use optimization procedures.

The ESA TROPOMI algorithm is less sensitive in waters where the concentrations of OWCs are high, which is in contrast to all other $K_d(\lambda)$ methods presented here. However, it shows much lower uncertainty in clear waters compared to the other $K_d(\lambda)$ retrievals (Begouen Demeaux et al., 2024). The method only applies where Fraunhofer lines in the emission spectrum can be detected, which will determine the minimum spectral band width, as well as the spectral band position that can be detected. So far, validation for the shortest UV band $K_d(\lambda)$ retrieval is limited by the low quantity and quality of in situ data.

Empirical methods to retrieve $K_d(\lambda)$ in the UV, such as those presented in Cao et al., 2014; Fichot et al., 2008; Johannessen et al., 2003; Morel and Maritorena, 2001; Smyth, 2011; Vasilkov et al., 2001 and summarized in Wang et al., 2022, were developed based on assumptions of the relationship between visible and UV wavelength ranges derived from specific in situ

dataset compilations. They have not been recently updated for application to satellite data that observe UV light. A first assessment and inter-comparison of these algorithms showed far less robustness to obtain $K_d(\lambda)$ in the UV as compared to the semi-analytical method by Lee et al., 2005 (Wang et al., 2022).

3.1.4 New and improved applications

Retrieving spectral IOPs and $K_d(\lambda)$ from in situ $R_{rs}(\lambda)$ has shown meaningful potential for a variety of applications. As elaborated in subchapters 3.4 and 3.7, phytoplankton pigment composition can be retrieved from $a_{ph}(\lambda)$ (Chase et al., 2017; Hoepffner and Sathyendranath, 1991), thus providing proxy information on phytoplankton community composition (Astoreca et al., 2009; Li et al., 2021; Organelli et al., 2017) and phytoplankton photophysiological state. Hyperspectral $a_{ph}(\lambda)$ can also be linked to biological niches in the global ocean (Holtrop et al., 2021), metrics of photoacclimation (Hintz et al., 2021), and harmful algal bloom (HAB) composition (Castagna et al., 2021). As described in subchapter 3.6, hyperspectral $a_{ph}(\lambda)$ can also improve the accuracy of primary production estimates when spectrally-resolved underwater light intensity is weighted by the efficiency of phytoplankton to absorb light (e.g., Zhao et al., 2023). Hyperspectral $a(\lambda)$ or $K_d(\lambda)$ data in the UV-to-blue wavelength region can help to quantify photo-degradation / photo-bleaching that leads to Deoxyribonucleic Acid (DNA) damage (Schuch et al., 2012; Teague et al., 2023).

Spectral IOPs and $K_d(\lambda)$ also provide valuable information in support of ocean and inland water quality and biodiversity monitoring; ecosystem and biogeochemical modelling and coupled ocean-biogeochemical modelling (Álvarez et al., 2022; Terzić et al., 2021); ecosystem management and conservation activities; and identification of new *Digital Twin of the Ocean* focus areas, which further improve ecosystem and biogeochemical modelling and enhance artificial intelligence (AI) developments. Hyperspectral IOPs and $K_d(\lambda)$ also enable improved estimates of particulate carbon components (e.g., Lian et al., 2024), as discussed in subchapter 3.5, and identification and characterization of "coastal darkening / lightning" (Lazzari, Becerro, et al., 2021). Finally, knowledge of IOPs and $K_d(\lambda)$ is thought to potentially improve ocean colour atmospheric correction and atmospheric studies, through improved separation of aerosols from hydrosols and CDOM, and quantification of shortwave radiation (including feedback to the atmosphere).

3.1.5 Progress towards addressing new science questions

Hyperspectral satellite missions are already, and will continue: enhancing our scientific understanding of aquatic radiative transfer; advancing approaches for inverse modelling of many existing and desired geophysical and optical products (e.g., PAR, primary production, CHL, phytoplankton community composition, a_{CDOM}, suspended matter, and particulate organic and inorganic carbon); and improving the retrieval of these geophysical products and their application across water types, with reduced uncertainties.

3.1.5.1 New science questions

The following emergent science questions specifically related to advancing IOP retrievals were identified:

- What is the impact of the underwater UV radiation on aquatic ecosystems? Is it a source of energy for phytoplankton? Does it prohibit phytoplankton growth? Can it contribute

to the photochemical transformation of dissolved organic matter? Can it affect the vertical movement of zooplankton? Can we observe trends in UV radiation, and do they link to aquatic ecosystem changes?

- How does UV radiation modulate the release of methane, aerosol precursors and other climate-related gases (e.g. isoprenes, halocarbons) by phytoplankton cells, which then directly feedback to the radiation budget in the atmosphere?
- What is the role of photo-bleaching in organic matter degradation?
- What is the geographical and temporal distribution of surface shortwave (UV-VIS-NIR) reflection, is there feedback to atmospheric radiation, and can it be related to global warming?

3.1.6 Perspectives

Advanced IOP and $K_d(\lambda)$ retrievals from hyperspectral radiometry offers possibilities for: obtaining more detailed information on particles and CDOM; lowering the uncertainties in derived products such as CHL, CDOM, TSM, particulate organic carbon (POC), particulate inorganic carbon (PIC), and PFTs (see subchapters 3.2 - 3.4); and enabling satellite retrievals in an expanded range of OWTs. In turn, these should facilitate improved biodiversity and water quality monitoring, and analysis of the feedback of climate change and other environmental factors in nearly all waters where satellite pixel size allows for the resolution of the related dynamics. In principle, all new scientific questions can possibly be addressed with new and improved products that rely on hyperspectral IOP and $K_d(\lambda)$ retrievals as intermediate or input products.

We identified the following gaps and/or activities, which, if addressed and pursued, would advance the retrieval and performance assessment of spectral IOPs and $K_d(\lambda)$ products:

- Test, extend, and adapt retrievals to hyperspectral sensors (e.g., DESIS, EnMAP, HICO, Hyperion, PRISMA, PACE, TROPOMI, UVN), in preparation for future missions (e.g., CHIME, SBG, S3NGO/AOLCI).
- Explore the development of $K_d(\lambda)$ algorithms to be applied to new atmospheric sensors, such as UVN on S4 and S5.
- Improve radiative transfer modelling for aquatic (e.g., Ecolight) and coupled ocean-atmosphere (e.g., SCIATRAN), and bio-optical models (e.g., Bi et al., 2023) to better connect OWC quantities with hyperspectral IOPs and AOPs across different environments. The degree of independent information in hyperspectral signals will depend on the water type (e.g., waters optically dominated by phytoplankton alone, other particles, or CDOM) and will determine whether different phytoplankton products can be independently derived from a given hyperspectral spectrum. This statistical-informational problem needs to be considered in the application of global and regional inversion algorithms.
- Inter-compare hyperspectral IOP and $K_d(\lambda)$ satellite products in round-robin exercises, including assessments at both regional and global scales.
- Develop additional frameworks for standardized uncertainty assessment and implementation, with pixel-level uncertainty retrievals in products.
- Extend in situ validation data acquisition to encompass more OWTs across multiple seasons, and promote round-robin exercises and inter-comparisons for method and uncertainty assessments.
- Enable the development, maintenance, and expansion of, and easy access to, global in

situ data compilations for algorithm development and validation of satellite products.

3.2 Dissolved Organic Matter (CDOM, DOM, DOC)

3.2.1 Societal application and user needs

The largest carbon pool in the ocean is in the form of dissolved organic matter (DOM; g/L; Hansell and Carlson, 2002). The predominant sources of DOM are humic substances from terrestrial plants and aquatic phytoplankton. Therefore, understanding DOM distribution and inputs from terrestrial environments to the ocean is important for predicting changes in the biogeochemical cycles. Additionally, DOM fluxes from the land to the ocean are anticipated to change due to an increase in permafrost thaw by global warming and other changes in human-activity and land-use. A fraction of DOM that strongly absorbs light in the UV-blue region of the spectrum with yellow-brown colour, CDOM, is detectable from satellite ocean colour sensors. Dissolved organic carbon (DOC) is a major component of DOM and its concentration frequently has high correlation with the absorption coefficient of CDOM. Satellite observations of CDOM on global and local scales remain an important way to obtain knowledge on the distribution of DOM and the process of its production and removal.

3.2.2 Inventory of existing algorithms: innovations and improvements to multi-spectral methods

Due to the spectral information available from heritage ocean colour instruments, remote-sensing estimates of $a_{CDOM}(\lambda)$ (often just abbreviated as CDOM, provided in m^{-1}) are traditionally derived from visible $R_{rs}(\lambda)$. Several algorithmic approaches currently exist. The simplest empirical $a_{CDOM}(\lambda)$ algorithms use blue-green or green-red ratios of $R_{rs}(\lambda)$ (e.g., Morel and Gentili, 2009). More complex algorithms estimate $a_{CDOM}(\lambda)$ or its spectral slope as a function of multiple regression, using $R_{rs}(\lambda)$ at several wavelengths (e.g., Aurin et al., 2018; Bricaud et al., 2012; Ciotti and Bricaud, 2006; Fichot et al., 2013). Semi-analytical algorithms, such as those discussed in subchapter 3.1, have also been developed. They most commonly separate the contributions of particulate backscattering and multiple absorption components to the observed $R_{rs}(\lambda)$, but typically retrieve the sum of $a_{CDOM}(\lambda)$ and $a_{NAP}(\lambda)$ as a single variable $a_{dg}(\lambda)$. Several ways to separate $a_{dg}(\lambda)$ have been attempted (Hirata, 2020; Matsuoka et al., 2013; Zheng et al., 2015). $a_{CDOM}(\lambda)$ (either at $\lambda = 350$ or 440 nm) can be used to estimate DOC empirically (Cao et al., 2018; Fichot et al., 2013; Mannino et al., 2008) or based on machine learning (ML) techniques (Bonelli et al., 2022). However, DOC retrieval is limited to the local scale because CDOM algorithms are only robust for coastal areas with higher availability of in situ samples to inform the relationship between DOC and CDOM.

3.2.3 Limitations and challenges associated with current algorithms or applications

Deriving $a_{CDOM}(\lambda)$ and $a_{NAP}(\lambda)$ individually, or separating them from a retrieved $a_{dg}(\lambda)$, is challenging because of the similarity between the absorption spectra of CDOM and NAP, both of which decrease exponentially with wavelength. Several methods have been attempted. These include, for example, expression of $a_{CDOM}(\lambda)$ as a function of $a_{CDOM}(\lambda)$ and $a_{NAP}(\lambda)$ (Hirata, 2020), and subtraction of $a_{NAP}(\lambda)$ expressed by a function of $R_{rs}(\lambda)$ from $a_{CDOM}(\lambda)$ and $a_{NAP}(\lambda)$

(Matsuoka et al., 2013). However, there is no robust algorithm that is applicable on both global and local scales.

Better retrievals of the spectral slopes are expected using hyperspectral data in the UV region compared to using multispectral data with wide bands. Optical signatures from the spectral shape of $a_{CDOM}(\lambda)$ in the UV region, such as spectral slopes ($S_{275\text{-}295}$ and $S_{350\text{-}400}$) and $a_{CDOM}(350)$, provide important information to trace water masses. This information includes photo-bleaching, terrestrial DOC, lignin, molecular weight of DOM, microbial activity, and mycosporine-like aminoacids (e.g., Fichot and Benner, 2012; Helms et al., 2008; Yamashita et al., 2013). However, ocean colour sensors measuring within the UV region are limited. Although estimation of the optical signatures in the UV region has been attempted using multiple regression or ML with visible spectral data, these bear large uncertainties as the spectral shape of $a_{CDOM}(\lambda)$ is not monotonical in the UV region (several peaks by degradation; e.g., Organelli et al., 2014).

NASA PACE OCI has hyperspectral radiometry in the UV region (e.g., from 315 to 400 nm) and data from OCI have potential to provide useful information to detect the optical signature of CDOM in the UV spectral region. However, algorithms to retrieve a_{CDOM} in the UV have uncertainties, and OCI does not cover the wavelengths for $S_{275\text{-}295}$. Therefore, development of algorithms to estimate a_{CDOM} in the UV, and CDOM proxy at shorter wavelengths, are required. While OCI provides radiances from 315 to 340 nm, validation is needed.

3.2.4 New and improved applications

The spectral slopes of CDOM in the UV range provide a useful optical signature of varied water masses (Hirawake et al., 2021; Oida et al., 2024) and information on the source of organic material. However, estimation of the slopes from multispectral satellite data requires extrapolation of CDOM data at several wavelengths from the VIS range. Hyperspectral radiometry will improve retrievals of the spectral slopes of CDOM, and measurements in the UV range will allow for less uncertain retrievals of CDOM proxies.

3.2.5 Progress towards addressing new science questions

Mapping CDOM parameters and their proxies is useful to track the CDOM distribution in waters from rivers / land into the ocean, and to better study the ocean carbon cycle from coastal to open ocean waters. CDOM optical proxies are indicators of degradation and remineralization processes of organic material. For example, the CDOM absorption coefficient has been linked to dissolved oxygen used by heterotrophic bacteria digesting organic particles (e.g., Nelson and Siegel, 2013) and has also been found to depend on changes in the phytoplankton community structure (e.g., Organelli and Claustre, 2019). The ability to obtain more accurate CDOM coefficients and spectral characteristics will thus help to disentangle chemistry- and biology-driven dynamics related to CDOM and DOC processes in the ocean, and quantify sources (Lazzari, Álvarez, et al., 2021).

3.2.5.1 New science questions

The following emergent science questions specifically related to advancing DOM retrievals were identified:

- How are biogeochemical dynamics between land and ocean changing under global warming?

- Can $a_{CDOM}(\lambda)$ and spectral characteristics help assess the direct role of phytoplankton in generating forms of dissolved organic material that is resistant to further degradation, thus becoming part of the carbon sequestered in the ocean?

3.2.6 Perspectives

We identified the following gaps and/or activities, which, if addressed and pursued, would advance the retrieval and performance assessment of DOM products:

- Conduct in situ hyperspectral measurements of CDOM and particle absorption as well as $R_{rs}(\lambda)$ over UV-VIS regions from coastal to offshore waters. These measurements would be utilized to develop robust algorithms for estimating CDOM absorption coefficients, for example, to improve modelling for partitioning a_{NAP} from a_{CDOM}.
- Develop or tune new algorithms using UV bands. Algorithms have been developed only for the VIS, while CDOM proxies based on UV are more accurate.
- Extend the wavelength range of ocean colour sensors to the UV region to improve retrievals of CDOM proxies.

3.3 Particle Concentration, Size and Composition

3.3.1 Societal application and user needs

Suspended particulate matter (SPM) in water plays a key role in many ocean and coastal processes, including biogeochemical cycles, nutrient balances, ecological dynamics, and carbon sequestration to the deep ocean. The composition and size of such particles influences their sinking rates, aggregation and disaggregation potentials, and nutritional value, as well as how they influence light penetration and local aquatic radiation budgets. In coastal areas, the study of suspended particle spatiotemporal variability is important for understanding sediment and land material transport and coastal erosion. These have large implications to coastal resource management, including responses to storm events, maintenance of beaches, management of fisheries and shellfisheries, and other efforts with socioeconomic and recreational relevance.

3.3.2 Inventory of existing algorithms: innovations and improvements to multispectral methods

In remote sensing studies, the concentration of TSM (g/m^3; also called SPM) that is estimated via the optical properties of suspended particles assumes, either directly or indirectly, a constant relationship between particle mass and particulate scattering or absorption (Ruddick et al., 2008). Different algorithms to estimate SPM from water reflectance have been developed that use either a single band, a band ratio, or multispectral remotely sensed information. Multispectral algorithms are quite varied but are generally based on a forward modelling of reflectance as a function of IOPs (e.g. simulated spectra using a radiative transfer model) and an inversion procedure (like artificial neural networks, NN) to find the reflectance spectra that best fits the measured spectra. This type of approach has been proposed to better deal with the non-linear and multivariate nature of the inversion problem and NNs have been shown to produce reasonable results in optically complex (Case-2) waters, like the Case 2 Regional CoastColour (C2RCC) and the OLCI Neural Network Swarm (ONNS). The C2RCC (Brockmann et al., 2016) is a comprehensive processor that includes atmospheric correction and retrieval of multiple water constituents and is used to generate the Case 2 water products in S3 OLCI

standard ESA products. The ONNS (Hieronymi et al., 2017) is a processing scheme that does not include the atmospheric correction of satellite data, and consists of several blended NNs that are optimized for waters with different optical properties that are applied after classifying the spectra in different OWTs. Single and band ratio algorithms have been widely used to provide good estimations of SPM using red and NIR spectral regions (e.g., Doxaran et al., 2002, 2012; Han et al., 2016; Hu et al., 2004; Miller and McKee, 2004; Nechad et al., 2010; Novoa et al., 2017; Ondrusek et al., 2012; Ouillon et al., 2008). However, SPM algorithms are regionally specific and cannot be applied globally because the relationship has been shown to depend on particle type, i.e., particle size and composition (Babin et al., 2003; Binding et al., 2005). The relationship between water reflectance and backscattering or water turbidity (a proxy to side-scattering), is more direct and can be retrieved first and then used to estimate SPM via regional relationships (Dogliotti et al., 2015).

Multispectral remote sensing algorithms exist for retrieving information on the particle composition, i.e., to estimate the organic (POC) and inorganic (PIC) fractions of suspended particles, or the POC/SPM ratio, which is a useful proxy for characterizing the contribution of organic particles to SPM. These two main types of particles generally have quite different indices of refraction, especially phytoplankton cells and mineral particles that influence the optical properties of the water body (Stramski et al., 2001). Both PIC and POC are part of the marine carbon cycle, which has a significant role in absorbing human-produced fossil fuel carbon as well as heat (Arico et al., 2021, and are thus key to the Earth system carbon budget. Current satellite algorithms for retrieving PIC, which is used to quantify a specific phytoplankton group called coccolithophores, which are covered by highly reflective carbonate calcium plaques, use two blue-green and three red/NIR bands for detecting non-bloom conditions (Balch et al., 2005; Mitchell et al., 2017), and turbid and high-reflectance blooms of coccolithophores (Gordon and Du, 2001), respectively. The blue-green algorithm (Tran et al. 2019) detects CHL absorption and PIC scattering peaks, while using the red/NIR bands minimizes the interfering effects of CHL and CDOM. However, studying coccolithophores and PIC over continental shelves can be challenging given that highly scattering re-suspended sediments can confound the algorithm (Daniels et al., 2012).

Multispectral global algorithms have been developed from ocean colour remote sensors that estimate POC (a mixture of live, i.e. phytoplankton, and non-living, i.e. detritus, particles) for open-ocean pelagic environments where properties are dominated primarily by phytoplankton and co-varying organic matter (Evers-King et al., 2017; Stramski et al., 2008 and references therein). These algorithms tend to fail in waters with a high proportion of mineral particles (Wozniak and Stramski, 2004) and regionally-specific algorithms are generally tuned using regional datasets.

Finally, different attempts have been made to retrieve information on the particle size distribution (PSD) from multispectral radiometry. The quantitative estimate of particle size in estuaries and shelf areas is important given their impact on oceanic processes, like the settling velocity of particles, carbon fixation (Nasiha et al., 2019; Xi et al., 2014), and light penetration through the water column (Baker and Lavelle, 1984). In order to retrieve PSDs from space, it is necessary to quantitatively link optical proxies and PSD parameters. Strong relationships (empirical models) have been found between median particle size and mass-specific back-scattering (Bowers et al., 2007) or water reflectance band ratios (Qing et al., 2014) from multispectral satellites. It has also been found that the spectral slope of the particulate backscattering coefficient can be related to the power law or "Junge-type" PSD slope parameter in coastal non-algal-dominated waters (Slade and Boss, 2015; Wozniak and Stramski, 2004) and

oceanic waters (Kostadinov et al., 2010), but this relationship was not always observed (Boss et al., 2018; Organelli et al., 2020; Reynolds et al., 2016).

The estimation of SPM using hyperspectral radiometry has been mainly performed using empirical algorithms, i.e., regressions between bands and in situ measurements, showing generally better results than the existing multispectral algorithms. The increased amount of spectral information allows the selection of specific band or band combinations that are not present in the existing multispectral missions, and different statistical approaches can be used. Simple linear or logarithmic regressions using single or multiple band combinations have been used, selecting the ones showing the highest correlation and minimal root-mean-square-error (Sterckx et al., 2007). Multivariate statistical approaches, like partial-least-squares regression, have been applied to retrieve SPM (Ali and Ortiz, 2016; Harringmeyer et al., 2024) and POC/SPM (Harringmeyer et al., 2024). These methods extract the main patterns of changes in the hyperspectral reflectance as they identify spectral bands that are more sensitive to specific optically-active constituents, thus reducing collinearity in complex datasets. Harringmeyer et al., 2024 found that the enhanced spectral information provided by hyperspectral radiometry improved the retrieval of SPM and POC/SPM. Partial-least-squares regression algorithms (in log-log scale) have been developed using in situ SPM and POC/SPM data, performing first a reduction in the number of variables (bands) using the Variable Importance Projection (VIP) score. The impact of the reflectance spectral resolution on the performance of these algorithms was assessed by downscaling the reflectance to coarser spectral resolutions, showing that the POC/SPM retrieval accuracy was more sensitive to spectral resolution than the SPM retrieval (Harringmeyer et al., 2024). Machine learning techniques have also been used to retrieve SPM concentration from hyperspectral remote sensing data. Combining clustering and ML regression, Kwon et al., 2022 proposed an algorithm to estimate SPM from hyperspectral data that improved the SPM retrieval in optically complex and shallow waters with different bottom properties. Probability-based hyperspectral clustering was used to classify the in situ dataset according to optical similarity, and then different ML regression models were developed using Recursive Feature Elimination for selecting the relevant bands for each cluster.

3.3.3 Limitations and challenges associated with current algorithms or applications

Even though many algorithms have been proposed to retrieve SPM, a single algorithm that can be applied globally remains a challenge. This is because these algorithms are generally limited regionally to where in situ data were collected and used to calibrate the algorithm, or they are limited in application by the quality and representativeness of the data (range and concentration of constituents) used to train the NNs. Dimensionality, and the effects of multicollinearity in hyperspectral remote sensing data also pose a challenge in retrieving stable models and accurate results.

Regarding the determination of the nature of particles, there is still an important limitation in disambiguating the organic vs mineral fraction. For example, considering and removing the effects of CDOM and other minerals on POC determination remains a challenge in coastal and estuarine waters where these constituents usually dominate. Recent efforts have attempted to separate POC related to phytoplankton vs detritus in coastal waters, with limitations, for which hyperspectral data could be useful, in determining the refractive index and efficiency factors, which require further study (Li, Organelli, et al., 2024).

Improvement in PSD modelling is a challenge that still needs to be addressed. It has been

shown that PSDs cannot be modelled simply as a power law, especially in waters dominated by organic particles. Indeed, strong deviations from a power law can exist in the presence of phytoplankton (Organelli et al., 2020). In this regard, more accurate in situ PSD measurements are needed. However, these measurements are not easily made, especially in the open ocean. Two major instruments exist: the Coulter counter and the Laser In Situ Scattering and Transmissometry (LISST). LISST instruments, based on laser diffraction, imaging, or digital inline holography, resolve in situ particle sizes and concentrations down to 1 µm, 3.4 µm, and 25 µm, respectively. Coulter counters can be used to directly characterize ex situ particle size and concentrations down to 0.6 µm, but the method is time-consuming, especially in low particle environments, because several replicates are required.

3.3.4 New and improved applications

Hyperspectral imagery could improve retrieving quantitative estimates of SPM, as well as the type (size) and composition (organic vs. inorganic) of particles. Satellite maps of SPM could be useful for automated detection of dredging and coastal plumes. Improved characterization of the fraction of organic vs. inorganic particles will improve our understanding of the connectivity of particle transport between coastal and open ocean waters, and how this connection might be related to circulation patterns, which can have an impact on the management of fisheries, and aquaculture. Improved retrieval of SPM, POC, and particle characteristics may help increase the accuracy of output from biogeochemical and ecosystem models used to mechanistically represent ocean and coastal environments, which can help to improve the accuracy of blue carbon estimations.

3.3.5 Progress towards addressing new science questions

Hyperspectral satellite missions are improving our understanding of the role of particle composition in coastal carbon cycling, which are affected by the strong land-sea exchange of organic and inorganic matter. Identifying the composition and contribution of diverse particle types within the marine POC pool enables more accurate estimation of ocean carbon budgets, as well as potential new investigations into the trophic web functioning (from primary producers to higher levels), especially in response to climate events. Improvements in coccolithophore PIC retrievals, specifically in the quantification of their abundance and distribution, will help to ascertain their responses to ocean acidification, and further improve estimates of the ocean carbon budget.

3.3.5.1 New science questions

The following emergent science questions specifically related to advancing particle concentration, size, and composition retrievals were identified:

- Is the geographical and temporal distribution of different particle types changing, and can it be related to global warming?
- Which type of materials, transported from the coast, are enhancing carbon production and sequestration and altering trophic webs in oligotrophic waters?
- Do large river plumes influence carbon characteristics, processes, and budget in the open ocean?

3.3.6 Perspectives

We identified the following gaps and/or activities which, if addressed and pursued, would advance the retrieval and performance assessment of particle concentration, size, and composition products:

- Improve the retrieval of particle backscattering spectral slope from hyperspectral reflectance to retrieve PSD-related parameters (a key parameter when studying biogeochemical cycles). The spectral slope changes from VIS to NIR due to particle absorption (Doxaran et al., 2009) thus a better spectral characterization of absorption will improve backscatter retrieval (Devred et al., 2013). See also subchapter 3.1.
- Develop new models to retrieve PSD-related parameters directly from hyperspectral reflectance or a combination of optical properties.
- Enhance the acquisition of in situ particle backscattering spectral slope and PSD data to evaluate general model assumptions (Mie theory for non-absorbing spherical particles with Junge type distribution). It has been shown that the relationship between particle backscattering spectral slope and PSD slope is not confirmed from in situ data across various trophic regimes (Boss et al., 2018; Organelli et al., 2020; Reynolds et al., 2016). Only recently two commercially available hyperspectral backscatter instruments exist: Hyper-bb, measuring spectral backscattering at a fixed ~135° angle across the visible spectrum (430-700 nm), with 5-nm channel spacing and ~9-14 nm spectral bandwidth (wavelength-dependent) (Mikkelsen et al., 2020); and a fixed-angle, hyperspectral fiber-optic backscatter instrument (HyFi-bb) that is capable of measuring scattering at a single angle but throughout the visible and partial UV and IR regions (320 - 850 nm) with a 2-nm spectral resolution (Novak et al., 2024).
- Exploit the hyperspectral resolution of the PIC reflectance spectra to improve coccolithophore PIC retrievals. Recent hyperspectral estimates of PIC backscattering cross-section suggest that it is more spectrally variant than previously thought (Balch and Mitchell, 2023).
- Develop new and better ways to characterize PSD (moving beyond the Junge slope for PSD characterization).
- Work on optical efficiency and refractive index derivation for better characterizing PSD and POC fractions (hyperspectral should help because light absorption is likely needed).
- Develop new algorithms that rely on multiple optical properties for deriving POC and PSD.

3.4 Phytoplankton Functional Types (PFTs)

3.4.1 Societal application and user needs

PFT characterizations serve to classify organisms by: their roles in biogeochemical or ecological processes; morphology; spatial and/or temporal dominance in specific environments. While PFT assignments often vary by study or user definition, they can be typically organized by size spectra (pico-, nano-, microplankton), ecological function (e.g., nitrogen fixation), pigment composition, or physiological trait(s) (Le Quéré et al., 2005). Broadly speaking, distinct PFT functions mean that their biomass and distribution dynamics can serve as direct proxies for marine environmental shifts and climate change impacts. Consequently, satellite monitoring of PFT spatiotemporal patterns is essential for understanding ecosystem responses

and improving climate predictions. PFTs directly influence society, the economy, and recreation, through their influence on fisheries, shellfisheries, and sport. Harmful algal blooms close beaches and contaminate drinking water. All of these activities carry substantial socioeconomic relevance. In this subchapter, we focus on general methods for PFT retrievals, but exclude rigorous discussion of harmful algal blooms, which are covered thoroughly in subchapter 3.7.

In response to climate impacts on marine ecosystems, the Intergovernmental Oceanographic Commission of the United Nations Educational, Scientific and Cultural Organization (IOC-UNESCO) established the Climate Change and Global Trends of Phytoplankton in the Oceans (TrendsPO) working group to assess phytoplankton community changes (which are critical indicators of ocean health), and develop conservation strategies (IOC-UNESCO, 2024). Hyperspectral remote sensing offers transformative potential towards this task. High-resolution, continuous spectral data enables unprecedented global-scale monitoring of PFT distribution and diversity over space and time. This capability provides vital insights into marine ecosystem responses to climate change, and supports improved assessments of marine biodiversity dynamics.

3.4.2 Inventory of existing algorithms: innovations and improvements to multispectral methods

PFT retrieval approaches broadly fall into two categories: abundance-based methods, where assignments are made based on empirical relationships to geophysical retrievals (e.g., a_{ph} or CHL concentration), and spectra-based methods that explore assignment through unique optical signatures of the target classifications (see Bracher, Bouman, et al., 2017; Mouw et al., 2017 for a thorough review). The focus here is to highlight how hyperspectral remote sensing surpasses multispectral systems in distinguishing PFTs due to higher spectral resolution and continuous bands, enabling more accurate detection (CEOS, 2018; Vandermeulen et al., 2017; Wolanin et al., 2016). The two categorizations are not discussed in detail, and traditional band ratio methods and phytoplankton abundance-based empirical models are excluded, as they rely on a few or limited spectral bands and are not capable of leveraging the full potential of hyperspectral radiometry. All algorithms discussed below are designed specifically for hyperspectral remote sensing, utilizing continuous spectral information to extract PFTs.

While hyperspectral remote sensing offers a promising avenue for overcoming limitations with multispectral retrievals, the historical scarcity of spaceborne hyperspectral missions has meant that most hyperspectral PFT algorithms have been developed from in situ hyperspectral R_{rs} data, with only a few subsequently applied to hyperspectral satellite data. In situ-based approaches include inversions via bio-optical modelling (e.g., Gege, 1998; Isada et al., 2015; Marie et al., 2025); cluster analysis of derivative spectra (e.g., Torrecilla et al., 2011; Xi et al., 2015); and statistical decomposition or spectral-fitting techniques such as empirical orthogonal functions (EOF), principal component analysis (e.g., Bracher et al., 2015; Lange et al., 2020; Taylor et al., 2013; Vishnu et al., 2025), and Gaussian deconvolution (e.g., Chase et al., 2017; Ye et al., 2019). Leveraging advances in AI technology, Zhu et al., 2020 developed a PFT retrieval framework that integrates in situ and simulated hyperspectral R_{rs} through transfer-learning and deep-learning techniques, demonstrating its application with the hyperspectral satellite HICO. Direct applications of hyperspectral satellite data remain rare. Notably, Bracher et al., 2009 applied data from SCIAMACHY, a satellite sensor designed for atmospheric applications (see Chapter 2) and developed the PhytoDOAS method which inverts observed top-of-atmosphere

radiometric signals using DOAS, to retrieve three phytoplankton groups (Bracher, Dinter, et al., 2017; Bracher et al., 2009; Sadeghi et al., 2012). This was done by accounting simultaneously for atmospheric and surface effects. Besides these applications, until today, only few of the other above-mentioned methods have been applied to hyperspectral satellite data: HICO (Zhu et al., 2020), DESIS (Bracher et al., 2021 and Bracher et al., 2025, respectively, using the Water Colour Simulator, WASI, by Gege, 2014 and PACE (operational processing using EOF-based algorithm of Lange et al., 2020).

3.4.3 Limitations and challenges associated with current algorithms or applications

A pervasive challenge in remote sensing of PFTs is the scarcity of concurrent in situ PFT measurements and hyperspectral optical data for algorithm training and validation (Dierssen et al., 2023). This data scarcity severely limits algorithm development and accuracy, as existing datasets are often sparse and regionally biased. This critical lack of hyperspectral $R_{rs}(\lambda)$-PFT matchups also directly hinders both validation and performance assessment of the remotely sensed PFT products. While major optical databases (e.g., SeaBASS) archive AOPs, they typically lack associated PFT measurements, although this has been widely acknowledged and is starting to change in recent years. Furthermore, global hyperspectral IOP collections (e.g., NOMAD; GLORIA, Lehmann et al., 2023; Valente et al., 2022) remain similarly limited, as they are often providing absorption data only, with backscattering properties sparse across wavelengths. Compounding these issues, spatiotemporal mismatches between satellite / airborne hyperspectral acquisitions and in situ PFT observations (e.g., from HPLC analysis) introduce significant validation uncertainties (Soppa et al., 2017).

Current satellite PFT classification faces constraints from excessive reliance on HPLC-based methods. While effective for distinguishing phylum-level classes, this approach inherently limits finer taxonomic resolution, precluding differentiation of subgroups or genera. This dependency on pigment proxies (HPLC / CHEMTAX) introduces critical calibration / validation uncertainties. Shared pigments across multiple phytoplankton groups generate ambiguous PFT assignments (Bracher, Bouman, et al., 2017; Catlett and Siegel, 2018), while treating HPLC as "ground truth" obscures algorithm biases for taxa with overlapping pigment suites. Issues with spatial representation arise when discrete bottle samples inadequately capture satellite pixel-scale variability. Emerging solutions integrate HPLC with hyperspectral fluorescence (Ilić et al., 2023), cellular morphology via imaging flow cytometry (Cetinić et al., 2024; Chase et al., 2022), and holographic quantification (Walcutt et al., 2020), complemented by ML techniques that correlate optical signatures with PFT composition to reduce chemical dependency (Orenstein et al., 2022). Ultimately, robust PFT databases require holistic integration of satellite observations, autonomous in situ sensors, and targeted chemical analyses (Catlett et al., 2023; IOCCG, 2018).

Retrieving multiple PFTs from a single hyperspectral spectrum remains an ill-posed problem in many situations, leading to spectral unmixing issues (see also subchapter 3.1). Even with 100+ bands, the ocean colour signal has limited independent information due to broad overlapping absorption features and the influence of external factors (sun angle, viewing geometry, etc.). As Bracher et al., 2022 emphasize, reliance on limited spectral indices creates significant inversion uncertainties, often yielding non-unique solutions where different PFT combinations can fit the same spectrum within error bounds. This instability is compounded by poor algorithm generalization. Methods optimized for specific regions or seasons frequently

fail when transferred to new environments due to shifting optical-PFT relationships. Coastal waters present particular difficulties, where sediment scattering and CDOM absorption mask phytoplankton signatures (hyperspectral algorithms may struggle to detect diatom blooms in turbid river plumes, for example). Addressing these issues requires incorporating ecological constraints (e.g., temperature-driven PFT covariance or competitive exclusion principles) to reduce solution space ambiguity, alongside multi-source data fusion to enhance unmixing robustness. Critical unmet needs include developing algorithms that are resilient across diverse OWTs and extreme conditions (e.g., highly sediment-laden waters or mixed blooms) to ensure reliable performance beyond localized calibration domains.

Finally, a fundamental challenge persists in deciphering PFT spectral fingerprints. It remains difficult to isolate the specific spectral signatures of individual PFTs from the confounding influences of CHL concentration, pigment composition, and environmental factors, particularly within mixed communities where multiple PFTs contribute similarly to the overall signal. While Bi et al., 2023 advanced understanding by modelling how specific absorption coefficients and environmental parameters (e.g., temperature, light) affect optical properties, key gaps remain. These include quantifying the impact of cell morphology on backscattering spectra, which lacks validation for complex in situ communities. Proposed concepts like the Spectral Diversity Index (SDI) for PFT classification (CEOS, 2018), although integrating hyperspectral and pigment data, suffer from limitations such as non-open-source algorithms and lack of independent validation.

3.4.4 New and improved applications

Hyperspectral data for PFT retrievals has a wide range of applications across various domains. Hyperspectral retrieval of PFTs enhances the accuracy of carbon export estimates by providing detailed information on phytoplankton community composition, which is essential for validating carbon output models. Related, early warnings of cyanobacterial blooms are now possible due to the detailed spectral signatures captured by hyperspectral instruments. Hyperspectral data could become instrumental in identifying HAB species, aiding in both early detection and spatial distribution mapping (see subchapter 3.7). This application is crucial for environmental protection and public health.

Beyond community succession, hyperspectral retrieval of PFTs offers valuable insights into how phytoplankton communities respond to broader environmental changes, including climate shifts. While they did not consider hyperspectral data, studies like Alvain et al., 2008; Konik et al., 2025; Soppa et al., 2016 illustrated how long-term records on phytoplankton composition can provide essential data on phytoplankton response to climate change, contributing significantly to ongoing climate change research. These retrievals also play roles in fisheries resource management, as accurate identification of spawning grounds is essential for sustainable fisheries management.

Finally, future ecosystem models are expected to assimilate hyperspectral retrieval of PFTs routinely, which will significantly improve their accuracy and predictive power. Near-real-time community composition enables improved simulation of food web dynamics and biogeochemical processes (e.g., carbon export, nitrogen fixation). A key advancement involves incorporating optical tracers (i.e., simulating phytoplankton spectral properties alongside biomass) for direct satellite data comparison. This advancement facilitates refined climate change scenario testing, such as assessing how observed community shifts impact carbon sequestration, thereby informing policy discussions.

3.4.5 Progress towards addressing new science questions

Improved PFT retrievals from hyperspectral radiometry offer a number of potential advantages and advancements. Related to marine biodiversity monitoring, advanced global detection of phytoplankton diversity, including harmful algal blooms, will offer new insights into ecosystem structure and dynamics. High spectral resolution also allows for more accurate tracking of phytoplankton community shifts over time, supporting the identification of seasonal or event-driven successions, as well as long-term changes in response to nutrient regimes, or ocean stratification. In addition, as various PFTs contribute differently to carbon export, advanced observations should improve quantification of the biological carbon pump, thereby enhancing global carbon budget assessments and coupled physical-biogeochemical and climate model accuracy. By better resolving the functional types of phytoplankton, hyperspectral remote sensing facilitates more accurate estimation of carbon fixation, nutrient uptake, and export production associated with different assemblages, thus improving marine carbon cycle models and strengthening our understanding of phytoplankton roles in climate regulation and feedback mechanisms. It also better informs operational applications such as water quality assessment and fisheries management, which requires evidence-based decision-making at local to global scales.

3.4.5.1 New science questions

The following emergent science questions specifically related to advancing PFT retrievals were identified:

- Can the spectral complexity derived from hyperspectral data be used to infer ecological biodiversity indices, and how do these indices vary geographically and temporally in relation to environmental gradients?
- Is there a quantifiable relationship between spectral diversity (e.g., richness of optical signatures) and phytoplankton community diversity, and can this relationship reveal novel microbial biogeographic patterns or previously undetected bloom dynamics?
- Could hyperspectral remote sensing enable the detection of previously unknown phytoplankton adaptations or rare bloom events that were not observable with traditional multispectral sensors?
- How can high-resolution PFT data derived from hyperspectral observations be integrated into monitoring frameworks for achieving Sustainable Development Goals (SDGs), such as SDG 13 (Climate Action) and SDG 14 (Life Below Water)?
- In what ways can hyperspectral PFT products enhance marine hazard early warning systems, for example, detecting harmful algal species near aquaculture zones, and how can these services be operationalized for coastal resource management?
- How can hyperspectral ocean colour data contribute to the development of *Digital Twins of the Ocean*, and what new insights into real-time ecosystem state and function can be gained by integrating PFT distributions into such models?

3.4.6 Perspectives

We identified the following gaps and/or activities which, if addressed and pursued, would advance the retrieval and performance assessment of PFT products:

- Establish standardized, comprehensive bio-optical and PFT databases. A robust data foundation is essential. This includes matched datasets of hyperspectral $R_{rs}(\lambda)$, IOPs,

and phytoplankton composition (via HPLC pigments, microscopy, flow cytometry, or genomics). Expanding and harmonizing repositories such as SeaBASS, particularly with contributions from under-sampled regions using autonomous platforms. Global coordination (e.g., via IOCCG or OBIS) and standard protocols for co-locating optical and biological measurements are also needed (Cetinić et al., 2024; Dierssen et al., 2020).

- ❖ Perform algorithm inter-comparison and validation across diverse waters. Systematic comparison of retrieval algorithms (empirical, semi-analytical, ML-based) on shared datasets will help identify strengths and weaknesses. Validation using independent in situ observations should include a range of water types and provide uncertainty estimates for each PFT product, an often missing but essential component for scientific and operational use.
- ❖ Enhance multi-sensor and multi-source integration. Combining hyperspectral data with multispectral and active sensors can improve spatial, spectral, and temporal resolution. Integrating model outputs and in situ data into retrieval workflows can further constrain and stabilize algorithm performance.
- ❖ Advance AI and analytical tools for bio-optical applications. Machine learning holds great promise, particularly when incorporating uncertainty quantification, explainable AI, and active learning. Hybrid models combining hyperspectral data with environmental variables (e.g., SST, PAR) can enhance ecological interpretation. Investment in computational infrastructure is needed to support these advanced approaches.

3.5 Phytoplankton Carbon

3.5.1 Societal application and user needs

Phytoplankton carbon (C_{phyto}; mg/m^3) refers to the fraction of the POC pool associated with living phytoplankton cells only. This pool is estimated to be around 0.78-1.0 Gt C in size (Falkowski et al., 1998; Sathyendranath et al., 2020) and has a key role in governing major processes in the ocean carbon cycle and in supplying energy to higher trophic levels. Knowing the concentration of C_{phyto} in the ocean, and how it varies spatially and temporally, is important to achieving more accurate estimates of primary production (Behrenfeld et al., 2005; Sathyendranath et al., 2009). Specifically, C_{phyto} enables improved assessments of CHL-to-carbon ratios (Sathyendranath et al., 2020), determinations of phytoplankton growth and loss rates (Behrenfeld and Boss, 2014; Sathyendranath et al., 2009), evaluations of the impact of photo-physiology on phytoplankton biomass changes (Bellacicco et al., 2016), and biomass changes in response to climate stress (Li, Organelli, et al., 2024).

3.5.2 Inventory of existing algorithms: innovations and improvements to multispectral methods

Since 2005, the remote sensing community has developed several algorithms to estimate C_{phyto} from multispectral satellite-derived ocean-colour observations. No existing algorithm directly infers C_{phyto} from $R_{rs}(\lambda)$, rather they exploit $R_{rs}(\lambda)$-derived products such as CHL and IOPs with various assumptions to describe co-variation with POC or size (e.g., PSDs, PFTs, or phytoplankton size classes). This array of paths to C_{phyto} has thus generated a variety of algorithms that can be broadly grouped into five main classes (Brewin et al., 2021):

1. **CHL-based empirical relationships** (Maranon et al., 2014; Sathyendranath et al., 2009). In these approaches phytoplankton CHL is used as an unambiguous measure for phyto-

plankton concentration. In Sathyendranath et al., 2009, because POC varied as a function of CHL, the minimum POC associated with a given CHL concentration returned the fraction of phytoplankton carbon biomass.

2. **Particle backscattering-based empirical approaches** (Behrenfeld et al., 2005; Bellacicco et al., 2016, 2018, 2020; Graff et al., 2015; Martínez-Vicente et al., 2013; Yang et al., 2024). In these approaches, the particulate optical backscattering is used since it is directly correlated to particle concentration and size (Organelli et al., 2018; Stramski et al., 2004) and widely applied as a proxy of POC. However, to infer C_{phyto}, the fraction of backscattering associated with NAP ($b_bNAP(\lambda)$) must be estimated first from the backscattering vs CHL relationships, then removed from the total particle backscattering, and finally converted to C_{phyto} through lab-tested scaling factors. Starting from considering $b_bNAP(\lambda)$ as a constant value across all the oceans, later studies and algorithms have demonstrated the spatial, temporal and depth variability of $b_bNAP(\lambda)$ in the global ocean (e.g., Bellacicco et al., 2019) and how this was helping to improve the accuracy of C_{phyto} retrievals (Bellacicco et al., 2020). Latest improvements target the use of photoacclimation models to better estimate $b_bNAP(\lambda)$ in subtropical oligotrophic regions (Yang et al., 2024).
3. **Particle-backscattering-based allometric semi-analytical models** (Kostadinov et al., 2009, 2016, 2023). These approaches attempt partitioning C_{phyto} into three different size classes (pico-, nano-, and micro-phytoplankton). Based on PSD derived from spectrally-resolved optical backscattering, the associated volume is converted to carbon concentration using allometric relationships that link the cellular carbon content to the cellular volume.
4. **Absorption-based allometric semi-analytical models** (Roy et al., 2017). Similarly to those based on particle optical backscattering, this semi-analytical model retrieves C_{phyto} partitioned in the three phytoplankton size classes. The model infers the phytoplankton size spectrum from the phytoplankton absorption coefficient at 676 nm (Roy et al., 2013), which is then related to carbon and CHL:C ratio using allometric relationships.
5. **Photoacclimation-based models** (Sathyendranath et al., 2020). Currently, the only existing approach computes C_{phyto} from the CHL:C ratio which varies as a function of the photoacclimation status of the phytoplankton community in response to PAR within the mixed layer through daylight hours. The satellite-derived CHL is divided by the model derived CHL:C ratio to estimate the phytoplankton carbon biomass.

Though each algorithm has been provided with its own performances against in situ data, major inter-comparison exercises have not been conducted or are currently underway. Bellacicco et al., 2020 inter-compared various particle backscattering-based empirical algorithms globally and found 24% as the best error in predictions. CHL-based empirical approaches show high correlations with in situ data. However, the lack of large in situ datasets of C_{phyto} is limiting algorithm improvements as well as uncertainty characterization. In the review by Brewin et al., 2023 (their Table 5) major priorities, challenges, gaps, and opportunities for improving C_{phyto} detection from space have been identified. However, the authors have not highlighted the role that hyperspectral remote sensing of ocean colour may have for C_{phyto} retrievals. At the time of writing, there are few, if any, published attempts to derive C_{phyto} from hyperspectral R_{rs} or derived products. Only particle-backscattering-based allometric semi-analytical models exploit spectrally-resolved optical properties, while the majority of available algorithms use particle optical backscattering or phytoplankton light absorption coefficients at a single band, in blue and red light.

3.5.3 Limitations and challenges associated with current algorithms or applications

This section describes the major challenges with C_{phyto} retrievals with the experience gained from multispectral remote sensing, as well as limitations for moving to hyperspectral ocean-colour-based applications.

The detection of C_{phyto} from space is difficult because field data to develop and validate algorithms are scarce and biased towards the picophytoplankton size class (see Martínez-Vicente et al., 2017). Several lab-based methodologies can be used (see Brewin et al., 2023 for details), but their outputs are not yet standardized. In addition, such measurements are rarely coupled with in situ IOPs and AOPs, which further limits new developments. Difficulties also arise when lab-based scaling factors and photoacclimation parameters are needed to convert observations to C_{phyto}. The scientific community has rarely invested in increasing these fundamental sets of parameters which should help substantially to improve retrieval performances at both global and regional scales. Nonetheless, the use of these limited in situ data and parameters, together with light availability and temperature, has shown promising results for advancing the estimation of C_{phyto}, including in historically challenging areas such as the mid-ocean oligotrophic gyres (Yang et al., 2024).

Despite demonstration of phytoplankton as a major source of optical backscattering at both single and multiple wavelengths (e.g., Organelli et al., 2018, 2020; Poulin et al., 2018), partitioning of living versus non-living fractions of particles in optical backscattering is unresolved. Across the Atlantic Meridional Transect, Organelli et al., 2020 found that the relative contribution of eukaryotic phytoplankton to the total pool of particles with size above 1 µm may vary by an order of magnitude, from 10% to 100% above the deep CHL maximum. The same authors also found that spectrally resolved optical backscattering significantly varies with the ratio of cyanobacteria to eukaryotic phytoplankton, and with light absorption coefficients. This suggests that hyperspectral remote sensing, and combinations of optical backscattering and absorption properties, might help disentangle the contribution of each fraction to backscattering, and thus improve the estimation of $b_bNAP(\lambda)$.

Given the large diversity of phytoplankton composition and particle size distributions, low understanding of how optical properties link to C_{phyto} also limits retrievals. Current C_{phyto} inversion approaches make use of single indicators of size and composition based on a single slope describing the whole community (Kostadinov et al., 2009, 2016; Roy et al., 2017), which strongly misrepresents the phytoplankton and particle size distribution in several oceanic waters (e.g., Organelli et al., 2020).

3.5.4 New and improved applications

Hyperspectral remote sensing could improve the accuracy of C_{phyto} retrievals and how these are linked with ecosystem structure and physiological status. Improved C_{phyto} could yield a more accurate estimate of primary production, and improve the evaluation of the ocean carbon budget, as hyperspectral imagery might better partition C_{phyto} into size classes and populations, and differentiate the contributions of NAP and photoacclimation. The possibility to better assign C_{phyto} to various phytoplankton communities will also improve evaluation of their carbon biomass (Li, Shen, et al., 2024).

Advanced retrievals of C_{phyto} could enable improved assessment and monitoring of ocean health. C_{phyto} retrievals provide a more robust proxy than CHL concentration for studying stress of algal blooms; changes in community composition in response to extreme weather

events; and cascading impacts to zooplankton (Li, Organelli, et al., 2024). C_{phyto} may also yield further assessment of long-term changes in phytoplankton biomass, including assessing current desertification trends in the ocean (Volta et al., 2025).

3.5.5 Progress towards addressing new science questions

The use of hyperspectral satellite missions to retrieve C_{phyto}, especially if partitioned into phytoplankton size classes and groups, will be highly relevant to better quantify the biological carbon pump in the ocean, and to understand the role biology plays in driving the carbon cycle and related processes. In addition, ecosystem modelling would gain mechanistic capability in describing ecosystem functioning and predicting biogeochemical quantities, including under climate change scenarios.

3.5.5.1 New science questions

The following emergent science questions specifically related to advancing phytoplankton carbon retrievals were identified:

- Can we better understand and monitor ocean health, scale up from phytoplankton to higher trophic levels, and aim towards improved ecosystem management of living resources (e.g., fisheries)?
- Can onset and evolution of harmful algal blooms be better identified and monitored?
- What is the role of multiple climatic stressors (i.e., compound events) on phytoplankton carbon biomass? How does C_{phyto} vary? What is the impact on primary production, export production, export efficiency and ocean carbon budget?
- What is the dependence between phytoplankton carbon biomass, primary production, phytoplankton diversity, particle remineralization, and dissolved organic matter? Does phytoplankton biomass production have a direct role in generating recalcitrant dissolved material?
- Can we understand more about phytoplankton growth and losses of the different size classes and functional types starting from refined measurements of C_{phyto} estimates?

3.5.6 Perspectives

We identified the following gaps and/or activities which, if addressed and pursued, would advance the retrieval and performance assessment of phytoplankton carbon products:

- Improved understanding of how optical properties, particle community composition and phytoplankton physiological status are related to phytoplankton carbon will improve retrieval quality.
- Enlarged in situ datasets with simultaneous hyperspectral optical properties, phytoplankton structure and carbon measurements across different water types and trophic status would further enable algorithm development and performance assessments.
- Improved modelling would support disentangling the contribution of NAP to total backscattering coefficients by exploiting combinations of spectrally-resolved backscattering and absorption properties.
- Developing synergies with AI, ecosystem modelling and autonomous platforms will improve the retrieval of phytoplankton carbon from hyperspectral ocean colour observations and expand its use for ecological and climate-related applications.

3.6 Photophysiology and primary production

3.6.1 Societal application and user needs

Primary production, driven by photosynthetic organisms such as phytoplankton, forms the base of aquatic food webs. Understanding phytoplankton physiology (e.g., nutrient uptake rates, photosynthetic efficiency, temperature adaptation) is, therefore, key to predicting ecosystem productivity and biodiversity. Physiological traits determine how species respond to environmental stressors, affecting fisheries, marine mammals, and global carbon cycling. As marine primary producers sequester approximately 50% of Earth's atmospheric CO_2 via the *biological pump*, their physiological responses to warming, acidification, and light availability directly influence carbon export to the deep ocean. Changes in physiology (e.g., altered growth rates or nutrient requirements) can disrupt this pump, accelerating or mitigating climate change. Studying marine physiology and primary production is vital to safeguarding biodiversity, climate stability, and human livelihoods. Remote sensing bridges scales, offering unparalleled insights into how physiological processes drive global ocean productivity, and how they are being reshaped by a changing planet.

3.6.2 Inventory of existing algorithms: innovations and improvements to multi-spectral methods

Multiple models have been developed to retrieve PP from (multispectral) ocean colour radiometry (e.g., Antoine and Morel, 1996; Arrigo et al., 2008; Behrenfeld and Falkowski, 1997; Sathyendranath et al., 1995; see also overview by Carr et al., 2006; Sathyendranath et al., 2020; Westberry et al., 2023). In general, there are three primary modelling strategies (Lee et al., 2014). The first is CHL-based, in which the vertically generalized production model (VGPM) (Behrenfeld and Falkowski, 1997) has been one of the most applied models to estimate PP from satellite ocean colour remote sensing. This kind of model's key input is CHL concentration. It is easy to implement and provides a comprehensive overview of spatio-temporal variations on both regional and global scales in the era of multi-band satellites. Its future application to hyperspectral satellite data may enhance the model's performance, as hyperspectral data is expected to lead to more accurate CHL derivation. The other two are based on phytoplankton absorption coefficients (Antoine and Morel, 1996; Hirawake et al., 2011; Lee et al., 1996, 2011) and or phytoplankton carbon (Behrenfeld et al., 2005; Westberry et al., 2008), where the former is termed as an absorption-based model (AbPM) and the latter termed as carbon-based model (CbPM). Both have already demonstrated their value by producing insightful results with multi-band satellite data (Behrenfeld et al., 2006; Bisson et al., 2022; Hirawake et al., 2011; Lee et al., 1996, 2011, 2015; Song et al., 2023). While the CbPM is fundamentally CHL-driven (Song et al., 2024; also see subchapter 3.7), the AbPM utilizes a scheme centered on the spectral information of phytoplankton absorption coefficients (Lee et al., 2014). Thus, models like AbPM are directly applicable to hyperspectral satellite data, and the use of hyperspectral phytoplankton absorption coefficients as input will certainly enhance their performance.

In addition to phytoplankton absorption coefficients, models like AbPM involve a key photo-physiological property, maximum quantum yield (ϕ_m; C (mol photons)$^{-1}$), which indicates phytoplankton photosynthetic efficiency. Variations of this property depend on environmental factors such as nutrients, light, and temperature (Wozniak et al., 2002). Zoffoli et al., 2018 optimized the relationship between ϕ_m and SST using data from two long-term observation stations, HOT (Hawaii Ocean Time-Series) and BATS (Bermuda Atlantic Time-series

Study). A relationship between ϕ_{m} and the absorption coefficient ratio ($a_{ph}(435)/a_{ph}(676)$) of different-sized (micro, nano, pico) phytoplankton has also been established experimentally (Deng et al., 2022; Xie et al., 2015). The combination of these SST- and absorption-dependent empirical functions will improve the estimation of ϕ_{m} from hyperspectral satellite data, especially since the absorption-based function can be largely refined with input of hyperspectral data, thereby facilitating the subsequent derivation of primary production using models like the AbPM.

While it has not been established to directly measure the absolute ϕ_{m} from space, its relative variability can be monitored using satellite CHL fluorescence (Behrenfeld et al., 2009; Hu et al., 2022). A low fluorescence yield indicates high photochemical efficiency (i.e., quantum yield is near its theoretical maximum), while a high fluorescence yield indicates physiological stress and a lower photochemical quantum yield. This provides a foundation for the CbPM and similar models, as their parameterization is sensitive to the same physiological changes that affect quantum yield.

The sun-induced fluorescence (SIF) of CHL near 685 nm is often a prominent feature in high spectral resolution reflectance data. Just like absorption features, this signal has been used for decades to derive CHL (Neville and Gower, 1977). However, SIF is strongly dependent on the physiological state and photosynthetic activity of the phytoplankton, namely the fraction of absorbed photons that are supplied to photosynthetic conversion, heat dissipation or fluorescence emission (Gupana et al., 2021 and references therein). This property can make the derivation of CHL based on SIF inconsistent, especially if the phytoplankton are increasingly engaged in non-photochemical quenching under increasing light intensity (Gupana et al., 2022; Morrison, 2003). SIF algorithms such as Fluorescence Line Height (FLH; Letelier and Abbott, 1996) or Fluorescence Peak Height (FPH; Kritten et al., 2020) can be used with a few spectral bands as available from sensors on MERIS, MODIS or OLCI. In principle the algorithm can be extended for application to hyperspectral satellite data. Various inversion methods using the Level-1 data of atmospheric sensors have also targeted SIF retrievals. Here, e.g., the DOAS technique has been applied to hyperspectral (<1 nm spectral resolution) top of atmosphere reflectances from SCIAMACHY (Wolanin et al., 2015), which directly accounts for atmospheric effects and is more flexible in retrieving SIF with variations to maximum peak height. Similar methods have been developed for the follow-up mission sensors GOME-2 and TROPOMI to SCIAMACHY (Joiner et al., 2016; Köhler et al., 2020).

In addition, CHL and $a_{ph}(\lambda)$ retrievals register changes in intracellular pigmentation originating from light-driven (photoacclimation) and nutrient-driven physiological responses, as well as indicate shifts in phytoplankton community composition. Behrenfeld et al., 2016 proposed a photoacclimation model, showing that the photoacclimation response is an important component of temporal CHL variability across the global ocean. A recent study using this model stressed that, in the center of the South Pacific Subtropical Gyre, photoacclimation alone could not explain the seasonal dynamics of CHL (Lian et al., 2024). Higher surface CHL in anticyclonic eddies than in cyclonic eddies in the subtropical gyres revealed by satellite observations (Dufois et al., 2016) were also suggested to be due to photoacclimation (He et al., 2021).

3.6.3 Limitations and challenges associated with current algorithms or applications

To evaluate and compare the performance of various PP models, a series of round-robin experiments have been conducted (Campbell et al., 2002; Carr et al., 2006; Friedrichs et al., 2009). Early findings showed that 10 out of 12 model estimates fell within a factor of two of in situ PP data (Campbell et al., 2002). Notably, none of the models successfully captured a broad-scale shift in the tropical Pacific, which went from low biomass-normalized productivity in the 1980s to higher values in the 1990s (Friedrichs et al., 2009). While current global annual PP estimates from contemporary models have largely converged, this apparent consensus masks substantial discrepancies in individual model performance. When validated against in situ PP measurements, model accuracy varies significantly, underscoring persistent uncertainties in their capacity to predict real-world PP dynamics (Westberry et al., 2023).

Specific to the three PP model strategies, the VGPM has been found to show larger uncertainties than the other two (CbPM and AbPM) in the estimated PP for a specific region and time (e.g. Song et al., 2023). This is because the parameter CHL-specific absorption coefficient, which varies widely, is implicitly embedded in the determination of both CHL and the maximum light-saturated rate of photosynthesis, the two key components of VGPM and many other CHL-based models (Lee and Marra, 2022). On the other hand, based on a sensitivity analysis, the CbPM results were recently found to be driven fundamentally by CHL (Song et al., 2024), rather than by phytoplankton carbon that is calculated from particle backscattering coefficients (Behrenfeld et al., 2005). In the AbPM, the parameterization of ϕ_{m} is unresolved, limiting its application to the global ocean. Current ϕ_{m} models face challenges either due to site dependency or difficulties in accessing input data from satellites.

The radiative transfer based inversion methods applied so far to atmospheric sensors with higher spectral resolution (<1 nm) are limited by their rather large footprints (from 3.5 by 5.5 km for TROPOMI, 30 by 60 km for SCIAMACHY, and 40 by 80 km for GOME-2).

3.6.4 New and improved applications

Hyperspectral IOPs and AOPs, particularly $a_{ph}(\lambda)$, are expected to lower uncertainties in PFT and PP retrievals, as the PFT composition influences the spectrum and magnitude of phytoplankton absorption (e.g., Bricaud et al., 1995; see also subchapter 3.4), and because the photo-physiological properties such as ϕ_{m} are different among PFTs. In addition, hyperspectral data will enable the development of better early warning systems by detecting anomalies in productivity (e.g., harmful algal blooms), thus enabling proactive management. For example, hyperspectral data is critical in identifying harmful algal bloom-forming species such as *Phaeocystis globosa* when a signal around 466 nm is required (Astoreca et al., 2008; Lubac et al., 2008; see also subchapter 3.7).

The limited spectral resolution of multispectral sensors allows only a rudimentary quantification of the SIF signal compared to hyperspectral in situ measurements, since the peak of SIF can shift based on phytoplankton composition and atmospheric conditions (Gupana et al., 2025). Alternatively, the DOAS technique can be applied to higher spectral resolution (<1 nm) data, as available from SCIAMACHY, for example (Wolanin et al., 2015), which directly accounts for atmospheric effects and maintains more flexibility in retrieving SIF with variations to maximum peak height. Similar methods have been developed for GOME-2 and TROPOMI (Joiner et al., 2016; Köhler et al., 2020; Wolanin et al., 2015), however, these atmospheric-type sensors have very large footprints.

3.6.5 Progress towards addressing new science questions

Once hyperspectral IOPs and PFTs are better retrieved using hyperspectral remote sensing data, advanced models of ϕ and PP can be expected. Then, the spatio-temporal variability of carbon-fixation in the global ocean, especially given potential shifts under climate change, will be better understood, owing to potentially more accurate remote sensing PP products. Biogeochemical prediction models can also be enhanced by other hyperspectral satellite retrievals. Knowledge and modelling of ϕ_{m} and fluorescence has additional potential for improvement with the emergence of advanced modelling tools, such as machine learning. These tools should aid the inference of spatio-temporal variability of physiological states from space, such as iron limitation in phytoplankton. A better understanding on how environmental factors shape physiological processes may follow, through related improvements in biogeochemical models and identification of regions under physiological stress.

Contiguous bands at high spectral resolution around the red CHL fluorescence peak will enable capturing characteristics of the peak under varying atmospheric conditions, as well as under varying CHL concentrations and phytoplankton taxonomic compositions. Advanced photophysiological products for aquatic ecosystems require accurate retrievals of spectral CHL absorption, plankton taxonomy, SIF and spectral diffuse attenuation. Simultaneous observations of these parameters could facilitate advanced modelling of gross aquatic PP with improved parameterization of photoadaptation, in particular non-photochemical quenching (Cesana et al., 2021), and specific phytoplankton communities.

Recent advances in atmospheric trace gas retrievals by Borger et al., 2025 have shown that the DOAS technique can be applied to hyperspectral sensors with larger spectral resolution (~6 nm), which indicates feasibility of application to PACE-OCI and EnMAP. Improved SIF measurements can be expected with the upcoming FLEX-FLORIS low resolution instrument (Coppo et al., 2017), which will collect radiometric measurements from 500 to 677 nm at 2 nm spectral steps, and from 677 to 780 at 0.5-0.65 nm spectral steps over land and aquatic ecosystems at 300 m pixel size. However, the 150 km swath of FLEX limits its revisit time to 27 days, which necessitates that high precision SIF retrievals will likely require synergy with OLCI or OCI SIF retrievals.

3.6.5.1 New science questions

The following emergent science questions specifically related to advancing photophysiology and primary production retrievals were identified:

- Can photoacclimation states and quantum yields of phytoplankton be tracked by quantifying changes in CHL-specific absorption coefficients?
- Can non-photochemical quenching (NPQ) and photoinhibition be tracked by separating signatures of photoprotective pigments (e.g., zeaxanthin, antheraxanthin) from photosynthetic ones (e.g., diadinoxanthin)?
- Can rapid adjustments in pigment composition, light-harvesting complex regulation, and NPQ over diel cycles be tracked by using high-temporal-resolution hyperspectral imaging (e.g., hourly satellite revisits or drone-based systems)?
- What conformational changes in Photosystem II (e.g., closure of reaction centres under high light) can be revealed through shifts in hyperspectral absorption/scattering properties?
- Can export production specific to diatoms, the most important carbon exporter, be retrieved based on estimates of diatom biomass (see subchapter 3.4), production rate,

and physiological state?

- ❖ Can nutrient limitation be inferred from altered pigment composition and photosynthetic light-use efficiency?
- ❖ Can ocean acidification be tracked via altered spectral backscattering to infer shifts in biogenic particle composition, which may be linked to acidification?

3.6.6 Perspectives

Hyperspectral remote sensing is poised to revolutionize our understanding of ocean primary production and photophysiology by bridging scales from molecular pigment dynamics to basin-wide ecosystem processes. We identified the following gaps and/or activities which, if addressed and pursued, would advance the retrieval and performance assessment of photophysiology and primary production products:

- ❖ Enhanced and higher volumes of in situ observations and process-oriented biogeochemical field campaigns that are closely aligned with satellite data will reduce a key bottleneck in algorithm development and performance assessments.
- ❖ Leveraging AI tools to improve retrieval algorithms, by identifying the most informative spectral regions for specific physiological processes, and aiding in the optimization of future sensor design would improve retrieval performance.
- ❖ Developing algorithms using hyperspectral data to retrieve photophysiological properties, such as photoacclimation proxies, photosynthetic pigment ratios, and sun-induced CHL fluorescence with its emission spectrum, as well as improving estimates of primary production, would advance the field.

3.7 Harmful Algal Blooms

3.7.1 Societal applications and user needs

Harmful Algal Blooms (HABs) represent a pervasive and escalating global concern, posing significant threats to aquatic ecosystems, human health, and various economic sectors, including aquaculture, seafood safety, and coastal tourism. Fishery agencies and related stakeholders face critical challenges in managing the impacts of HABs. The increasing frequency and intensity of HAB events worldwide, often exacerbated by climate change and anthropogenic nutrient loading, underscore an urgent need for advanced, robust, and precise monitoring and prediction systems. Hyperspectral remote sensing, with its superior spectral resolution, offers a potentially transformative solution by enabling the detailed analysis of unique spectral signatures associated with different algal species and water constituents. Consideration of the full visible spectrum, for example, provides an opportunity to improve distinction between harmful and non-harmful algal species, as well as the identification of the specific toxic species or their composition. This is crucial for targeted risk assessment and management, as not all blooms are harmful. The additional information provided by hyperspectral radiometry may also enable quantification of the biomass or cell density of HABs, which is vital for assessing bloom severity and potential toxicity. This information directly informs public health decisions, such as guiding beach and shellfish bed closures or water treatment strategies. Such advanced monitoring from space will aid in determining the spatial extent and temporal variations of HAB outbreaks, as well as facilitate improved forecasting of their occurrence and expansion. The ability to predict HABs days to weeks in advance allows for proactive management, minimizing economic losses in industries like aquaculture and enhancing public safety.

The superior spectral resolution of hyperspectral sensors could enable more detailed analysis of unique spectral signatures associated with different algal species and water constituents, offering new opportunities to improve detection, quantification, and forecasting of HABs.

3.7.2 Inventory of existing algorithms: innovations and improvements to multispectral methods

While remote sensing has made significant strides in HAB monitoring, current algorithmic capabilities with multispectral data remain actively in development. Algorithms for detecting the presence of algal blooms are generally the most common. These often rely on identifying elevated CHL or other pigment-specific spectral features (Ahn and Shanmugam, 2006; Cannizzaro et al., 2008; Hu et al., 2005; Ishizaka et al., 2006; Liu et al., 2022; Noh et al., 2018; Stumpf, 2001). A lingering significant challenge lies in justifying the thresholds used for presence / absence identification. This is because the optical signal of HAB waters is influenced not only by the concentration of other water constituents (CDOM, sediments), but also by species-specific differences in spectral characteristics, both of which make accurate estimation of bloom biomass highly uncertain.

Algorithms for quantifying bloom characteristics, such as biomass or cell density, remain less common than detection algorithms (Baek et al., 2025; Cannizzaro et al., 2008; Gitelson et al., 2007; Kim et al., 2023; Noh et al., 2018). Even fewer efforts have been made to move beyond simple detection towards differentiating or classifying HABs (Hunter et al., 2008; Kim et al., 2016; Kurekin et al., 2014; Shang et al., 2014; Shin et al., 2022; Tao et al., 2017). Except for Gitelson et al., 2007, which relied on field-measured hyperspectral data, the other works largely employed multispectral satellite sensors such as GOCI, MODIS, MERIS, and OLCI. Algorithms using hyperspectral data, for example from HICO or PRISMA, have been developed for the detection of cyanobacteria (Begliomini et al., 2023; O'Shea et al., 2021). More recently, Legleiter et al., 2022 demonstrated the potential for genus-level differentiation of cyanobacteria based on laboratory hyperspectral data.

3.7.3 Limitations and challenges associated with current algorithms or applications

While ongoing research and technological advancements are rapidly transforming known challenges into promising opportunities, several limitations currently hinder full operationalization of HAB monitoring. For example, laboratory studies have demonstrated the potential of hyperspectral radiometry to separate bloom-forming taxa with high accuracy, but extending this capability to natural waters remains constrained by both environmental complexity and biological variability. From an environmental perspective, the measured remote-sensing reflectance represents the bulk effect of overlapping absorption and scattering by water, phytoplankton, CDOM, and NAP. This bulk effect complicates isolation of bloom signals under heterogeneous field conditions, especially in the presence of sensor noise or imperfect atmospheric correction. From a biological perspective, harmful algal species often share broadly similar pigment suites with non-harmful taxa, so absorption spectra alone rarely enable reliable species-level discrimination. Although minor pigment differences can introduce measurable variability, such features are easily confounded in natural waters where phytoplankton co-occur with CDOM and NAP. Scattering and backscattering, influenced by cell size, morphology, and intracellular structure, may, in principle, provide additional separability, but in practice these signals are weak and strongly affected by non-phytoplankton constituents.

Systematic species-specific IOP datasets remain sparse, and their acquisition still requires specialized instruments and controlled measurements both in situ and in the laboratory.

Validation of remote sensing-based HAB detection and quantification algorithms remains particularly challenging. Unlike standard CHL retrievals, which can often be evaluated against relatively abundant in situ measurements, HAB validation requires coincident observations under far more restrictive conditions. In practice, researchers must first locate an active bloom, then obtain samples during favourable weather and within the narrow time window of satellite or airborne overpasses. Even under such circumstances, ensuring that field samples and remote-sensing pixels correspond spatially and temporally is difficult, as HABs are typically patchy, small in scale, and highly dynamic in both species composition and biomass. Vertical heterogeneity of the water column further complicates comparisons, while logistical constraints such as vessel drift and sensor instability add additional uncertainty. These limitations mean that even hyperspectral measurements collected directly above the water surface may not perfectly align with the water actually sampled. As a result, the scarcity of rigorous matchup datasets significantly constrains algorithm development and evaluation, underscoring the need for coordinated field campaigns and standardized validation protocols tailored specifically to HAB monitoring.

3.7.4 New and improved applications

3.7.4.1 Improved Quantification

Hyperspectral data provides better correction for non-algal contributions in water. Hyperspectral sensors, with their many narrow bands, can better resolve the distinct absorption and scattering characteristics of these different components, allowing for more accurate removal of their influence and, thus, a more precise estimation of algal biomass (Dall'Olmo and Gitelson, 2005; Mishra and Mishra, 2012).

Hyperspectral measurements provide better capacity to account for atmospheric variability. Atmospheric conditions (e.g., cloud cover, aerosols) significantly impact the quality of remote sensing data, leading to data gaps and inaccuracies. Accurate retrieval of water-leaving radiance from satellite data, especially in optically complex waters, is challenging due to aerosol concentrations. Variants of the atmospheric correction algorithm Polymer (Karthick et al., 2024; Soppa et al., 2021; Zhang et al., 2019) leverage hyperspectral data (e.g., using UV and VIS-NIR bands) to more realistically estimate aerosol contributions and improve the accuracy of water-leaving radiance retrievals, even in highly turbid or phytoplankton-dominated waters. This is vital because the water surface is much darker than terrestrial surfaces, making the signal from water easily obscured by the atmosphere.

3.7.4.2 Advanced Species Identification

Studies have successfully used hyperspectral imaging to identify and map the distribution of specific HAB species, such as *Karenia brevis* in the Gulf of Mexico (Cannizzaro et al., 2008), demonstrating its capability to distinguish between different algal species and other water features. Lab-based studies examining 140 hyperspectral images of five bloom-forming cyanobacteria genera (*Microcystis, Planktothrix, Aphanizomenon, Chrysosporum, Dolichospermum*) achieved high classification accuracies (e.g., >95% for *Microcystis* and *Chrysosporum*) using VIS/NIR reflectance and machine learning models (Fournier et al., 2024). This research involved growing cultures under various light and nutrient conditions to mimic natural vari-

ability, and demonstrating the stability of signatures within species. Preliminary results from prototype hyperspectral sensors such as HICO show their ability to accurately capture the detailed spectral features of certain HABs (e.g., *Trichodesmium, Noctiluca*) when the phytoplankton cells aggregate heavily on the water surface. The success of these studies highlights the ability of hyperspectral imagery to resolve subtle spectral differences that are often missed by multispectral sensors.

3.7.4.3 Resolving Vertical Profiles

Remote sensing techniques have historically been limited in monitoring the vertical distribution of HABs due to the optical complexity of inland waters. However, recent academic findings demonstrate significant progress. Hong et al., 2021 successfully applied a deep NN model to drone hyperspectral imagery, combined with in situ measurements and meteorological data, to monitor the vertical distribution of CHL, phycocyanin, and turbidity. This advancement moves beyond surface-level observations, providing crucial insights into the 3D structure of blooms, which is essential for understanding bloom dynamics, toxin distribution, and environmental impacts that are not always evident from the surface.

3.7.5 Progress towards addressing new science questions

Recent studies have taken complementary approaches to address the fundamental challenges of HAB detection and quantification using advanced optical methods. Lomas et al., 2024 developed a comprehensive phytoplankton optical fingerprint library by directly measuring absorption, scattering, backscattering, and hyperspectral reflectance across more than 50 strains, providing a standardized dataset that enables the design and evaluation of next-generation ocean colour algorithms. Similarly, Reynolds and Stramski, 2019 analyzed phytoplankton assemblages in the western Arctic Ocean, demonstrating how community composition influenced inherent optical properties and remote-sensing reflectance, and underscoring the importance of accounting for NAP and CDOM when interpreting bloom signals. Expanding the spectral domain, Zheng et al., 2025 evaluated near-blue and UV R_{rs} from multiple sensors (VIIRS, PACE OCI, and Global Change Observation Mission - Climate (GCOM-C) Second Generation Global Imager(SGLI)), showing that these bands carry valuable information for aerosol correction and phytoplankton / CDOM absorption retrieval, while also highlighting the sensitivity of retrievals to sensor design. Clementson et al., 2022 identified distinct UV-absorption peaks associated with *Trichodesmium spp.* in Great Barrier Reef waters, linking them to mycosporine-like amino acids and demonstrating how such features can both aid discrimination and introduce biases into algorithms that ignore UV absorption. Finally, Deglint et al., 2018 demonstrated the feasibility of classifying six algal taxa using fluorescence-based spectral and morphological features acquired from a custom multispectral imaging microscope. Neural network classifiers achieved the highest accuracy (~96%) when combining fluorescence spectra with morphological traits, significantly outperforming morphology alone. The study highlights the strong potential of fluorescence hyperspectral features for species-level algal discrimination under controlled laboratory conditions. As a contribution towards more open-access spectral reference information for HAB-related algorithm development, a *Nodularia spumigena* bloom in the German Banter See (Lake Bant) was surveyed and documented using a suite of proximal hyperspectral measurements (i.e., reflectance, absorption coefficients, absorbance, fluorescence) combined with identification based on microscopic analyses, DNA extraction and sequencing (Garaba et al., 2023).

3.7.5.1 New science questions

The following emergent science questions specifically related to advancing HAB retrievals were identified:

- Can species-level discrimination of HABs, whether based on absorption, scattering (volume scattering function (VSF), BRDF), or fluorescence, be achieved with current hyperspectral sensors, or will it require instruments with higher sensitivity, finer bandwidths, and optimized spectral placement?
- What level of hyperspectral data precision is required for species-level discrimination of HABs, considering both absolute band uncertainty and relative inter-band accuracy? What in situ IOP observations, instruments, and ancillary measurements are necessary to achieve such precision from raw data?
- How do intra- and interspecific IOPs of HAB-forming taxa differ? How do absorption, scattering, and backscattering behave under high or ultra-high biomass conditions, and can such regimes be accurately reproduced in laboratory experiments? If not, what approaches are needed to translate laboratory IOP measurements into field-representative conditions?
- Can machine learning and (self-)supervised approaches achieve reliable species-level discrimination of HABs when trained on laboratory or in situ hyperspectral and fluorescence measurements, and how transferable are these models to natural, optically complex waters?

3.7.6 Perspectives

Progress on the emerging science questions outlined above would collectively redefine the future of HAB remote sensing. The ability to resolve species-level differences hinges first on building a comprehensive library of species-specific IOPs, which captures both absorption and scattering behaviour under realistic bloom conditions. Achieving this goal requires not only extensive laboratory work but also a clear strategy to ensure that such measurements are transferable to the natural environment, where particle assemblages and community dynamics differ fundamentally from controlled cultures. At the same time, the precision of hyperspectral measurements (both absolute sensitivity and inter-band stability) must reach a level that allows these subtle species-dependent signals to be detected consistently above the background of CDOM, sediments, and atmospheric perturbations. Once such precision is attainable, advanced algorithms can begin to exploit these signatures with confidence, reducing reliance on empirical thresholds. Machine learning approaches offer a path forward, but their promise will only be realized if they are trained on data that capture the diversity of laboratory and in situ conditions, ensuring that classification models remain robust when confronted with the optical complexity of real waters. Addressing these linked challenges will shift HAB monitoring from qualitative bloom detection toward quantitative, species-resolved, and operationally validated products.

If the current science questions are addressed, the outcome would be transformative for end-users. Detection products could distinguish harmful from benign blooms rather than grouping them together; maps could report bloom intensity in meaningful biomass units instead of relative anomalies; and confidence levels could be attached to each detection. In practice, these outcomes would shift satellite monitoring from vague warnings to precise, actionable detection tools, allowing agencies to respond more selectively, aquaculture to prepare more accurately, and coastal managers to act before visible damage occurs.

3.8 Floating Matter

3.8.1 Societal applications and user needs

Both natural and man-made floating matter have been reported in various regions of global oceans, riverine systems, and lakes. These include floating macroalgae (e.g., *Sargassum fluitans/natans, Sargassum horneri, Ulva prolifera, Macrocystis pyrifera, Nereocystis luetkeana*), microalgae scums (*Microcystis*, *Trichodesmium*, *Noctiluca*), marine mucilage (sea snot), brine shrimp eggs, pollens, wracks of floating seagrass or other plants, driftwood, pumice, oil slicks, kelp, foam/whitecaps, plastics, and other non-plastic debris/litter, which can all be detected from space (Fig. 3.1; Garaba and Park, 2024; Park et al., 2021; Qi et al., 2020; Smith and Garaba, 2025).

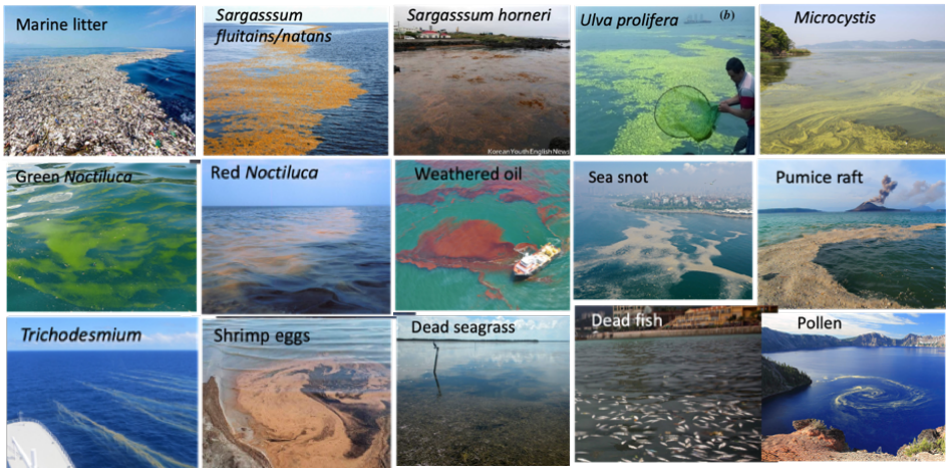

Figure 3.1 The many types of floating matter reported in oceans and lakes. Adapted from Hu, 2025

Remotely-sensed data products of floating matter have wide applications as they are relevant to many interdisciplinary science studies (e.g., management, biodiversity, ocean biology and ecology, nutrient and carbon cycles, fisheries science, turtle migrations) and user-based applications (e.g., response to harmful algal blooms, pollution mitigation, aquaculture, beach management and economic and human health impact). Hyperspectral sensors is expected to improve spectral discrimination, reduce uncertainties in biomass estimates, and provide insights to physiological states of floating vegetation.

3.8.2 Inventory of existing algorithms: innovations and improvements to multi-spectral methods

Nearly all algorithms to retrieve floating matter have been based on multi-band satellite data (MODIS, MERIS, OLCI, VIIRS, MSI, Operational Land Imager (OLI), Landsat, WorldView, GeoEye, PlanetScope, etc.) with one or more of the following steps: detecting image features based on certain indices or through machine learning; discriminating the type of floating matter by analyzing the spectral shape or using a combination of indices; and quantifying floating matter amount by spectral unmixing (Bell et al., 2023; Cózar et al., 2024; Garaba and Park, 2024; Gendall et al., 2023; Hu et al., 2025; Mora-Soto et al., 2024). Some algorithms have been implemented to generate operational data products (e.g., floating algae density) and made available in near real-time, while others have been developed for research. For a certain type of float-

ing matter, four types of data products have been developed: quicklook images; presence / absence thematic maps; density maps; and composite maps (Hu et al., 2025). Some hyperspectral data collected from airborne sensors or other pathfinder sensors (e.g., PRISMA, DESIS, HICO) have been used for demonstration purposes (Bell et al., 2015; Dierssen et al., 2015; Hu, 2022), yet algorithms remain to be developed. Validation of such algorithms / data products often rely on cross-sensor comparisons as well as on limited field data to verify presence / absence. In addition to optical sensors, Synthetic Aperture Radar (SAR) sensors have also been attempted, with variable success (Qi et al., 2022).

In addition to spectral discrimination and new ways to reduce uncertainties, hyperspectral reflectance of floating algae carries new information about plant physiology. For example, it has been shown that differences in several red bands can be used as an index for the C:CHL ratio of giant kelp (Bell et al., 2015). Likewise, McKinna, 2010 showed two different colours of *Trichodesmium*: orange/brown (healthy), and bright green (undergoing pigment leaching and cell lysis) where such subtle changes in colour are difficult to measure with multi-band sensors, but possible with hyperspectral sensors.

3.8.3 Limitations and challenges associated with current algorithms or applications

Largely due to variations in satellite instrument design and performance, it remains challenging to achieve consistency and accuracy in presence / absence detection, where the lower detection limits are inversely proportional to sensor SNR in the NIR bands, and proportional to image pixel size (or spatial resolution). For example, the lower detection limit is 0.5% of the 300-m pixel for OLCI (or 450 m^2), and 2% of the 10-m pixel (or 2 m^2) for MSI (Qi and Hu, 2021). Table 3.1 lists the lower detection limits of several commonly used satellite sensors. These detection limits are not for the size of individual floating mats, but for total floating mats within a pixel. If the integrated size of total floating mats within a pixel is smaller than the detection limit, then the floating mats are simply not detectable.

Table 3.1 Lower detection limits (for presence / absence of signal anomalies) of commonly used satellite sensors, expressed as both sub-pixel macroalgae coverage of pixel size (%) and absolute area coverage (m^2, in parenthesis). Also listed are the SNRs of the sensors' NIR bands (mostly around 750 nm) when measuring the oceans, taken from published literature. Spectral discrimination limits to determine floating matter type are typically 3-4 times higher than the lower detection limits (Qi and Hu, 2021)

Sensor	SNRs (NIR)	Lower detection limit	Satellite(s)
MODIS (250 m)	200	1.0% (625 m^2)	Terra (2000 –) & Aqua (2002 –)
MODIS (1 km)	1000	0.2% (2,000 m^2)	Terra (2000 –) & Aqua (2002 –)
VIIRS (750 m)	400	0.5% (2,800 m^2)	SNPP (2012 –), NOAA20 (2017 –)
OLCI (300 m)	400	0.5% (450 m^2)	Sentinel-3A (2016 –) & 3B (2018 –)
GOCI (500 m)	500	0.4% (1,000 m^2)	COMS (2010 – 2021)
OCI (1.2 km)	630 (865 nm)	0.3% (4,320 m^2)	PACE (2024 –)
OLI (30 m)	40	2.0% (180 m^2)	Landsat-8 (2013 –)
MSI (20 m)	34	2.0% (80 m^2)	Sentinel-2A (2015 –) & 2B (2017 –)

Spectral discrimination of floating matter types remains an ongoing challenge (see subchapters 3.4 and 3.7 for additional context). Most algorithms assume a single type of floating matter in a study region (e.g., *Sargassum fluitans/natans* in the Atlantic Ocean, *Ulva prolifera* in the Yellow Sea, kelp along the Pacific west coast near Alaska / California / British Columbia,

etc.) based on either *a priori* local knowledge or spectral analysis of high-intensity pixels. This is because differences in spectral shapes of floating matter are mostly observed in visible wavelengths as opposed to NIR (with the exception of plastic litter, where the diagnostic bands are in the SWIR), and such differences require higher detection of floating matter beyond presence / absence within a pixel in order to reveal the characteristics of spectral shape. The spectral discrimination limit is often 3-4 times higher than the presence / absence detection limit in order to separate different types of macroalgae (Qi and Hu, 2021; Table 3.1). This limit may be higher for other types of floating matter. In certain cases, it is very difficult, if not impossible, to discriminate types of floating matter because of the lack of specific diagnostic spectral bands. This is particularly true for floating plastic litter, as their spectral signature is in the SWIR (Castagna et al., 2023; Garaba and Dierssen, 2020). Similarly, differentiating *Trichodesmium* surface scum from *Sargassum* mats requires several blue-green spectral bands that are sensitive to the specific pigment absorption of *Trichodesmium*, yet these bands are mostly missing in multispectral sensors.

While not related specifically to hyperspectral radiometry itself, the spatial resolution or temporal revisit times of various satellite platforms inhibits ideal detection of floating matter. Medium-resolution satellite sensors have frequent revisits (1-2 days) but their pixel sizes are too large to detect small-scale features (Table 3.1). Higher-resolution sensors are the opposite: they can capture small patches of floating matter, but they do not have near-daily revisits and they do not cover most open-ocean waters, making it difficult to monitor these fast-changing features.

Nearly all floating matter is spatially patchy and temporally dynamic, making a direct validation using field measurements nearly impossible except for presence / absence validation. It is difficult to co-locate an image pixel with the exact location and timing of the patchy floating matter, and difficult to collect or estimate *all* floating matter from a relatively large area to validate the satellite-derived floating matter quantity. Related to the validation are the uncertainties associated with the submerged fraction of floating matter, which are either underestimated or completely missed because of their exponentially decreased NIR signals with increasing depth (Timmer et al., 2022). How to estimate and correct such uncertainties remains a challenge. Difficulty in masking confusing image features such as cloud shadows, ship wakes, small clouds, and image artifacts, such as striping noise, poses another technical challenge. Specific image processing techniques are required, but it is challenging to maintain an appropriate balance between under-masking these unwanted features and over-masking the real image features caused by floating matter.

Although it is difficult to estimate surface reflectance of pixels containing floating matter due to their unknown contributions to the NIR signals that are used for atmospheric correction, the use of $R_{rs}(\lambda)$ (and therefore a rigorous atmospheric correction) is not necessary. Subtraction of the signal from nearby water pixels is required in order to minimize the impact of background water on the reflectance of mixed pixels covered by both floating matter and water. Such a subtraction serves as an effective atmospheric correction, regardless of whether the input signals are total radiance, total reflectance, or Rayleigh-corrected reflectance, none of which require full atmospheric correction.

3.8.4 New and improved applications

The most significant improvement gained by using hyperspectral sensors is through their capacity to spectrally discriminate floating matter types (e.g., Hu, 2022). Various types of floating

matter often have different spectral shapes (Fig. 3.2) that can be captured entirely by hyperspectral satellite sensors, whereas it is difficult to use multi-band sensors to differentiate these spectral shapes. Fig. 3.2 shows spectral reflectance of many types of floating matter compiled from the literature, many of which have narrow-band features due to specific pigments contained in the floating vegetation, while others have wide-band shapes. Once hyperspectral reflectance over water pixels is derived from satellite measurements, the reflectance can be compared with a spectral dataset through the use of a similarity index or other measure to determine the floating matter type. Of particular importance are the hyperspectral SWIR bands, which may be used to fingerprint plastic litter (Castagna et al., 2023; de Vries et al., 2023; GIZ, 2023; Ohall et al., 2025).

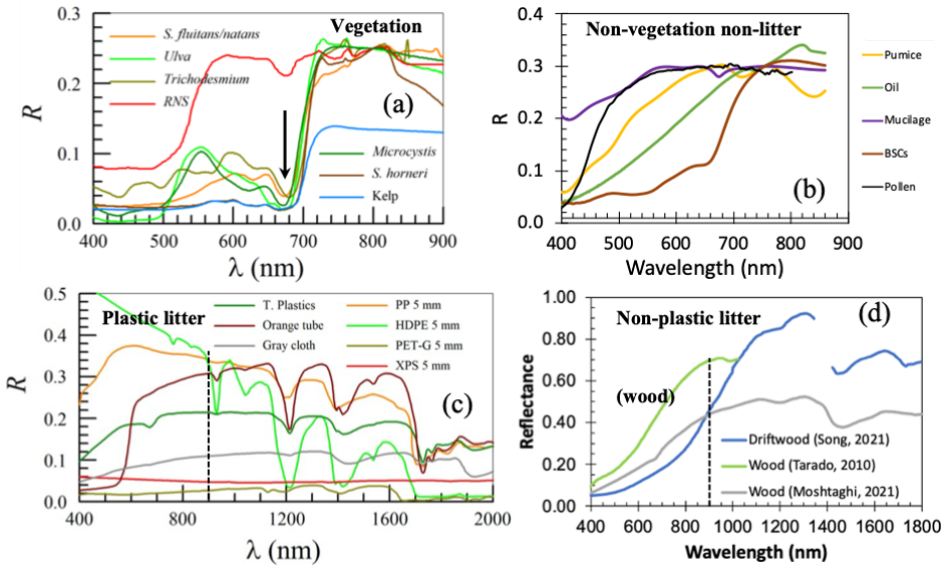

Figure 3.2 Spectral reflectance of various types of floating matter found in natural aquatic environments, compiled from the literature. Adapted from Hu, 2025

3.8.5 Progress towards addressing new science questions

Currently, floating matter submerged in water can cause large uncertainties in their quantitative estimates. This is because the NIR reflectance signal from the submerged matter decreases almost exponentially with increasing depth (Timmer et al., 2022). New indices designed from hyperspectral NIR bands may help reduce such uncertainties since different NIR bands respond to submerged floating matter differently, making a depth-invariant index possible (Hu, 2024). Furthermore, the development of hyperspectral indices, particularly within the visible spectral wavelengths, may enable the quantitative assessment of the physiological status of floating matter, including estimations of nutrient and pigment concentrations (Bell et al., 2015).

3.8.5.1 New science questions

The following emergent science questions specifically related to advancing floating matter retrievals were identified:

- Can all the different types of floating matter be identified?
- How much floating matter exists on the water surface?

- What ecological, environmental, and societal impacts does floating matter have?
- How has floating matter changed over the past decades? What caused such changes and can we predict changes in the future?
- What is the health status of vegetated floating matter?
- How can remote sensing be used to help various stakeholders mitigate adverse impacts caused by large quantities of floating matter in coastal environments?

3.8.6 Perspectives

We identified the following gaps and/or activities which, if addressed and pursued, would advance the retrieval and performance assessment of floating matter products:

- Uncertainties should be assessed through field observations, which provide direct validation of the remote detections of certain floating matter types. However, it is very difficult to quantitatively assess uncertainties in the remotely estimated amounts because of the inherent difficulties in matching field observations with image pixels, as described above.
- Uncertainties should be assessed through the use of spectral signatures of certain types of floating matter (e.g., *Trichodesmium* scums, *Noctiluca* scums, *Sargassum* macroalgae, wood, pollen, floating kelps) for spectral discrimination, and through the use of independent satellite data for cross validation and uncertainty estimates.
- Uncertainties should be assessed through cross-sensor comparisons, especially when using high-resolution sensors to evaluate lower-resolution sensors (e.g., Qi et al., 2023).

3.9 Benthic Mapping

3.9.1 Societal applications and user needs

Benthic habitats are foundational components of marine ecosystems, supporting biodiversity, regulating nutrient cycles, and buffering coastlines. They provide critical ecosystem services, including biodiversity support, fisheries, coastal protection, and carbon sequestration. Benthic habitats such as coral reefs, seagrass meadows, sediment, and macroalgal beds are vital for marine ecosystems and coastal communities.

User needs related to these habitats range from habitat classification and resource management to climate adaptation planning. Scientifically, key questions include understanding how benthic communities change over time, their interaction with environmental drivers, and the ecological consequences of human-induced changes. Systematic monitoring and spatial mapping of these habitats allow us to evaluate marine ecological health, guide conservation and resource management, and assess carbon sequestration and carbon dioxide removal strategies.

Traditional in situ surveys, while accurate, are often limited in spatial extent, expensive, and time-consuming. As a result, remote sensing has become increasingly vital for large-scale and repeated assessments of benthic environments. Among remote sensing techniques, hyperspectral remote sensing stands out for its ability to capture detailed spectral signatures that allow for the discrimination of diverse benthic features, as well as to accurately remove the water column contributions to the total signals. In this section, we outline general topics and include only a few specific references when necessary. For more specific references, see reviews on this topic (e.g. CEOS, 2018; Dekker et al., 2011; Dierssen et al., 2021; Giardino et al., 2019; Kutser et al., 2020; Muller-Karger et al., 2018).

3.9.2 Inventory of existing algorithms: innovations and improvements to multi-spectral methods

Hyperspectral sensors have increasingly been adapted for airborne and spaceborne platforms targeting mapping of aquatic benthic environments. Airborne platforms, such as AVIRIS and PRISM, provide high spatial and spectral resolution, while proposed upcoming spaceborne missions (e.g., SBG and CHIME) promise global coverage at a nominal resolution of 30 m on the ground with routine acquisitions. In support of this, spectral libraries have been developed to catalogue reflectance signatures of various benthic materials – considered *endmembers* for classification purposes (Fig. 3.3). These libraries are essential for both empirical classification and validation of physically-based models. Existing databases include spectral information for corals, seagrasses, macroalgae, and sediment (e.g., clay, sand, rubble). Some of these libraries have been collected in the field to represent natural variability in the benthos and others in more controlled laboratory conditions to ensure consistency. These spectral libraries showed that the current multi-band satellite sensors are unable to capture all diagnostic spectral shapes, which can be characterized well with hyperspectral data collected by satellites.

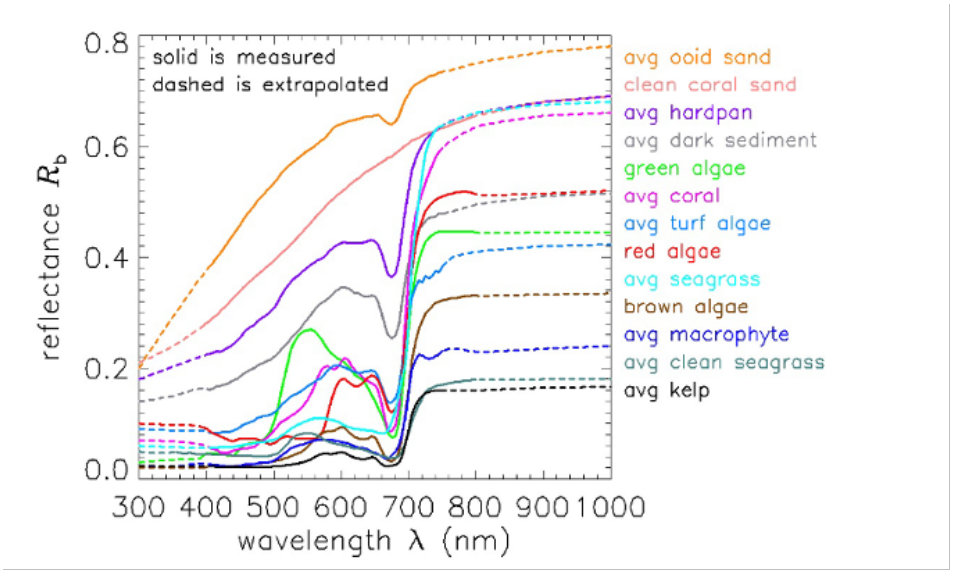

Figure 3.3 Benthic reflectance endmembers provided with the current Hydrolight radiative transfer code. Solid lines are measured; dashed lines are subjective extrapolations. Adapted from Hedley and Mobley, 2021.

Remote sensing has matured to the point where several methodological frameworks are in use for benthic habitat mapping. Forward models simulate expected reflectance by modelling the interaction of light with the sea surface, water column, and benthic surface. Spectrum matching is then conducted to find the spectra that most closely resembles the measured water-leaving reflectance (e.g., Mobley et al., 2005). Inversion models work in reverse by estimating benthic depth, reflectance, and water column optical properties from observed reflectance (e.g., HOPE model, Lee et al., 1998; review of 5 physics based inversion models and one empirical model in Dekker et al., 2011). Several of these models simultaneously incorporate atmospheric components into the inversion or optimization scheme (Thompson et al., 2019). Subchapter 3.1 provides additional details on spectral matching and inverse modelling. Empirical algorithms (such as the Spectral Angle Mapper), derivative-based approaches, ma-

chine learning classifiers, and object-based image analysis, provide tools often based on training data and/or *tuning* to specific images, regions, or environmental conditions (e.g., Kuhwald et al., 2022; Phinn et al., 2012). Hybrid models combine elements of the above to improve performance, reduce uncertainty, and reduce computation time (e.g., Garcia et al., 2020).

Mixed pixels are common because most benthic environments are spatially heterogeneous, especially at moderate spatial resolutions (30 m or coarser). Algorithms can incorporate the fractional composition of different benthic types within a single pixel. Most commonly, inversion models aim to simultaneously derive fractional amounts of a single bottom type versus sediment, like coral, seagrass or macroalgae (e.g., Casal et al., 2012). Some hyperspectral algorithms derive ecological parameters like Leaf Area Index of a seagrass meadow, for example, rather than fractional coverage (Hedley et al., 2017; Hill et al., 2014). Several modelling approaches also offer quantification of uncertainties, allowing users to evaluate confidence in classification outputs (e.g., Hedley et al., 2017). This can be important for applications requiring risk assessment or decision-making, such as marine spatial planning and habitat restoration.

To date, most hyperspectral benthic mapping efforts have targeted coral reefs and seagrass meadows. These ecosystems are ecologically significant, visually distinct, and often located in optically clear waters conducive to remote sensing. However, focus has been expanding to other benthic types such as benthic micro- and macroalgae and rocky substrates.

3.9.3 Limitations and challenges associated with current algorithms or applications

Many challenges exist in image processing for benthic remote sensing. Atmospheric correction over optically shallow water remains challenging due to interference of the shallow bottom to the spectral bands used for atmospheric correction. Water column corrections that account for absorption and scattering effects of the overlying water distort the benthic signal and often require interrogation of nearby deeper water. But, water column optical properties for offsite deep waters may not be representative of the optical properties in nearshore benthic habitats (Russell et al., 2019). Such a correction often requires *a priori* knowledge of bottom depth and/or benthic substrate type. Geometric correction and tidal corrections are critical to align imagery with surface features and to reduce uncertainties in water column corrections, especially in dynamic coastal zones. Spectral smoothing helps reduce noise, which is common to many high spatial resolution images. However, smoothing data may obscure important spectral features, making it difficult to differentiate benthic types.

Even with perfect image processing, many benthic types are not resolvable at the spectral resolution available from satellites. This is particularly true for separating green benthos such as macroalgae and seagrass. The presence of cyanobacterial films at the seafloor can appear identical to red macroalgae (Kutser et al., 2020). Even with higher spectral resolution sensors like MERIS or OLCI, seagrass is not spectrally resolvable from brown macroalgae or grapestone sediment containing bioalgal films (Garcia et al., 2020). Within such uncertainty, spectral unmixing within mixed pixels remains complex.

Inversion models can suffer from long computation times, sensitivity to initial parameters, and the inability to differentiate absorption and scattering from the water column versus that from an optically complex benthic habitat. Hybrid methods often incorporate machine learning approaches to increase efficiency of analytical models.

Another limitation is that existing benthic reflectance measurements are limited in both

scope and dimensionality. Field validation is limited by the scarcity of co-located in situ datasets, especially at the scale of satellite imagery (e.g., 10 m or 30 m resolution).

Future work involves developing better methods to quantify reflectance of canopies (seagrass, kelp, etc.) where vertical structure influences the observed benthic reflectance; assessing three-dimensionality of the benthos with shadows and varying heights (e.g., Hedley et al., 2018); and expanding point measurements to the scale of a pixel. Environmental noise, such as waves, turbidity, and changing solar angles, further complicate interpretation.

3.9.4 New and improved applications

Hyperspectral imagery significantly enhances benthic mapping capabilities compared to multispectral data (Hochberg and Atkinson, 2003; Kutser et al., 2003; O'Neill and Costa, 2013; Vahtmäe et al., 2020). It promises to enable finer discrimination between benthic types and allows for fractional coverage estimates in mixed pixels. The expansion into NIR wavelengths can provide additional information in some optically shallow habitats. New applications include detecting subtle changes in coral health, assessing algal phase shifts and health status, mapping ecosystem productivity, and characterizing habitat heterogeneity. The ability to estimate more accurate bathymetry and water column properties marks a notable advancement.

3.9.5 Progress towards addressing new science questions

Potential upcoming hyperspectral satellite missions, such as NASA SBG and ESA CHIME, aim to provide frequent, high-quality observations with aquatic retrievals at a nominal resolution of 30 m globally. These platforms offer the potential for routine benthic monitoring at large scales. Their high spectral resolution offers the ability to improve habitat classification if the SNRs are sufficiently high. Global spectral coverage will be useful for change detection and long-term trend analysis. Integration with biophysical models may link remote sensing metrics to ecological processes such as primary productivity and biodiversity. Improved geolocation accuracy will further enhance retrieval reliability for trend detection.

3.9.5.1 New science questions

The following emergent science questions specifically related to advancing benthic retrievals were identified:

- Can spectral heterogeneity serve as a reliable proxy for ecological resilience or habitat quality?
- How do photophysiological traits vary across benthic types and water conditions?
- To what extent can early stress indicators, like sedimentation, nutrient loading, bleaching or disease, be detected remotely?
- What are the spectral signatures of functional traits, and how do they relate to ecosystem services?

3.9.6 Perspectives

We identified the following gaps and/or activities which, if addressed and pursued, would advance the retrieval and performance assessment of benthic mapping products

- Data fusion of imagery from a variety of sensors with different spectral and spatial resolutions and with different sensing capabilities should be pursued. This includes pan-sharpening techniques and fusion with acoustic and LiDAR data.

- New and underutilized methods such as polarimetry and its potential for benthic classification should be explored.
- Recent advances in hyperspectral sensor miniaturization, which provide exciting opportunities for observing heterogeneous benthic habitats at high spatial resolution from autonomous platforms (such as drones and submersible vehicles), should be explored to further develop and validate classification and mapping approaches.
- Better techniques for making benthic measurements across spatial scales relevant to remote sensing for both algorithm development and validation are needed.
- Linking benthic reflectance to physiology and ecology of benthic habitats and other ecological metrics (e.g., environmental DNA, or eDNA) is critical.

Chapter 4

Retrieval and Assessment of Water-leaving Reflectance

Jeremy Werdell, Amir Ibrahim, Malik Chami, Astrid Bracher, Heidi Dierssen, Chuanmin Hu

Broadly speaking, multispectral ocean colour radiometers adeptly retrieve bulk aquatic geophysical properties that drive first-order variations in spectral $R_{rs}(\lambda)$, such as concentrations of total CHL, total spectral absorption and backscattering coefficients, and sub-surface light attenuation. Yet, the scientific goals and methodologies that guided such efforts have been superseded by considerably more sophisticated and ambitious research objectives. The composition of phytoplankton communities, for example, affects fisheries productivity, human health, and the effectiveness of carbon and nutrient cycling processes and, therefore, may be potentially more critical to resolve from space than understanding variations in concentrations of CHL or carbon stocks. While remote sensing methods for identifying different phytoplankton groups exist (see, e.g., Bracher, Bouman, et al., 2017; Mouw et al., 2017, Chapter 3.4), these algorithms rely on accurate retrieval of second-order factors that influence ocean colour (e.g., contributions by accessory pigments) and have been shown to benefit from hyperspectral measurements of at least 5-nm resolution (Lee et al., 2007; Vandermeulen et al., 2017; Wolanin et al., 2016). Given the emergence of hyperspectral space-borne assets (see Chapter 2), now is the time to ensure that hyperspectral retrievals of $R_{rs}(\lambda)$ are of the highest possible quality.

In this Chapter, we address the current state-of-the-art of *processes* and *methods* that ultimately produce and evaluate $R_{rs}(\lambda)$, which is used as input into the algorithms and approaches presented in Chapter 3. Briefly, satellite ocean colour instruments measure the spectral radiance exiting the TOA at wavelengths typically spanning the UV to NIR and SWIR depending on the sensor. Atmospheric correction algorithms are used to remove the atmospheric contribution from this total signal, generating estimates of $R_{rs}(\lambda)$ that represent the light exiting water, normalized to a hypothetical scenario of an overhead sun and no atmosphere (see references in subchapter 4.2). All prelaunch, temporal, and system vicarious calibrations are applied to TOA radiances prior to atmospheric correction. Bio-optical algorithms are subsequently applied to $R_{rs}(\lambda)$ to produce estimates of the geophysical properties discussed in Chapter 3. The quality and ultimate utility of geophysical properties derived from satellite ocean colour (ignoring the efficacy of the bio-optical algorithms) depend explicitly on instrument calibrations, the atmospheric correction approach used and its associated uncertainties, and the final performance and uncertainty assessments of the retrieved $R_{rs}(\lambda)$ used as input into the bio-optical algorithms.

Method development for these processes enjoys a rich history in support of decades of multispectral ocean colour remote sensing (e.g., IOCCG, 2010, 2013, 2019 and others in the IOCCG Report Series; Frouin et al., 2019; Zibordi et al., 2025). While many multispectral approaches can be easily applied to hyperspectral measurements, the additional information provided by the latter offers opportunities to improve or reconsider these tasks that have yet

to be fully investigated and exploited. As such, the emphasis of this chapter is highlighting additional requirements, gaps, and needs to advance retrievals of hyperspectral $R_{rs}(\lambda)$, while also proposing what additional value hyperspectral instruments might offer the processes themselves. We concentrate specifically on methods and needs for system vicarious calibration (SVC), atmospheric correction, and validation and performance assessments, with some interspersed commentary on temporal calibrations. Our primary goal is to highlight areas that will benefit from additional attention and research. The intended audiences are those who can fund such efforts and individuals who can pursue them. Note that our focus is *processes* and *methods*, not the *resources* needed to pursue them (e.g., in situ data or infrastructure availability), unless such resources do not yet exist.

4.1 System Vicarious Calibration

In the ocean colour paradigm, SVC provides a radiometric gain adjustment that includes the instrument as well as the processing algorithm for atmospheric correction. Its goal is to maximize the agreement or reduce the bias between remotely sensed water-leaving radiances obtained after atmospheric correction and expected water-leaving radiances. This goal is achieved through adjustment of the sensor-plus-algorithm system to account for unknown uncertainties in pre-launch instrument calibrations and components of the atmospheric correction algorithm. Gordon, 1987 provided the first complete outline for SVC of a satellite ocean colour instrument, namely the NASA CZCS. General evolution of the approach since the late 1990s is described in Eplee et al., 2001; Franz et al., 2007; Gordon, 1998, with a recent overview and perspective provided in Zibordi et al., 2025. The latter muses that SVC is "*the process applied to satellite ocean colour missions to achieve the required accuracy over time for data products targeting climate and global long-term operational applications*" (Zibordi et al., 2025). SVC has been applied in some form to nearly all ocean colour satellite instruments since the CZCS era.

For a given satellite-to-truth (in situ) match-up, SVC begins by propagating the known spectral water-leaving radiances to the TOA using the coincident satellite-specific geometric conditions and derived atmospheric parameters. An individual spectral gain adjustment for this match-up is then calculated as the ratio of propagated TOA radiance to satellite-measured TOA radiance. Over time, individual gains for each wavelength are assessed for quality via a series of exclusion criteria and average values are calculated for use as final spectral gain adjustments. In the flow of standard ocean colour data processing, these final values are applied to measured TOA radiances following the application of pre-launch and temporal (lunar and solar) calibration adjustments, but prior to atmospheric correction.

In standard operation, this process remains generally agnostic to the truth data source. While this section focuses on future methods and needs for hyperspectral SVC other than data sources, we note for completeness that assets used as ground (sea) truth for visible wavelength SVC have typically been hyperspectral and, thus, remain suitable for future needs. Commonly used hyperspectral instrument systems are listed in Table 4.1. Their architectures, deployment strategies and locations, and rationales are described in detail in the provided references. Alternative *truth* sources for SVC have been explored, including the AErosol RObotic NETwork Ocean Colour (AERONET-OC; Bailey et al., 2008; Mélin and Zibordi, 2010) and an ocean reflectance model (Werdell et al., 2007). NIR and SWIR wavelengths are most often calibrated assuming negligible water-leaving radiances as the *truth* values over oligotrophic

oceans such as the south pacific gyre.

Table 4.1 Commonly used hyperspectral instrument systems used for System Vicarious Calibration (SVC).

Name	Duration	Location	Reference
MOBY	1996-present	Lanaii, Hawaii	Clark et al., 1997
BOUSSOLE	2001-2023	Mediterranean Sea	Antoine et al., 2008
HyperNAV	2024-present	Various sites	Barnard et al., 2024
MarONet	2024-present	near Perth, Australia	

4.1.1 Status

Historically, operational multispectral SVC methods calculate a gain individually for each band following Franz et al., 2007 or with minor process adjustments (e.g., Barnes et al., 2022; Wang et al., 2016). In practice, this involves first calculating NIR and/or SWIR gains at open-ocean site(s) where atmospheric aerosols are assumed to be well-known, and water-leaving radiances in this spectral range are assumed to be negligible; then calculating individual visible gains at the site of an SVC instrument system. To our knowledge, this approach has been generally adopted for most on-orbit multi- and hyperspectral instruments (e.g., Ahn et al., 2015; Concha et al., 2019; Dash et al., 2012; Ibrahim et al., 2018; Song et al., 2019). For example, through its second full mission reprocessing (Version 3.1; August 2025) PACE OCI adopted the band-by-band approach for its SVC calculations (Fig. 4.1). After multiple iterations of SVC calculations across different OCI processing versions, unity gains were adopted for the NIR bands, as evidence indicated that they were already well-calibrated after absolute and temporal on-orbit calibration, making the separate NIR approach unnecessary.

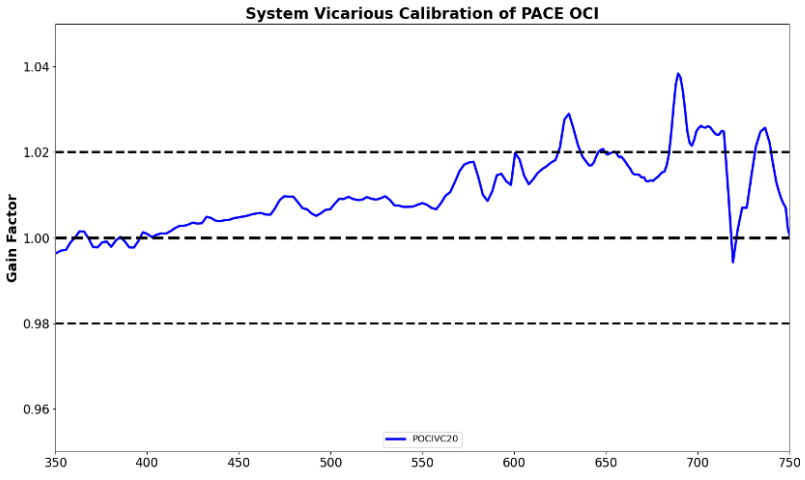

Figure 4.1 PACE Version 3.1 OCI SVC gains (https://oceancolor.gsfc.nasa.gov/data/reprocessing/)

The SVC gains presented in Fig. 4.1 reveal several issues in PACE OCI Version 2 processing that warranted attention. In this case, four distinct Hybrid Perception for Object-Oriented Navigation (HyperNav) sites exhibited inconsistent gains, with a spread of less than

5%. These sites were sampled at geographically disparate locations, each characterized by unique oceanic and atmospheric conditions, thereby raising concerns regarding the relative accuracy of atmospheric correction across sites. Furthermore, in spectral regions affected by strongly absorbing gas features, such as the oxygen A- and B-bands, residual gain structures were evident. These artifacts, arising from imperfect correction of sharp absorption features, likely introduced uncertainties in the retrieval of water-leaving radiance within these bands. Some of these observations were only possible due to the rapid collection of SVC data early in the mission, which advocates for future consideration of instrument systems that further enable routine and rapid data collection. In this example of OCI SVC, algorithm updates for Version 3.1 processing enabled the prompt resolution of issues that arose in the gain sets, which were hypothesized to be attributed to either algorithmic limitations or calibration errors. For completeness, a short list of alternative approaches is included in Table 4.2. These approaches have all been applied to multispectral instruments and do not necessarily address the challenges, gaps, and opportunities for hyperspectral SVC explored in the remainder of this chapter.

Table 4.2 Brief list of alternative methodological approaches to SVC.

Approach / Source	**Instruments considered**	**Reference**
Rayleigh scattering	SeaWiFS, MERIS	Fougnie and Bach, 2008; Hagolle et al., 2008
Desert sites	MERIS, MODIS, OLCI, Sentinel-2	Bouvet and Ramoino, 2010; Cosnefroy et al., 1996; Thome, 2001
Deep Convective Clouds	MODIS, VIIRS	Fougnie and Bach, 2008
Instrument Cross-calibration	Traceable Radiometry Underpinning Terrestrial- and Helio-Studies (TRUTHS, benchmark mission), cross-calibration with Sentinel and others, CLARREO Pathfinder	Gorroño et al., 2024; Roithmayr et al., 2014

4.1.2 Gaps in SVC methodologies

The heritage band-by-band approach works mechanically for hyperspectral instruments. Intuitively, however, we expect hyperspectral information to be better exploited. As an important example of this, we note that current operational methods do not explicitly consider band-to-band relationships that likely become increasingly important when assessing an observed continuous spectrum. As shown in Fig. 4.2, SVC gains were computed for each band independently, without accounting for spectral correlation. This band-by-band treatment introduced sharp spectral structures in the gains, primarily due to imperfect atmospheric gas correction, such as the oxygen absorption feature near 685 nm. Since such features originate from well-characterized atmospheric absorption, they are not attributable to instrument calibration. A more rigourous approach would separate atmospheric correction errors from calibration effects, the latter expected to be spectrally smooth. Incorporating spectral covariance into the SVC process could mitigate these artifacts, enable an independent assessment of instrument calibration, and improve the atmospheric correction itself.

Spectral curvature has been explored for multispectral instruments, but methods have not been routinely applied in practice. Stumpf and Werdell, 2010, for example, used spectral

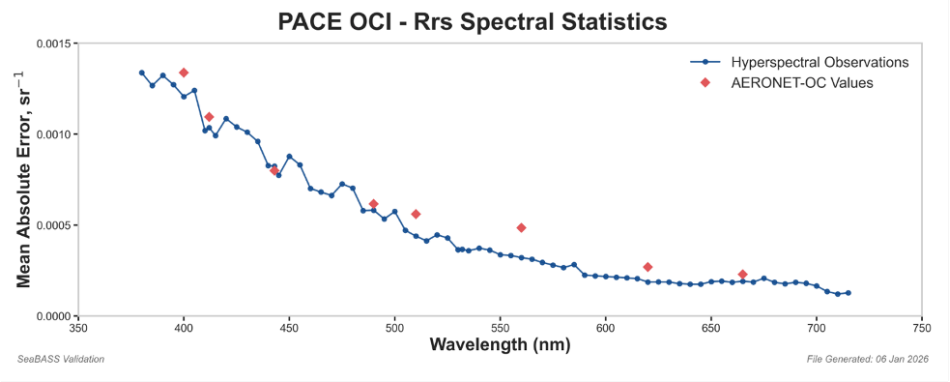

Figure 4.2 OCI mean absolute errors in $R_{rs}(\lambda)$ as a function of wavelength in comparison to coincident hyperspectral measurements (blue connected dots) and AERONET-OC observations (red diamonds). These are results for OCI version 3.1 and were generated in January 2026 (https://pace.oceansciences.org/pace_data_matchups.html)

shapes to identify a relative temporal shift between the blue bands of MODIS-Aqua that was otherwise invisible given calibration uncertainties. Analysis of this trend revealed a potential calibration change that could address this temporal shift. A key concern in hyperspectral SVC, however, lies in the potential suppression, smoothing, or artificial introduction of spectral features in the retrieved reflectance. The ultimate objective of hyperspectral ocean colour is to extract geophysical information from subtle spectral signatures, which are often magnified in derivative space, particularly through second-derivative analyses. Any alteration of these features risks introducing biases that propagate into derived products. Moreover, because SVC approaches may be inadvertently tuned to the specific observational conditions under which the in situ data were collected, the resulting spectral features may reflect site-specific biases rather than true instrument or atmospheric characteristics.

Mitigating these limitations requires the explicit inclusion of uncertainty constraints in the SVC process. Both the satellite instrument and the in situ reference data carry radiometric uncertainties that must be rigourously accounted for, including their full covariance across spectral bands. Without this covariance-aware framework, error propagation can distort the spectral shape, particularly in regions where fine features are most critical for geophysical retrievals. Advanced approaches such as Bayesian inference, including hierarchical Bayesian models suited to multi-site SVC, or machine learning techniques designed to capture nonlinear error structures, offer promising pathways forward. Such methods have the added advantage of providing confidence intervals for the SVC gains themselves, with uncertainties naturally decreasing as additional data are collected and sample sizes accumulate over time.

Several fundamental questions remain unresolved. For example, the role of spectral coherence in constraining SVC deserves closer examination: can curvature or derivative-based analyses be systematically leveraged to refine SVC gains? Similarly, it is unclear whether SVC might be more effective if applied directly in derivative space, where spectral features are most pronounced. Uncertainty quantification also demands greater rigour, both in terms of incorporating input uncertainties from the *truth* source and in the calculation and reporting of output uncertainties from the SVC process, which is often an overlooked problem.

In addition to methodological concerns, the integration of external information may offer a path to improved outcomes. Atmospheric and aquatic conditions, including aerosol optical depths, aerosol type, cloud cover, and water optics characteristics such as VSF, could provide important contextual data for constraining SVC. At the same time, revisiting existing NIR and

SWIR approaches, which were originally designed for multispectral sensors, may reveal useful adaptations for the hyperspectral paradigm, such as the utilization of the aerosol information at the SVC sites. Rapid expansion of matchup sample sizes is another issue. For example, the number of available Marine Optical Network (MarONET) or Marine Optical BuoY (MOBY)-Refresh matchups is dwarfed by those of HyperNAV in the PACE context, raising challenges for statistical robustness. Reconciling differences in SVC gains across multiple sites, such as among different HyperNAV deployments, requires careful consideration to avoid introducing geographic or environmental biases. Importantly, the quality and rigour of these independent systems may vary, as their levels of measurement uncertainty differ.

Finally, the criteria for matchup selection and quality assurance must be reexamined in the hyperspectral domain. Conventional exclusion criteria that aggressively discard data when a single band is suspected to be an outlier risk eliminating valuable information and may be inadequate in the context of increased spectral dimensionality. Emerging tools such as Apparent Visible Wavelength (AVW) and Quality Water Index Polynomial (QWIP), applied jointly to both in situ and satellite spectra, could provide new pathways for refining exclusion criteria and ensuring more consistent quality analysis/control standards.

Taken together, these challenges highlight the need for a comprehensive rethinking of hyperspectral SVC. Progress will depend on integrating advanced statistical frameworks, expanding matchup datasets, and refining quality control procedures. Such developments will be essential to ensure that hyperspectral ocean colour measurements achieve their full potential in delivering unbiased, geophysically meaningful products.

4.2 Atmospheric Correction

Since water bodies are typically much darker than land or atmosphere, the determination of water leaving radiance from satellite remote sensing observation techniques, which informs the bio-optical properties of the suspended and dissolved matter within the water column, remains a challenging task. This is because the water signal typically represents only a few percent (<10%) of the photons that could reach a spaceborne sensor. The atmospheric correction procedure refers to the algorithms or techniques used to subtract the contribution of all atmospheric effects from the at-sensor radiance. Those atmospheric effects include gaseous absorption, light scattered by air molecules (Rayleigh) and aerosols, and the influence of the air-water interface (sun and sky-glint). Specific challenges include the consideration of absorbing aerosols, the detection and masking of clouds, the quantification of adjacency effects (i.e., photons originating from the neighbouring pixels of the observed target), and the analysis of the influence on the water leaving radiance of the reflection of light from the benthos in shallow waters.

4.2.1 Inventory of existing algorithms: both innovations and improvements to multispectral methods

Various robust radiative transfer models have been proposed to develop relevant atmospheric correction algorithms and retrieve aerosol optical properties of the water-atmosphere system. The radiative transfer equation is modelled using different methods such as Monte Carlo ray tracing technique (e.g., Kattawar and Adams, 1989; SMART-G, Ramon et al., 2019), discrete ordinates (DISORT, Stamnes et al., 1988; CRTM, Jin and Stamnes, 1994; COART, Jin et al., 2006; SCIATRAN, Rozanov et al., 2014, 2017), successive orders of scattering (6SV, Kotchenova et

al., 2006; Zhai et al., 2010; OSOAA, Chami et al., 2015), adding-doubling (MOMO, Chowdhary et al., 2006; Fell and Fischer, 2001; PCOART, He et al., 2010) and the finite element method (FEM, Bulgarelli et al., 1999; Kisselev et al., 1995).

Most of the existing atmospheric correction algorithms that are applied to multispectral and hyperspectral imagery over aquatic water bodies have been recently reported in Frouin et al., 2019, Dierssen et al., 2021, and references therein. Examples of current commonly used algorithms are (see Acronyms section for full names of abbreviations): ACOLITE, ACORN, ATREM, CASIDA, COSHISE, FLAASH, HATCH, ICOR, ISOFIT, MIP, Polymer, SCAPE-M, SEADAS Hyperspectral (MBAC), MIP (EnMap). The performances of many of these methods applied over approximately 250 PRISMA images and 50 EnMAP images can be found in the literature (Giardino, Pahlevan, et al., 2025; Giardino, Pellegrino, et al., 2025; Soppa et al., 2024. In addition to these algorithms that are based on radiative transfer, there are also algorithms developed using machine learning (Schiller and Doerffer, 1999). These include OC-SMART (Fan et al., 2021), CSAC (Lee et al., 2024), and ACA-SIM (Li et al., 2025), showing various success in oceanic and/or coastal regions. All of the atmospheric correction algorithms can be classified into two general categories: pixel-wise and image-wise. The former carries out atmospheric correction for each pixel independently, while the latter assumes some spatial coherence.

The atmospheric correction algorithms used for turbid waters are based on various methods such as: the use of a semi-empirical radiative transfer model; a neural network approach; a spectral matching method; a UV-NIR-SWIR approach; a SWIR exponential approach; SWIR Dark Spectrum Fitting (DSF); a SWIR band at 1.38 µm for the removal of thin cirrus radiance; and physics-based approaches that rely on an inversion of radiance or reflectance spectra back to water optical properties and water constituents (e.g., MIP by Heege et al., 2014; PhytoDOAS with latest update in Oelker et al., 2022).

Algorithms that are dedicated to correct for the atmosphere over inland waters include methods such as the spatial extension of aerosol information retrieved from nearby land pixels (e.g., SCAPE-M, ICOR); the DSF approach; machine learning approaches; removal of the sole molecular Rayleigh contribution to obtain various diagnostic products (e.g., blooms, floating vegetation); and glint correction, as in Polymer.

The atmospheric correction routines that are specifically applied to hyperspectral satellite measurements using a pixel-wise approach often include the following features:

- simulation of water leaving reflectance shapes and retrieval of spectra based on some type of *a priori* spectral library,
- retrieval of all components on a pixel-by-pixel basis,
- independent retrieval of the water and atmospheric properties,
- an optimization procedure that is based on patterns in the imagery to help constrain one or more parameters in the solution for the entire scene under investigation.

4.2.2 Gaps in atmospheric correction approaches

The main limitations and challenges that are associated with the current atmospheric correction algorithms are as follows:

- Atmospheric correction over the global deep ocean has been robust, however, challenges remain in coastal and in land waters, where uncertainties in water reflectance remain high and depend on the optical water types (Pahlevan et al., 2021), thus impacting water quality products.
- Sunglint and whitecaps can limit the utility of data even with the most advanced cor-

rection routines. Wind speed is typically provided to the algorithms from ancillary data sources such as NASA's Modern-Era Retrospective analysis for Research and Applications, Version 2 (MERRA-2), NOAA's National Centers for Environmental Prediction (NCEP), or the European Centre for Medium-Range Weather Forecasts (ECMWF). These datasets are generally available at coarser spatial resolution than satellite observations, which introduces additional uncertainties.

- Adjacency effects remain a difficult issue to address. These effects could be defined as the influence of the reflectance from adjacent land/ice pixels that can be scattered into the field of view of the sensor, thus contaminating the water signal. They are particularly problematic for water near bright ice surfaces, sand or bare soil, and for inland waters surrounded by bright land and vegetation. The problem is confounded by the fact that the same land / water settings can cause different adjacency effects due to variable solar/viewing geometry relative to the land / water settings, and also confounded by the sensor's bright target recovery design (Feng and Hu, 2016, 2017). It is currently a challenging task to make correction approaches for adjacency effects applicable across all diverse landscapes.
- For hyperspectral sensors, additional difficulty arises from residual errors of correction for absorbing gases such as H_2O, NO_2, and O_2, and these errors can lead to artificial spectral features in specific bands that can interfere with algorithms using those bands.
- The BRDF remains a challenge, particularly in complex waters where the particle VSF deviates significantly from the assumptions typically used in BRDF models (e.g., Morel et al., 2002).
- Atmospheric correction in the UV remains a challenge due to the strong contribution of Rayleigh scattering and the additional uncertainties introduced by the presence of absorbing aerosols.

An exhaustive list of algorithmic shortcomings is provided in Frouin et al., 2019.

4.2.3 Other considerations

Gaps that need to be filled in order to advance analysis of hyperspectral imagery over aquatic ecosystems could be summarized as follows.

- **Removal of moderate sunglint and sky glint from hyperspectral data**: The removal of sun and sky glint from hyperspectral data could be performed using image-driven approaches (UV, oxygen-A), a SWIR-based semi-analytical approach or multidirectional and polarization-based approach.
- **Use of hyperspectral imagery from UV to SWIR**: A great improvement of atmospheric correction robustness is expected through the analysis of the satellite measurements acquired in the UV and SWIR bands. The UV and SWIR bands are particularly helpful to improve the estimation of absorbing aerosols as well as the estimation of the aerosol layer height (UV range, oxygen-A and oxygen-B).
- **Inversion algorithm based on simultaneous retrieval of both ocean and atmosphere variables**: The development of advanced inversion methods that are able to simultaneously retrieve parameters from a coupled ocean-atmosphere system without individual atmospheric correction routines should be strengthened (e.g., MIP, Polymer, SCIATRAN-based-PhytoDOAS). This is an area of future growth. AI-based methods should greatly contribute to improving the performance of the retrievals.
- **Multidirectional polarized measurements**: Multidirectional polarized measurements

of satellite radiance, as measured by the PACE sensor, should significantly improve the performance of atmospheric correction algorithms by providing additional physical constraints (i.e., directional and polarization effects of atmospheric components) to reduce the number of solutions within the inversion process. Such types of measurements are also helpful for performing simultaneous retrievals of water reflectance and aerosol properties.

- **Minimize the residual errors from corrections of absorbing gases**: Residual artifacts from imperfect gas corrections, particularly those associated with H_2O, O_2, and O_4, can introduce alterations in the spectral shape of $R_{rs}(\lambda)$. To mitigate these effects, it is critical to develop algorithms that explicitly account for the coupled interactions of scattering and absorption processes, thereby reducing systematic errors in the retrieved spectra.

4.3 Validation and performance assessments

In remote sensing of ocean colour, assessing the performance and uncertainties of $R_{rs}(\lambda)$ is fundamental and takes many forms. Ultimately, these assessments serve to evaluate the quality of the spectral radiometry that underpins algorithms for deriving aquatic geophysical properties of interest. In other words, because the reliability of derived geophysical variables depends heavily on the accuracy of the input $R_{rs}(\lambda)$, quantifying uncertainties in satellite-measured $R_{rs}(\lambda)$ at regional to global scales remains of critical importance. To this end, space agencies and their partners invest heavily in in situ data collection, the development of measurement protocols, and subsequent data analysis to support performance evaluations (e.g., Giardino, Pellegrino, et al., 2025; Seegers et al., 2018; Werther et al., 2025).

4.3.1 Status

Ocean colour satellite performance assessments most commonly emphasize coincident satellite-to–in situ match-ups (Bailey and Werdell, 2006), though additional approaches, such as time-series analysis, population statistics, and satellite-to-satellite intercomparisons, are also routinely pursued. Historically, multispectral analyses have relied on comparing in situ and satellite reflectances one wavelength at a time. These comparisons employ a wide range of techniques, including regression statistics, scatter plots, and Bland-Altman plots; multi-dimensional visualizations such as Taylor, Target, and Star diagrams; histograms and distribution functions across space and time scales; and time-series analyses at varying resolutions.

More recently, assessments have expanded beyond individual wavelengths to consider properties or metrics derived from the full spectrum (e.g., AVW, QWIP; Dierssen et al., 2022; Vandermeulen et al., 2020). Additional methods, such as evaluating spectral shape using spectral angle (Kruse et al., 1993), applied, for example, in Soppa et al., 2021, 2024, provide complementary insight into the fidelity of spectral information.

IOCCG, 2019 provided a valuable framework for translating validation statistics into meaningful uncertainty metrics. In contrast to traditional approaches that focus narrowly on regression slopes, scatter plots, or bias at specific wavelengths, the report emphasizes the need to formalize how those quantities reflect true uncertainty in $R_{rs}(\lambda)$ and derived products. It highlights that metrics for validation should not only quantify the magnitude of satellite-in situ differences (e.g., mean bias, standard deviation, root mean squared error; see Seegers et al., 2018), but also account for the quality and uncertainty of the in situ data (e.g., McKinna et

al., 2021), as well as mismatches in time, space, and spectral sampling (IOCCG, 2019). In this way, commonly used validation metrics (bias, σ, mean absolute error, median relative difference) are repositioned within a structured framework of uncertainty propagation, helping to distinguish between random noise, systematic error, and representativeness effects (Werther et al., 2025). This perspective underscores the importance of reporting performance assessments in a way that can support long-term application, such as climate data records, where consistent and interpretable validation metrics are essential.

4.3.2 Gaps in performance assessment methods

While heritage band-by-band approaches remain mechanically possible for hyperspectral instruments, the presentation of scatter plots or massive tables quickly becomes impractical, and often uninterpretable, when more than 200 wavelengths are available. Consequently, novel and standardized approaches to visualizing hyperspectral validation results are essential. One straightforward method is to plot statistical metrics of interest (y-axis) as a function of wavelength (x-axis; Fig. 4.2). Such plots are intuitive, scalable, and can be implemented with existing statistical pipelines. Yet several open questions remain. Can a preferred suite of hyperspectral validation metrics be recommended? There are alternative graphical methods that can consolidate or compress full-spectrum information into more interpretable formats (e.g., principal component representations, heatmaps, or spectral similarity measures). While wavelength-by-wavelength plots such as Fig. 4.2 are useful, they also raise important methodological considerations:

- **Necessity of full spectral coverage**: Does every available wavelength require independent validation? For example, are assessments at both 442 nm and 444 nm truly independent or practically useful? One consideration is the combination of hyperspectral and multispectral validation data. A representative plot of validation metrics that merges, for example, hyperspectral data collected in open ocean conditions with AERONET-OC (multispectral), could produce discontinuities in spectral metrics due to marked performance differences between coastal waters and open ocean regimes.
- **Spectral covariance**: How should covariances across bands be quantified and incorporated into performance assessments? Hyperspectral retrievals depend not only on accurate individual bands but also on the spectral coherence across bands. Field measurements of hyperspectral $R_{rs}(\lambda)$ confirm that most bands are not independent but correlated (Lee et al., 2014; Sun et al., 2015). In practice, information in a subset of key spectral bands can reproduce much of the variance in other bands, suggesting that uncertainty estimates could be prioritized for these informative wavelengths. Meanwhile, uncertainties in other bands might be evaluated through assessment of spectral shapes or metrics derived from the full spectrum.
- **Spectral and spatial coherence**: For derivative-based algorithms, spectral coherence is critical; for sub-pixel retrievals, spatial coherence is equally necessary. This becomes particularly important as emerging geophysical algorithms increasingly exploit spectral derivatives. For instance, second-derivative methods are gaining traction (e.g., Kramer et al., 2024), yet it remains uncommon to evaluate spectral curvature in the context of performance assessments. Could second-derivative metrics provide a pathway to capture spectral coherence and subtle absorption features? Similarly, proxy metrics of spectral shape (such as AVW or QWIP) may serve as compact, interpretable alternatives to exhaustive band-by-band assessments. In the same vein, approaches that quan-

tify spectral curvature (e.g., Stumpf and Werdell, 2010) could be adapted to validation frameworks to emphasize continuity and coherence across the spectrum.

- **Spatiotemporal variability in matchups**: Another unresolved challenge is the treatment of spatiotemporal variability between satellite pixels and field observations (Nasiha et al., 2022). A 5×5 pixel box centred on an in situ station may capture natural spatial heterogeneity (due to gradients, fronts, or submesoscale features) that contributes to differences in observed reflectance, even in the absence of measurement error. Similarly, temporal mismatches, even within ±3 hours, can introduce variability due to tidal cycles, atmospheric transients, or phytoplankton patchiness and blooms. This spatiotemporal mismatch is often treated as *noise*, but in reality it represents a fundamental component of the matchup uncertainty budget. Spatial and temporal variability could be correlated. Distinguishing between natural environmental variability and true sensor or algorithm error remains a key research need. Approaches such as variance decomposition or geostatistical modelling (e.g., kriging) could provide more principled ways to attribute observed mismatch to either natural variability or sensor performance.
- **Treatment of uncertainties in both satellite and field data**: Issues of uncertainty are not unique to hyperspectral sensors, but they underscore a persistent gap in performance assessments—the treatment of uncertainties in the *truth* data. Field measurements are often assumed to be error-free, yet they carry their own sources of uncertainty, including instrumental, methodological, and representativeness errors. Reliable estimates of these uncertainties, such as those demonstrated by McKinna et al., 2021, are critical for closing the loop. Without them, validation results risk conflating sensor errors with uncertainties inherent in in situ observations.

4.3.3 Other considerations

While not the focus of this report, the fact remains that in situ data for validation remains sparse, both temporally and geographically. The community needs investment from agencies and institutions to remedy this limitation. The scarcity of data introduces important limitations:

- **Sampling bias**: Existing matchup datasets are often concentrated in the Northern Hemisphere, near established observing networks (e.g., AERONET-OC, MOBY, or coastal moorings). This leads to over-representation of certain environments (e.g., temperate coastal waters) while under-sampling others (e.g., oligotrophic gyres, polar seas, and much of the Southern Hemisphere). Validation metrics derived from these biased samples risk being unrepresentative when generalized to the global ocean.
- **Lack of representativeness**: Without sufficient coverage of diverse bio-optical regimes, subtle sensor or algorithm errors may remain undetected in under-sampled regions. For instance, waters with distinct phytoplankton communities, high CDOM absorption, or unusual aerosol conditions may show different error characteristics than those observed in well-sampled sites.
- **Temporal gaps**: Matchup opportunities are clustered around campaign periods or long-term observatories, but many dynamic environments (upwelling zones, river plumes, polar blooms) lack sustained observations. As a result, seasonal and interannual variability is often poorly represented in current matchup databases.
- **Southern Hemisphere gap**: In particular, the Southern Hemisphere remains markedly under-observed compared to the Northern Hemisphere. Large expanses of the South

Pacific, South Atlantic, and Southern Ocean lack systematic matchup coverage. This asymmetry undermines the ability to validate satellite products on a global basis, particularly in regions critical for carbon cycling, climate feedback, and fisheries.

Addressing these gaps will require targeted investment in new observing platforms (e.g., autonomous systems such as gliders, floats, and uncrewed surface vehicles equipped with hyperspectral radiometers), expansion of existing networks into underrepresented regions, and stronger international collaboration to pool resources and datasets. Importantly, validation strategies must explicitly account for sampling bias when interpreting matchup results, for example, by weighting results by bio-optical province rather than relying on unbalanced global statistics.

Chapter 5

Summary and Key Recommendations for Actions

Ana I. Dogliotti, Astrid Bracher, Jeremy Werdell, Malik Chami, Maycira Costa, Heidi Dierssen, Claudia Giardino, Toru Hirawake, Chuanmin Hu, Amir Ibrahim, Wonkook Kim, Emanuele Organelli, Shaoling Shang, Fang Shen

5.1 Summary

The advent of aquatic hyperspectral remote sensing marks a pivotal advancement in Earth observation, transitioning the community from the reliable but limited scope of multispectral radiometry to a richer, continuous spectral capability. This report documented the current status, highlighted the substantial benefits, and critically assessed the remaining challenges and gaps.

Hyperspectral data, defined here as the continuous measurement of light in incremental steps across the UV-to-NIR spectrum, provides fundamentally improved capacity to:

- accurately resolve the spectral signatures of aquatic constituents, thereby lowering uncertainties in core products such as CHL, CDOM, and total suspended matter across the optical water types;
- enable the retrieval of new and improved products, including detailed inherent optical properties, PFTs, spectral water reflectance and underwater light properties, photophysiological parameters, carbon-related products, and the spectral discrimination of various floating matter and benthic habitats;
- address pressing global and regional science questions concerning water quality, biodiversity, and the carbon cycle, particularly where multispectral sensors have reached their limits.

Despite these clear advantages and the existing hyperspectral missions, the full operational potential of aquatic hyperspectral remote sensing is not yet realized. Key constraints identified across Chapters 2 - 4 present a crucial roadmap for future action.

- **Sensor Limitations:** Current spaceborne high-spatial-resolution sensors often suffer from a low SNR (<400) inadequate for dark ocean waters (where SNR >500 is often required). Furthermore, sensors appropriate for coastal and inland waters (spatial resolution <100 m) typically possess a narrow swath and poor temporal revisit frequency, which is insufficient for characterizing highly dynamic fine-scale processes.
- **Retrieval Challenges:** The methods for system vicarious calibration and atmospheric correction face critical gaps, including effectively removing adjacency effects in complex coastal / inland environments, and residual errors from absorbing gas correction. The successful operational application of novel products requires the advancement of coupled ocean-atmosphere retrieval techniques and the exploitation of new methodologies such as polarized and multidirectional measurements.
- **Validation Gaps:** The validation and performance assessment of hyperspectral prod-

ucts is severely constrained by the limited spatial and temporal coverage of in situ matchup data, necessitating a concerted community effort toward standardization and uncertainty quantification.

Ultimately, no single sensor can meet the combined requirements of high spatial, temporal, and spectral resolution with sufficient SNR for all aquatic applications. Therefore, the future of aquatic hyperspectral remote sensing depends on the *synergistic integration* of data streams and a focused investment in resolving the technological and methodological gaps outlined in the following recommendations.

5.2 Key Recommendations

Based on the current status, challenges, and perspectives identified throughout this report, the following core recommendations for satellite missions, associated research, and the broader aquatic radiometry community are proposed.

5.2.1 Technology & Sensor Development

1. **Prioritize high-resolution aquatic missions:** Agencies must prioritize and fund the development and operation of satellite imaging spectroscopy sensors specifically designed to meet the critical requirements for coastal and inland waters. This specifically means missions featuring high spatial resolution (<30 m, or below, specifically for benthic and floating matter needs) and significantly enhanced signal-to-noise ratios to ensure accurate measurements in optically complex and darker waters.
2. **Synergistic data combination:** Future efforts should systematically combine data from multiple satellite platforms, including both hyperspectral and multispectral sensors, as well as Earth observation missions (such as land and atmosphere), to overcome the limitations of individual systems.
3. **Integrate commercial data:** Explore and support pathways for integrating data from the rapidly growing number of commercial hyperspectral satellite missions for scientific and applied use, recognizing their potential for high-spatial resolution, and local-to-regional applications.
4. **Ensure operational transition:** Current and planned research-focused hyperspectral missions (e.g., PRISMA, EnMAP) must be strategically transitioned into operational platforms to ensure the routine, reliable, and continuous monitoring of water quality and ecological variables over the long term.
5. **Sustain airborne and autonomous platforms:** Public and commercial operators should maintain and augment airborne and drone hyperspectral capabilities. These platforms provide essential, high-quality, fine-scale data crucial for:
   - ❖ testing and validating new satellite-based algorithms and mission requirements (e.g., PRISMA, EnMAP, SBG);
   - ❖ conducting fine-scale mapping and real-time hazard identification;
   - ❖ developing and validating new classification and mapping approaches for heterogeneous environments like benthic habitats.

5.2.2 Targeted Investment in Calibration and Validation Infrastructure

6. **Expand observing networks**: Invest in new and expanded observing platforms, such as autonomous systems (Argo floats, gliders, uncrewed surface vehicles) equipped with

hyperspectral radiometers, to address the profound data gaps, particularly in the Southern Hemisphere and dynamic environments like upwelling zones.

7. **Improve detection of 3D structures:** Develop better techniques for making and expanding benthic reflectance measurements (including canopy structure and 3D effects) at the spatial scales relevant for satellite pixel sizes for both algorithm development and validation.
8. **Hyperspectral ground truth:** Enlarge in situ bio-optical data collection (e.g. expand WATERHYPERNET) and establish a centralized, internationally collaborative data system or hub to collate high-quality, fully characterized, co-located hyperspectral in situ validation datasets, including water and optical constituents, benthic reflectance, and floating matter.
9. **Hyperspectral system vicarious calibration:** Current SVC methods, which treat each band independently, can introduce spectral artifacts from imperfect atmospheric gas correction. A more rigorous approach must be adopted that incorporates spectral covariance and spectral shape into the SVC process to separate true instrument calibration errors from atmospheric effects, thereby improving the atmospheric correction itself.

5.2.3 Algorithm and Methodology Advancement

10. **Advanced atmospheric correction:** Research efforts must focus on improving atmospheric correction robustness for hyperspectral data, with a specific emphasis on:
    - ❖ developing robust, sensor-independent methods to address **adjacency effects** in diverse landscapes (e.g., inland waters near bright land/ice, coastal ecosystems);
    - ❖ strengthening **inversion algorithms** that perform the simultaneous retrieval of both ocean and atmosphere variables (coupled ocean-atmosphere approaches), leveraging the full spectral range and advanced methods such as **artificial intelligence** techniques provided that they are combined with physical-based methods;
    - ❖ exploiting the full spectral range, including **UV and SWIR bands**, to improve the estimation of absorbing aerosols and the aerosol model over highly scattering turbid water scenes;
    - ❖ exploring the potential of **multidirectional and polarized measurements** to further refine the separation of water and atmospheric signals.
11. **Hyperspectral product development:** The community must intensify efforts to transition established hyperspectral-enabled products from research to operational status, focusing on:
    - ❖ developing and testing robust algorithms for an expanded range of products (e.g., PFTs, IOPs, phytoplankton carbon, DOC, benthic and floating matter classification and health status) that rely on continuous spectral information;
    - ❖ Exploring **data fusion** techniques (e.g., with acoustic and LiDAR data) and **polarimetry** to advance the retrieval and classification of complex products like benthic habitats.
12. **Improve uncertainty quantification:** All new and improved products must incorporate advanced uncertainty quantification methodologies. Uncertainty characterization must be a core component of validation protocols to allow for the effective harmonization of international missions and to provide users with essential information on product reliability.

Acronyms

3SAA	Three-step Semi-Analytical Algorithm
6SV	Second Simulation of a Satellite Signal in the Solar Spectrum
AbPM	Absorption-based Production Model
AC	Atmospheric Correction
ACA-SIM	Atmospheric Correction based on Satellite–In situ Matchup data
ACOLITE	Atmospheric Correction for OLI 'lite'
ACORN	Atmospheric CORrection Now
AERONET-OC	AErosol RObotic NETwork Ocean Colour
AI	Artificial Intelligence
AISA	Airborne Imaging Spectrometer for Applications
AHSI	Advanced Hyperspectral Imager
AOP	Apparent Optical Property
AOD	Aerosol Optical Depth
AODN	Australian Ocean Data Network
AOLCI	Advanced Ocean and Land Colour Imager
AOT	Aerosol Optical Thickness
APEX	Airborne Prism EXperiment
ASI	Agenzia Spaziale Italiana (Italian Space Agency)
ATREM	ATmospheric REMoval program
AVIRIS-NG	Airborne Visible/Infrared Imaging Spectrometer – Next Generation
AVW	Apparent Visible Wavelength
BATS	Bermuda Atlantic Time-series Study
BRDF	Bidirectional Reflectance Distribution Function
C2RCC	Case 2 Regional CoastColour
Cal/Val	Calibration and Validation
CASI	Compact Airborne Spectrographic Imager
CASIDA	Combined Atmospheric and Surface Interaction Data Analysis
CbPM	Carbon-based Production Model
CCRR	CoastColour Round Robin
CDOM	Chromophoric Dissolved Organic Matter
CHIME	Copernicus Hyperspectral Imaging Mission for the Environment
CHEMTAX	CHEMical TAXonomy
CHL	Chlorophyll-a
CHRIS	Compact High Resolution Imaging Spectrometer
COART	Coupled Ocean–Atmosphere Radiative Transfer
COSHISE	COupled Surface–atmosphere Hyperspectral Imaging Spectral Extraction
CRTM	Community Radiative Transfer Model
CSAC	Cross-Satellite Atmospheric Correction
CZCS	Coastal Zone Color Scanner
DC	Default Configuration

DISORT	DIScrete Ordinate Radiative Transfer
DESIS	DLR's Earth Sensing Imaging Spectrometer
DLR	Deutsches Zentrum für Luft- und Raumfahr (German Aerospace Center)
DNA	Deoxyribonucleic Acid
DOAS	Differential Optical Absorption Spectroscopy
DOC	Dissolved Organic Carbon
DOM	Dissolved Organic Matter
DSF	Dark Spectral Fitting
EAGLE	Enhanced Airborne Geophysical / Geological and Environmental Imaging Spectrometer
ECMWF	European Centre for Medium-Range Weather Forecasts
eDNA	environmental Deoxyribonucleic Acid
EMIT	Earth Surface Mineral Dust Source Investigation
EnMAP	Environmental Monitoring and Analysis Program
Envisat	Environmental Satellite
EO	Earth Observation
EOF	Empirical Orthogonal Function
ESA	European Space Agency
EUMETSAT	European Organisation for the Exploitation of Meteorological Satellites
FEM	Finite Element Method
FENIX	Flexible Experimental Imaging Spectrometer
FLAASH	Fast Line-of-sight Atmospheric Analysis of Spectral Hypercubes
FLEX	FLuorescence EXplorer
FLH	Fluorescence Line Height
FLORIS	Fluorescence Imaging Spectrometer
FOV	Field Of View
FPH	Fluorescence Peak Height
GCOM-C	Global Change Observation Mission - Climate
GIOP	Generalized Inherent Optical Property
GALENE	Global Assessment of Limnological, Estuarine and Neritic Ecosystems
GOME-2	Global Ozone Monitoring Experiment-2
GLI	Global Land Imager
GLORIA	GLObal Reflectance community dataset for Imaging and optical sensing of Aquatic environments
GSM	Garver-Siegel-Maritorena model
HAB	Harmful Algal Bloom
HATCH	Hyperspectral Atmospheric Correction Tool for CHRIS
HICO	Hyperspectral Imager for the Coastal Ocean
HIUSI	Hyperspectral Imager Suite
HOPE	Hyperspectral Optimization Process Exemplar
HOT	Hawaii Ocean Time-Series
HPLC	High Performance Liquid Chromatography
HyperNAV	Hybrid Perception for Object-Oriented Navigation
Hyplant-DUAL	Hyperspectral Plant imaging spectrometer, in dual mode
HyMap	Hyperspectral Mapper
ICOR	Image CORrection for atmospheric effects
IFOV	Instantaneous Field Of View
IOC	Intergovernmental Oceanographic Commission

IOP	Inherent Optical Property
IR	Infrared
ISOFIT	Imaging Spectrometer Optimal FIT
ISS	International Space Station
JAXA	Japan Aerospace Exploration Agency
JPL	Jet Propulsion Lab
LiDAR	Light Detection and Ranging
LISST	Laser In Situ Scattering and Transmissometry
LS2	Loisel-Stramski Version 2
LUT	Look-up Table
MarONet	Marine Optical Network
MBAC	Model-Based Atmospheric Correction
MERIS	Medium Resolution Imaging Spectrometer
MERRA-2	Modern-Era Retrospective analysis for Research and Applications, Version 2
MetOp	Meteorological Operational satellites
MIP	Modular Inversion and Processing system
MIVIS	Multispectral Infrared and Visible Imaging Spectrometer
MOBY	Marine Optical BuoY
MODIS	Moderate resolution Imaging Spectroradiometer
MOMO	Matrix-Operator-MOdel
ML	Machine Learning
MSI	MultiSpectral Instrument
NAP	Non-Algal Particles
NASA	National Aeronautics and Space Administration (USA)
NCEP	National Centers for Environmental Prediction (USA)
NIR	Near Infra-Red
NOAA	National Oceanic and Atmospheric Administration (USA)
NOMAD	NASA Bio-optical Marine Algorithm Dataset
NN	Artificial Neural Networks
NPQ	Non-Photochemical Quenching
OAC	Optically Active Constituent
OBIS	Ocean Biodiversity Information System
OBPG	Ocean Biology Processing Group (NASA)
OC-CCI	Ocean Colour - Climate Change Initiative
OC-SMART	Ocean Color - Simultaneous Marine and Aerosol Retrieval Tool
OCI	Ocean Colour Imager
OCR	Ocean Colour Radiometry
OLCI	Ocean and Land Colour Imager
OLI	Operational Land Imager
OMI	Ozone Monitoring Instrument
ONNS	OLCI Neural Network Swarm
OPAC	Optical Properties of Aerosols and Clouds
OSOAA	Ocean–Surface–Ocean–Atmosphere Algorithm
OWC	Optical Water Constituent
OWT	Optical Water Type
PACE	Plankton, Aerosol, Cloud, ocean Ecosystem

PAR	Photosynthetically Active Radiation
PCOART	Polarized Coupled Ocean–Atmosphere Radiative Transfer
PIC	Particulate Inorganic Carbon
PFT	Phytoplankton Functional Type
POC	Particulate Organic Carbon
PP	Primary Production
PRISMA	PRecursore IperSpettrale della Missione Applicativa
PROBA	Project for On-Board Autonomy
PSD	Particle Size Distribution
PUR	Photosynthetic Usable Radiation
QWIP	Quality Water Index Polynomial
RTM	Radiative Transfer Model
S2	Sentinel-2
S3	Sentinel-3
S4	Sentinel-4
S5	Sentinel-5
S5P	Sentinel-5 Precursor
S5P-PAL	Copernicus S5P Product Algorithm Laboratory
S3NGO	Sentinel-3 Next Generation Optical
SAR	Synthetic Aperture Radar
SBG	Surface Biology and Geology
SCAPE-M	Self-Contained Atmospheric Parameters Estimation for MERIS data
SCIAMACHY	Scanning Imaging Absorption Spectrometer for Atmospheric Chartography
SCIATRAN	SCIAMACHY radiative TRANsfer model
SDG	Sustainable Development Goal
SDI	Spectral Diversity Index
SeaBASS	SeaWiFS Bio-optical Archive and Storage System
SeaDAS	SeaWiFS Data Analysis System
SeaWiFS	Sea-viewing Wide Field-of-view Sensor
SGLI	Second Generation Global Imager
SIF	Sun-induced Fluorescence
SLSTR	Sea and Land Surface Temperature Radiometer
SMART-G	Speed-up Monte-Carlo Advanced Radiative Transfer – GPU
SNAP	Sentinel Application Platform
S-NPP	Suomi National Polar-orbiting Partnership
SNR	Signal-to-Noise Ratio
SPM	Suspended Particulate Matter
SSI	Spectral Sampling Interval
SST	Sea Surface Temperature
SQ	Science Question
SVC	System Vicarious Calibration
SWIR	Shortwave Infra-Red
TOA	Top of Atmosphere
TROPOMI	TROPOspheric Monitoring Instrument
TRUTHS	Traceable Radiometry Underpinning Terrestrial- and Helio-Studies
TSM	Total Suspended Matter

UNESCO	United Nations Educational, Scientific and Cultural Organization
UV	Ultraviolet
UVN	Ultraviolet, Visible, Near-infrared light spectrometer
VIIRS	Visible Infrared Imaging Radiometer Suite
VIP	Variable Importance Projection
VIS	Visible
VGPM	Vertically Generalized Production Model
VRS	Vibrational Raman Scattering
VSF	Volume Scattering Function
WASI	Water Colour SImulator

Mathematical Notation

Symbol	Description	Typical Units
λ	wavelength	nm
a	spectral absorption	m^{-1}
a_{ph}	absorption by phytoplankton	m^{-1}
a_{NAP}	absorption by non-algal particles	m^{-1}
a_{CDOM}	absorption by chromophoric dissolved organic matter	m^{-1}
a_{dg}	combined absorption of NAP + CDOM	m^{-1}
a_w	absorption by seawater	m^{-1}
b_b	backscattering coefficients	m^{-1}
b_{bp}	backscattering by particles	m^{-1}
b_{bw}	backscattering by seawater	m^{-1}
b_b(NAP)	fraction of backscattering associated with non-algal particles	m^{-1}
C_{phyto}	phytoplankton carbon	mg/m^3
K_d	average attenuation coefficient for downwelling irradiance	m^{-1}
R_{rs}	remote sensing reflectance	sr^{-1}
ϕ_m	maximum quantum yield	C (mol photons)$^{-1}$

Bibliography

Ahn, J. H., Park, Y. J., Kim, W., Lee, B., & Oh, I. S. (2015). Vicarious calibration of the geostationary ocean color imager. *Optics express*, 23: (18), 23236–23258.

Ahn, Y.-H., & Shanmugam, P. (2006). Detecting the red tide algal blooms from satellite ocean color observations in optically complex northeast-asia coastal waters. *Remote Sensing of Environment*, 103: (4), 379–386.

Ali, K. A., & Ortiz, J. D. (2016). Multivariate approach for chlorophyll-a and suspended matter retrievals in case ii type waters using hyperspectral data. *Hydrol. Sci. J.*, 61: (1), 200–213.

Alvain, S., Moulin, C., Dandonneau, Y., & Loisel, H. (2008). Seasonal distribution and succession of dominant phytoplankton groups in the global ocean: A satellite view. *Global Biogeochemical Cycles*, 22: (3), 15.

Álvarez, E., Losa, S. N., Bracher, A., Thoms, S., & Völker, C. (2022). Phytoplankton light absorption impacted by photoprotective carotenoids in a global ocean spectrally-resolved biogeochemistry model. *Journal of Advances in Modeling Earth Systems*, 14, e2022MS003126: https://doi.org/10.1029/2022MS003126

Antoine, D., d'Ortenzio, F., Hooker, S. B., Bécu, G., Gentili, B., Tailliez, D., & Scott, A. J. (2008). Assessment of uncertainty in the ocean reflectance determined by three satellite ocean color sensors (meris, seawifs and modis-a) at an offshore site in the mediterranean sea (boussole project). *Journal of Geophysical Research: Oceans*, 113(C7): https://doi.org/10.1029/2007JC004472

Antoine, D., & Morel, A. (1996). Oceanic primary production: 1. adaptation of a spectral light-photosynthesis model in view of application to satellite chlorophyll observations. *Global Biogeochemical Cycles*, 10: 43–55. https://doi.org/10.1029/95GB02831

Arico, S., Arrieta, J. M., Bakker, D. C. E., Boyd, P. W., Cotrim da Cunha, L., Chai, F., Dai, M., Gruber, N., Isensee, K., Ishii, M., Jiao, N., Lauvset, S. K., McKinley, G. A., Monteiro, P., Robinson, C., Sabine, C., Sanders, R., Schoo, K. L., Schuster, U., … Rojas Aldana, A. (2021). *Integrated ocean carbon research: A summary of ocean carbon research, and vision of coordinated ocean carbon research and observations for the next decade*. UNESCO.

Arrigo, K. R., van Dijken, G. L., & Bushinsky, S. (2008). Primary production in the southern ocean, 1997–2006. *Journal of Geophysical Research: Oceans*, 113: (C8). https://doi.org/10.1029/2007JC004551

Astoreca, R., Rousseau, V., Ruddick, K., Knechciak, C., Van Mol, B., Parent, J. Y., & Lancelot, C. (2009). Development and application of an algorithm for detecting phaeocystis globosa blooms in the case 2 southern north sea waters. *Journal of Plankton Research*, 31: (3), 287–300. https://doi.org/10.1093/plankt/fbn116

Astoreca, R., Rousseau, V., Ruddick, K., Knechciak, C., Van Mol, B., Parent, J.-Y., & Lancelot, C. (2008). Development and application of an algorithm for detecting phaeocystis globosa blooms in the case 2 southern north sea waters. *Journal of Plankton Research*, 31: (3), 287–300. https://doi.org/10.1093/plankt/fbn116

Aurin, D., Mannino, A., & Lary, D. J. (2018). Remote sensing of cdom, cdom spectral slope, and dissolved organic carbon in the global ocean. *Applied Sciences*, 8: 2687. https://doi.org/10.3390/app8122687

Austin, R. W., & Petzold, T. J. (1981). The determination of the diffuse attenuation coefficient of sea water using the coastal zone color scanner. In J. F. R. Gower (Ed.), *Oceanography from space* (pp. 239–256). Boston, MA.

Babin, M., Morel, A., Fournier-Sicre, V., Fell, F., & Stramski, D. (2003). Light scattering properties of marine particles in coastal and open ocean waters as related to the particle mass concentration. *Limnol. Oceanogr.*, 48: 843–859. https://doi.org/10.4319/lo.2003.48.2.0843

Baek, S., Koh, S., Son, M., Park, S., & Kim, W. (2025). A red tide quantification approach for an inexpensive multispectral camera onboard an aircraft. *IEEE Transactions on Geoscience and Remote Sensing*.

Bailey, S. W., et al. (2008). Sources and assumptions for the vicarious calibration of ocean color satellite observations. *Appl. Opt.*, 47: (12), 2035–2045.

Bailey, S. W., & Werdell, P. J. (2006). A multi-sensor approach for the on-orbit validation of ocean color satellite data products. *Remote Sensing of Environment*, 102: 12–23.

Baker, E. T., & Lavelle, J. W. (1984). The effect of particle size on the light attenuation coefficient of natural suspensions. *Journal of Geophysical Research*, 89: 8197–8203. https://doi.org/10.1029/jc089ic05p08197

Balch, W. M., Gordon, H. R., Bowler, B. C., Drapeau, D. T., & Booth, E. S. (2005). Calcium carbonate budgets in the surface global ocean based on moderate!resolution imaging spectroradiometer data. *J. Geophys. Res.*, 110: C07001. https://doi.org/10.1029/2004JC002560

Balch, W. M., & Mitchell, C. (2023). Remote sensing algorithms for particulate inorganic carbon (pic) and the global cycle of pic. *Earth-Science Reviews*, 239: 104363. https://doi.org/10.1016/j.earscirev.2023.104363

Barnard, A., Boss, E., Haëntjens, N., Orrico, C., Frouin, R., Tan, J., Chamberlain, P., et al. (2024). Design and verification of a highly accurate in-situ hyperspectral radiometric measurement system (hypernav) [Article 1369769]. *Frontiers in Remote Sensing*, 5: https://doi.org/10.3389/frsen.2024.1369769

Barnes, B. B., Bailey, S. W., Hu, C., & Franz, B. A. (2022). Vicarious calibration of the long near infrared band: Cross-sensor differences in sensitivity. *IEEE Transactions on Geoscience and Remote Sensing*, 60: 1–9.

Begliomini, F. N., Barbosa, C. C., Martins, V. S., Novo, E. M., Paulino, R. S., Maciel, D. A., Lima, T. M., O'Shea, R. E., Pahlevan, N., & Lamparelli, M. C. (2023). Machine learning for cyanobacteria mapping on tropical urban reservoirs using prisma hyperspectral data. *ISPRS Journal of Photogrammetry and Remote Sensing*, 204: 378–396. https://doi.org/10.1016/j.isprsjprs.2023.09.019

Begouen Demeaux, C., & Boss, E. (2022). Validation of remote-sensing algorithms for diffuse attenuation of downward irradiance using bgc-argo floats. *Remote Sens.*, 14: 4500. https://doi.org/10.3390/rs14184500

Begouen Demeaux, C., Boss, E., Frouin, R., et al. (2023). *Bgc-argo matchups with satellite sensors updated for 2023*. ZENODO. https://doi.org/10.5281/zenodo.8228243

Begouen Demeaux, C., Boss, E., Tan, J., & Frouin, R. (2024). Algorithms to retrieve the spectral diffuse attenuation coefficient of light in the ocean from remote sensing. *Opt Express*, 32: (2), 2507–2526. https://doi.org/10.1364/OE.505497

Behrenfeld, M. J., et al. (2006). Climate-driven trends in contemporary ocean productivity. *Nature*, 444: (7120), 752–755.

Behrenfeld, M. J., et al. (2009). Satellite-detected fluorescence reveals global physiology of ocean phytoplankton. *Science*, 326: (5955), 1403–1403.

Behrenfeld, M. J., Boss, E., Siegel, D., & Shea, D. M. (2005). Carbon-based ocean productivity and phytoplankton physiology from space. *Glob. Biogeochem. Cycles*, 19. https:// GB1006: https://doi.org/10.1029/2004GB002299

Behrenfeld, M. J., & Boss, E. S. (2014). Resurrecting the ecological underpinnings of ocean plankton blooms. *Annual Review of Marine Science*, 6: 167–194.

Behrenfeld, M. J., & Falkowski, P. G. (1997). A consumer's guide to phytoplankton primary productivity models. *Limnology Oceanogr.*, 42: (7), 1479–1491.

Behrenfeld, M. J., O'Malley, R. T., Boss, E. S., Westberry, T. K., Graff, J. R., Halsey, K. H., Milligan, A. J., Siegel, D. A., & Brown, M. B. (2016). Revaluating ocean warming impacts on global phytoplankton. *Nat. Clim. Chang*, 6: 323–330.

Bell, T. W., Cavanaugh, K. C., Saccomanno, V. R., Cavanaugh, K. C., Houskeeper, H. F., Eddy, N., et al. (2023). Kelpwatch: A new visualization and analysis tool to explore kelp canopy dynamics reveals variable response to and recovery from marine heatwaves [https]. *PLoS ONE*, 18: (3), e0271477. https://doi.org/10.1371/journal.pone.0271477

Bell, T. W., Cavanaugh, K. C., & Siegel, D. A. (2015). Remote monitoring of giant kelp biomass and physiological condition: An evaluation of the potential for the hyperspectral infrared imager (hyspiri) mission. *Remote Sens Environ.*, 167: 218–228. https://doi.org/10.1016/j.rse.2015.05.003

Bellacicco, M., Cornec, M., Organelli, E., Brewin, R. J. W., Neukermans, G., Volpe, G., Barbieux, M., Poteau, A., Schmechtig, C., D'Ortenzio, F., Marullo, S., Claustre, H., & Pitarch, J. (2019). Global variability of optical backscattering by non-algal particles from a biogeochemical-argo data set. *Geophys. Res. Lett.*, 46: 9767–9776.

Bellacicco, M., Pitarch, J., Organelli, E., Martinez-Vicente, V., Volpe, G., & Marullo, S. (2020). Improving the retrieval of carbon-based phytoplankton biomass from satellite ocean color observations. *Remote Sens.*, 12: 3640.

Bellacicco, M., Volpe, G., Briggs, N., Brando, V., Pitarch, J., Landolfi, A., et al. (2018). Global distribution of non-algal particles from ocean color data and implications for phytoplankton biomass detection. *Geophysical Research Letters*, 45: (15), 7672–7682.

Bellacicco, M., Volpe, G., Colella, S., Pitarch, J., & Santoleria, R. (2016). Influence of photoacclimation on the phytoplankton seasonal cycle in the mediterranean sea as seen by satellite. *Remote Sens. Environ.*, 184: 595–604.

Bi, S., Hieronymi, M., & Röttgers, R. (2023). Bio-geo-optical modelling of natural waters [Article 1196352]. *Frontiers in Marine Science*, 10: https://doi.org/10.3389/fmars.2023.1196352

Binding, C. E., Bowers, D. G., & Mitchelson-Jacob, E. G. (2005). Estimating suspended sediment concentrations from ocean colour measurements in moderately turbid waters; the impact of variable particle scattering properties. *Remote sensing of Environment*, 94: (3), 373–383. https://doi.org/10.1016/j.rse.2014.01.005

Bisson, K. M., Siegel, D. A., & DeVries, T. (2022). Diagnosing mechanisms of ocean carbon export in a satellite-based food web model [Article e2021GB007223]. *Global Biogeochemical Cycles*, 36: (5).

Bolpagni, R., Bresciani, M., Laini, A., Pinardi, M., Matta, E., Ampe, E. M., Giardino, C., Viaroli, P., & Bartoli, M. (2014). Remote sensing of phytoplankton-macrophyte coexistence in shallow hypereutrophic fluvial lakes. *Hydrobiologia*, 737: (1), 67–76.

Bonelli, A. G., Loisel, H., Jorge, D. S. F., Mangin, A., d'Andon, O. F., & Vantrepotte, V. (2022). A new method to estimate the dissolved organic carbon concentration from remote sensing in the global open ocean. *Remote Sensing of Environment*, 281: 113227. https://doi.org/10.1016/j.rse.2022.113227

Borger, C., Beirle, S., Butz, A., Scheidweiler, L. O., & Wagner, T. (2025). High-resolution observations of no2 and co2 emission plumes from enmap satellite measurements. *Environmental Research Letters*, 20: (044034), 2025.

Boss, E., Sherwood, C. R., Hill, P., & Milligan, T. (2018). Advantages and limitations to the use of optical measurements to study sediment properties. *Appl. Sci.*, 8: (12), 2692. https://doi.org/10.3390/app8122692

Bouvet, M., & Ramoino, F. (2010). Radiometric intercomparison of aatsr, meris, and aqua modis over dome concordia (antarctica). *Canadian Journal of Remote Sensing*, 36: (5), 464–473.

Bowers, D. G., Binding, C. E., & Ellis, K. M. (2007). Satellite remote sensing of the geographical distribution of suspended particle size in an energetic shelf sea. *Estuarine Coastal Shelf Sci.*, 27: 457–466.

Bracher, A., Banks, A. C., Xi, H., Dessailly, D., Gossn, J., Lebreton, C., Röttgers, R., Kwiatkowska, E., Chaikalis, S., Mehdipour, E., Pitta, E., Soppa, M. A., Wevers, J., & Zeri, C. (2025). Assessment of olci absorption coefficients for non-water components across all optical water classes. *Frontiers in Remote Sensing*, 6: https://doi.org/10.3389/frsen.2025.1545664

Bracher, A., Bouman, H. A., Bricaud, A., Brewin, R. W. J., Brotas, V., Ciotti, A. M., Clementson, L., Devred, E., Di Cicco, A. M., Dutkiewicz, S., Hardman-Mountford, N. J., Hickman, A. E., Hieronymi, M., Hirata, T., Losa, S. N., Mouw, C. B., Organelli, E., Raitsos, D. E., Uitz, J., … Wolanin, A. (2017). Obtaining phytoplankton diversity from ocean color: A scientific roadmap for future development. *Frontiers in Marine Science*, 4: 00055. https://doi.org/10.3389/fmars.2017.00055

Bracher, A., Brewin, R., Ciotti, A., Clementson, L., Hirata, T., Kostadinov, T., Mouw, C., & Organelli, E. (2022). Chapter 7 - applications of satellite remote sensing technology to the analysis of phytoplankton community structure on large scales. In L. A. Clementson, R. S. Eriksen, & A. Willis (Eds.), *Advances in phytoplankton ecology* (pp. 217–244). Elsevier. https://doi.org/10.1016/B978-0-12-822861-6.00015-7

Bracher, A., Dinter, T., Wolanin, A., Rozanov, V. V., Losa, S. N., & Soppa, M. A. (2017). Global monthly mean chlorophyll a surface concentrations from august 2002 to april 2012 for diatoms, coccolithophores and cyanobacteria from phytodoas algorithm version 3.3 applied to sciamachy data, in supplement to: Losa, svetlana n; soppa, mariana a; dinter, tilman; wolanin, aleksandra; brewin, robert j w; bricaud, annick; oelker, julia; peeken, ilka; gentili, bernard; rozanov, vladimir v; bracher, astrid (2017): Synergistic exploitation of hyper- and multi-spectral precursor sentinel measurements to determine phytoplankton functional types (synsenpft). frontiers in marine science, 4(203), 22 pp. *Frontiers in Marine Science*, 4: 203. https://doi.org/10.1594/PANGAEA.870486

Bracher, A., Soppa, M. A., Gege, P., Losa, S. N., Silva, B., Steinmetz, F., & Dröscher, I. (2021). Extension of atmospheric correction polymer to hyperspectral sensors: Application to hico and first results for desis data. *2021 IEEE International Geoscience and Remote Sensing Symposium IGARSS*, 1237–1240. https://doi.org/10.1109/IGARSS47720.2021.9553568

Bracher, A., Taylor, B. B., Taylor, M., Dinter, T., Röttgers, R., & Steinmetz, F. (2015). Using empirical orthogonal functions derived from remote sensing reflectance for the prediction of concentrations of phytoplankton pigments. *Ocean Science*, 11: 139–158.

Bracher, A., Vountas, M., Dinter, T., Burrows, J. P., Röttgers, R., & Peeken, I. (2009). Quantitative observation of cyanobacteria and diatoms from space using phytodoas on sciamachy data. *Biogeosciences*, 6: (5), 751–764.

Brewin, R. J., Sathyendranath, S., Kulk, G., Rio, M. H., Concha, J. A., Bell, T. G., et al. (2023). Ocean carbon from space: Current status and priorities for the next decade. *Earth-Science Reviews*, 240: 104386.

Brewin, R. J. W., Sathyendranath, S., Platt, T., Bouman, H., Ciavatta, S., Dall'Olmo, G., Dingle, J., Groom, S., Jonsson, ¨. B., Kostadinov, T. S., Kulk, G., Laine, M., MartínezVicente, M., Psarra, S., Raitsos, D. E., Richardson, K., Marie-H´el'ene, R., Rousseaux, C. S., Salisbury, J., … Walker, P. (2021). Sensing the ocean biological carbon pump from space: A review of capabilities, concepts, research gaps and future developments. *Earth Sci. Rev.*, 217: 103604.

Bricaud, A., Ciotti, A. M., & Gentili, B. (2012). Spatial-temporal variations in phytoplankton size and colored detrital matter absorption at global and regional scales, as derived from twelve years of seawifs data (1998–2009). *Global Biogeochemical Cycles*, 26: https://doi.org/10.1029/2010gb003952

Bricaud, A., Morel, A., Babin, M., Allali, K., & Claustre, H. (1998). Variations of light absorption by suspended particles with chlorophyll a concentration in oceanic (case 1)waters: Analysis and implications for bio-optical models. *Journal of Geophysical Research: Oceans*, 103: (C13), 31033–31044. https://doi.org/10.1029/98JC02712

Bricaud, A., Babin, M., Morel, A., & Claustre, H. (1995). Variability in the chlorophyll-specific absorption coefficients of natural phytoplankton: Analysis and parameterization. *Journal of Geophysical Research: Oceans*, 100: (C7), 13321–13332. https://doi.org/https://doi.org/10.1029/95JC00463

Brockmann, C., Doerffer, R., Peters, M., Stelzer, K., Embacher, S., & Ruescas, A. (2016). Evolution of the c2rcc neural network for sentinel 2 and 3 for the retrieval of ocean color products in normal and extreme optically complex waters. *Proceeding of Living Planet Symposium (Prague*.

Bulgarelli, B., Kisselev, V. B., & Roberti, L. (1999). Radiative transfer in the atmosphere–ocean system: The finite-element method. *Applied Optics*, 38: (9), 1530–1542.

Campbell, J., Antoine, D., Armstrong, R., Arrigo, K., Balch, W., Barber, R., Behrenfeld, M., Bidigare, R., Bishop, J., Carr, M.-E., Esaias, W., Falkowski, P., Hoepffner, N., Iverson, R., Kiefer, D., Lohrenz, S., Marra, J., Morel, A., Ryan, J., … Yoder, J. (2002). Comparison of algorithms for estimating ocean primary production from surface chlorophyll, temperature, and irradiance. *Global Biogeochemical Cycles*, 16: (3), 9-1-9–15. https://doi.org/10.1029/2001GB001444

Cannizzaro, J. P., Carder, K. L., Chen, F. R., Heil, C. A., & Vargo, G. A. (2008). A novel technique for detection of the toxic dinoflagellate, karenia brevis, in the gulf of mexico from remotely sensed ocean color data. *Continental Shelf Research*, 28: 137–158.

Cao, F., Fichot, C. G., Hooker, S. B., & Miller, W. L. (2014). Improved algorithms for accurate retrieval of uv/visible diffuse attenuation coefficients in optically complex, inshore waters. *Remote Sensing of Environment*, 144: 11–27.

Cao, F., Tzortziou, M., Hu, C., Mannino, A., Fichot, C. G., Del Vecchio, R., Najjar, R. G., & Novak, M. (2018). Remote sensing retrievals of colored dissolved organic matter and dissolved organic carbon dynamics in north American estuaries and their margins. *Remote Sensing of Environment*, 205: 151–165. https://doi.org/10.1016/j.rse.2017.11.014

Carr, M. E., Friedrichs, M. A., Schmeltz, M., Aita, M. N., Antoine, D., Arrigo, K. R., Yamanaka, Y., et al. (2006). A comparison of global estimates of marine primary production from ocean color [Article 741-770. II: Topical Studies in Oceanography]. *Deep Sea Research Part*, 53: 5–7.

Casal, G., Sánchez-Carnero, D.-G., Kuster, T., & Freire, J. (2012). Assessment of ahs (airborne hyperspectral scanner) sensor to map macroalgal communities on the ría de vigo and ría de aldán coast (nw spain). *Marine Biology*, 159: 1997–2013.

Casey, K. A., Rousseaux, C. S., Gregg, W. W., Boss, E., et al. (2020). A global compilation of in situ aquatic high spectral resolution inherent and apparent optical property data for remote sensing applications. *Earth System Science Data*, 12: (2), 1123–1139. https://essd.copernicus.org/articles/12/1123/2020/

Castagna, A., Dierssen, H. M., Devriese, L. I., Everaert, G., Knaeps, E., & Sterckx, S. (2023). Evaluation of historic and new detection algorithms for different types of plastics over land and water from hyperspectral data and imagery. *Remote Sens. Environ.*, 298: 113834. https://doi.org/10.1016/j.rse.2023.113834

Castagna, A., Dierssen, H. M., Organelli, E., Bogorad, M., Mortelmans, J., Vyverman, W., & Sabbe, K. (2021). Optical detection of harmful algal blooms in the belgian coastal zone: A cautionary tale of chlorophyll c3 [Sci., Sec. Ocean Observation]. *Front.*, 8: 770340. https://doi.org/10.3389/fmars.2021.770340

Catlett, D., & Siegel, D. A. (2018). Phytoplankton pigment communities can be modeled using unique relationships with spectral absorption signatures in a dynamic coastal environment. *Journal of Geophysical Research-Oceans*, 123: 246–264.

Catlett, D., Siegel, D. A., Matson, P. G., Wear, E. K., Carlson, C. A., Lankiewicz, T. S., & Iglesias-Rodriguez, M. D. (2023). Integrating phytoplankton pigment and dna meta-barcoding observations to determine phytoplankton composition in the coastal ocean. *Limnology and Oceanography*, 68: (2), 361–376. https://doi.org/https://doi.org/10.1002/lno.12274

Cawse-Nicholson, K., Townsend, P. A., Schimel, D., Assiri, A. M., et al. (2021). Nasa's surface biology and geology designated observable: A perspective on surface imaging algorithms. *Remote Sensing of Environment*, 257: 112349. https://doi.org/10.1016/j.rse.2021.112349

CEOS. (2018). Feasibility study for an aquatic ecosystem earth observing sensor. In A. G. Dekker (Ed.), *Ceos report 2018*. CSIRO.

Cesana, I., Bresciani, M., Cogliati, S., Giardino, C., Gupana, R. S., Manca, D., Santabarbara, S., Pinardi, M., Austoni, M., Lami, A., & Colombo, R. (2021). Preliminary investigation on phytoplankton dynamics and primary production models in an oligotrophic lake from remote sensing measurements. *Sensors*, 21: https://doi.org/10.3390/s21155072

Cetinić, I., Rousseaux, C. S., Carroll, I. T., et al. (2024). Phytoplankton composition from space: Requirements, opportunities, and challenges. *Remote Sensing of Environment*, 302: 113964. https://doi.org/10.1016/j.rse.2023.113964

Chami, M., Bracher, A., Briottet, X., Costa, M., Damm-Reiser, A., Dekker, A., Garaba, S., Gege, P., Giardino, C., Knaeps, E., Kutser, T., Lucas, R., Odermatt, D., Otter, G., Pahlevan, N., Pinnel, N., Sterckx, S., & Turpie, K. (2025). Galene: A proposed future satellite mission dedicated to the observation of coastal and inland aquatic ecosystems, including the monitoring of water quality and the detection of marine plastics. one ocean science congress 2025, nice, france, 3-6 jun 2025. *OOS2025-262*, 2025: https://doi.org/10.5194/oos2025-262

Chami, M., Lafrance, B., Fougnie, B., Chowdhary, J., Harmel, T., & Waquet, F. (2015). Osoaa: A vector radiative transfer model of coupled atmosphere-ocean system for a rough sea surface application to the estimates of the directional variations of the water leaving reflectance to better process multi-angular satellite sensors data over the ocean. *Optics Express*, 23: (21), 27829–27852.

Chase, A. P., Boss, E., Cetinic´, I., & Slade, W. (2017). Estimation of phytoplankton accessory pigments from hyperspectral reflectance spectra: Toward a global algorithm. *Journal of Geophysical Research: Oceans*, 122: 9725–9743. https://doi.org/10.1002/2017JC012859pALACIOS

Chase, A. P., Boss, E. S., Haëntjens, N., Culhane, E., Roesler, C., & Karp-Boss, L. (2022). Plankton imagery data inform satellite-based estimates of diatom carbon. *Geophysical Research Letters*, 49: (13), e2022GL098076. https://doi.org/https://doi.org/10.1029/2022GL098076

Chowdhary, J., Cairns, B., & Travis, L. D. (2006). Contribution of water-leaving radiances to multiangle, multispectral polarimetric observations over the open ocean: Bio-optical model results for case 1 waters. *Applied optics*, 45: (22), 5542–5567.

Ciotti, A. M., & Bricaud, A. (2006). Retrievals of a size parameter for phytoplankton and spectral light absorption by colored detrital matter from water-leaving radiances at seawifs channels in a continental shelf region off brazil. *Limnol. Oceanogr. Methods*, 4: 237–253.

Clark, D. K., Gordon, H., Voss, K., Ge, Y., Broenkow, W., & Trees, C. (1997). Validation of atmospheric correction over the oceans. *Journal of Geophysical Research: Atmospheres*, 102: 17209–17217.

Clementson, L. A., Oubelkheir, K., Ford, P. W., & Blondeau-Patissier, D. (2022). Distinct peaks of uv-absorbing compounds in cdom and particulate absorption spectra of near-surface great barrier reef coastal waters, associated with the presence of trichodesmium spp. (ne australia). *Remote Sensing*, 14: (15). https://doi.org/10.3390/rs14153686

Cogliati, S., Sarti, F., Chiarantini, L., Cosi, M., Lorusso, R., Lopinto, E., Colombo, R., et al. (2021). The prisma imaging spectroscopy mission: Overview and first performance analysis. *Remote sensing of environment*, 262: 112499.

Concha, J., Mannino, A., Franz, B., Bailey, S., & Kim, W. (2019). Vicarious calibration of goci for the seadas ocean color retrieval. *International Journal of Remote Sensing*, 40: (10), 3984–4001.

Coppo, P., Taiti, A., Pettinato, L., Francois, M., Taccola, M., & Drusch, M. (2017). Fluorescence imaging spectrometer (floris) for esa flex mission. *Remote Sensing*, 9: (7), 649. https://doi.org/10.3390/rs9070649

Cosnefroy, H., Leroy, M., & Briottet, X. (1996). Selection and characterization of saharan and arabian desert sites for the calibration of optical satellite sensors. *Remote Sensing of Environment*, 58: (1), 101–114.

Cózar, A., Arias, M., Suaria, G., et al. (2024). Proof of concept for a new sensor to monitor marine litter from space. *Nature Comm.*, 15: 4637. https://doi.org/10.1038/s41467-024-48674-7

Dall'Olmo, G., & Gitelson, A. A. (2005). Effect of bio-optical parameter variability on the remote estimation of chlorophyll-a concentration in turbid productive waters: Experimental results. *Applied Optics*, 44: 412.

Daniels, C. J., Tyrrell, T., Poulton, A. J., & Pettit, L. (2012). The influence of lithogenic material on particulate inorganic carbon measurements of coccolithophores in the bay of biscay. *Limnol. Oceanogr.*, 57: (1), 145–153. https://doi.org/10.4319/lo.2012.57.1.0145

Dash, P., Walker, N., Mishra, D., D'Sa, E., & Ladner, S. (2012). Atmospheric correction and vicarious calibration of oceansat-1 ocean color monitor (ocm) data in coastal case 2 waters. *Remote Sensing*, 4: (6), 1716–1740.

de Vries, R. V. F., Garaba, S. P., & Royer, S. J. (2023). Hyperspectral reflectance of pristine, ocean weathered and biofouled plastics from a dry to wet and submerged state. *Earth System Science Data*, 15: (12), 5575–5596. https://doi.org/10.5194/essd-15-5575-2023

Defoin-Platel, M., & Chami, M. (2007). How ambiguous is the inverse problem of ocean color in coastal waters? *Journal of Geophysical Research-Oceans*, 112: (C3), C03004. https://doi.org/10.1029/2006JC003847

Deglint, J. L., Wong, A., Lamm, M. S., & Clausi, D. A. (2018). Preprint: The feasibility of automated identification of six algae types using neural networks and fluorescence-based spectral-morphological features.

Dekker, A. G., Phinn, S. R., Anstee, J., et al. (2011). Intercomparison of shallow water bathymetry, hydro-optics, and benthos mapping techniques in australian and caribbean coastal environments. *Limnol Oceanogr*, 9: 396–425.

Deng, L., Zhou, W., Xu, J., Cao, W., Liao, J., & Zhao, J. (2022). Estimation of vertical size-fractionated phytoplankton primary production in the northern south China sea. *Ecological Indicators*, 135: 108546.

Devred, E., Turpie, K. R., Moses, W., Klemas, V. V., Moisan, T., Babin, M., Toro-Farmer, G., Forget, M.-H., & Jo, Y.-H. (2013). Future retrievals of water column bio-optical properties using the hyperspectral infrared imager (hyspiri). *Remote Sensing*, 5: (12), 6812–6837. https://doi.org/10.3390/rs5126812

Dierssen, H. M., Ackleson, S. G., Joyce, K. E., Hestir, E. L., Castagna, A., Lavender, S., & McManus, M. A. (2021). Living up to the hype of hyperspectral aquatic remote sensing: Science, resources and outlook. *Frontiers in Environmental Science*, 9: 649528.

Dierssen, H. M., Bracher, A., Brando, V., Loisel, H., & Ruddick, K. (2020). Data needs for hyperspectral detection of algal diversity across the globe. *Oceanography*, 33: 74–79.

Dierssen, H. M., Chlus, A., & B., R. (2015). Hyperspectral discrimination of floating mats of seagrass wrack and the macroalgae sargassum in coastal waters of greater florida bay using airborne remote sensing. *Remote Sens. Environ.*, 167: 247–258. https://doi.org/10.1016/j.rse.2015.01.027

Dierssen, H. M., Gierach, M., Guild, L. S., Mannino, A., Salisbury, J., Schollaert Uz, S., Werdell, P. J., et al. (2023). Synergies between nasa's hyperspectral aquatic missions pace, glimr, and sbg: Opportunities for new science and applications [Article e2023JG007574]. *Journal of Geophysical Research: Biogeosciences*, 128: (10).

Dierssen, H. M., Vandermeulen, R. A., Barnes, B. B., Castagna, A., Knaeps, E., & Vanhellemont, Q. (2022). Qwip: A quantitative metric for quality control of aquatic reflectance spectral shape using the apparent visible wavelength. *Frontiers in Remote Sensing*, 3: 869611.

Dinter, T., Rozanov, V., Burrows, J. P., & Bracher, A. (2015). Retrieval of light availability in ocean waters utilizing signatures of vibrational raman scattering in hyper-spectral satellite measurements. *Ocean Science*, 11: 373–389.

Dogliotti, A. I., Ruddick, K. G., Nechad, B., Doxaran, D., & Knaeps, E. (2015). A single algorithm to retrieve turbidity from remotely-sensed data in all coastal and estuarine waters. *Remote Sens. Environ.*, 156: 157–168. https://doi.org/10.1016/j.rse.2014.09.020

Doxaran, D., Ehn, J., Bélanger, S., Matsuoka, A., Hooker, S., & Babin, M. (2012). Optical characterisation of suspended particles in the mackenzie river plume (canadian arctic ocean) and implications for ocean colour remote sensing. *Biogeosciences*, 9: 3213–3229. https://doi.org/10.5194/bg-9-3213-2012

Doxaran, D., Froidefond, J. M., Lavender, S. J., & Castaing, P. (2002). Spectral signature of highly turbid waters: Application with spot data to quantify suspended particulate matter concentrations. *Remote Sens. Environ.*, 81: 149–161. https://doi.org/10.1016/S0034-4257(01)00341-8

Doxaran, D., Ruddick, K., McKee, D., Gentili, B., Tailliez, D., Chami, M., & Babin, M. (2009). Spectral variations of light scattering by marine particles in coastal waters, from the visible to the near infrared. *Limnol. Oceanogr.*, 2009: (54), 1257–1271.

Dufois, F., Hardman-Mountford, N. J., Greenwood, J., Richardson, A. J., Feng, M., & Matear, R. J. (2016). Anticyclonic eddies are more productive than cyclonic eddies in subtropical gyres because of winter mixing. *Science Advances*, 2(5), e1600282: https://doi.org/10.1126/sciadv.1600282

Eplee, R. E., Robinson, W. D., Bailey, S. W., Clark, D. K., Werdell, P. J., Wang, M., Barnes, R. A., & McClain, C. R. (2001). Calibration of seawifs. ii. vicarious techniques. *Appl. Opt.*, 40: (36), 6701–6718. https://doi.org/10.1364/AO.40.006701

EUMETSAT. (2018). *Sentinel-3 olci inherent optical properties website. link to algorithm theoretical basis document (atbd)*. Retrieved November 18, 2024, from https://www.eumetsat.int/S3-OLCI-IOP

Evers-King, H., Martinez-Vicente, V., Brewin, R. J. W., Dall'Olmo, G., Hickman, A. E., Jackson, T., Kostadinov, T. S., Krasemann, H., Loisel, H., Röttgers, R., Roy, S., Stramski, D., Thomalla, S., Platt, T., & Sathyendranath, S. (2017). Validation and intercomparison of ocean color algorithms for estimating particulate organic carbon in the oceans. *Frontiers in Marine Science*, 4: 251. https://doi.org/10.3389/fmars.2017.00251

Falkowski, P. G., Barber, R. T., & Smetacek, V. (1998). Biogeochemical controls and feedbacks on ocean primary production. *Science*, 281: (5374), 200–206.

Fan, Y., Li, W., Chen, N., Ahn, J.-H., Park, Y.-J., Kratzer, S., Schroeder, T., Ishizaka, J., Chang, R., & Stamnes, K. (2021). Oc-smart: A machine learning based data analysis platform for satellite ocean color sensors. *Remote Sensing of Environment*, 253:

Fell, F., & Fischer, J. (2001). Numerical simulation of the light field in the atmosphere–ocean system using the matrix-operator method. *Journal of Quantitative Spectroscopy and Radiative Transfer*, 69: (3), 351–388.

Feng, L., & Hu, C. (2016). Cloud adjacency effects on top-of-atmosphere radiance and ocean color data products: A statistical assessment. *Remote Sens. Environ.*, 174: 301–313. https://doi.org/10.1016/j.rse.2015.12.020

Feng, L., & Hu, C. (2017). Land adjacency effects on modis aqua top-of-atmosphere radiance in the shortwave infrared: Statistical assessment and correction. *J. Geophys. Res. Oceans*, 122: 4802–4818. https://doi.org/10.1002/2017JC012874

Fichot, C. G., & Benner, R. (2012). The spectral slope coefficient of chromophoric dissolved organic matter (s275-295) as a tracer of terrigenous dissolved organic carbon in river-influenced ocean margins. *Limnology and Oceanography*, 57: 1453–1466. https://doi.org/10.4319/lo.2012.57.5.1453

Fichot, C. G., Kaiser, K., Hooker, S. B., Amon, R. M., Babin, M., Belanger, S., Walker, S. A., & Benner, R. (2013). Pan-arctic distributions of continental runoff in the arctic ocean. *Scientific reports*, 3: 1053. https://doi.org/10.1038/srep01053

Fichot, C. G., Sathyendranath, S., & Miller, W. L. (2008). Seauv and seauvc: Algorithms for the retrieval of uv/visible diffuse attenuation coefficients from ocean color. *Remote Sensing of Environment*, 112: 1584–1602.

Fougnie, B., & Bach, R. (2008). Monitoring of radiometric sensitivity changes of space sensors using deep convective clouds: Operational application to parasol. *IEEE Transactions on Geoscience and Remote Sensing*, 47: (3), 851–861.

Fournier, C., Quesada, A., Cirés, S., & Saberioon, M. (2024). Discriminating bloom-forming cyanobacteria using lab-based hyperspectral imagery and machine learning: Validation with toxic species under environmental ranges. *Science of the Total Environment*, 932: 172741.

Franz, B. A., Bailey, S. W., Werdell, P. J., & McClain, C. R. (2007). Sensor-independent approach to the vicarious calibration of satellite ocean color radiometry. *Applied Optics*, 46: (22), 5068–5082.

Friedrichs, M. A., Carr, M. E., Barber, R. T., Scardi, M., Antoine, D., Armstrong, R. A., Winguth, A., et al. (2009). Assessing the uncertainties of model estimates of primary productivity in the tropical pacific ocean. *Journal of Marine Systems*, 76: (1-2), 113–133.

Frouin, R. J., Franz, B. A., Ibrahim, A., Knobelspiesse, K., Ahmad, Z., Cairns, B., Zhai, P. W., et al. (2019). Atmospheric correction of satellite ocean-color imagery during the pace era. *Frontiers in earth science*, 7: 145. https://doi.org/10.3389/feart.2019.00145

Garaba, S. P., Albinus, M., Bonthond, G., Flöder, S., Miranda, M. L. M., Rohde, S., Yong, J. Y. L., & Wollschläger, J. (2023). Bio-optical properties of the cyanobacterium nodularia spumigena. *Earth System Science Data*, 15: (9), 4163–4179. https://doi.org/10.5194/essd-15-4163-2023

Garaba, S. P., & Dierssen, H. M. (2020). Hyperspectral ultraviolet to shortwave infrared characteristics of marine-harvested, washed-ashore and virgin plastics. *Earth System Science Data*, 12: (1), 77–86. https://doi.org/10.5194/essd-12-77-2020

Garaba, S. P., & Park, Y.-J. (2024). Riverine litter monitoring from multispectral fine pixel satellite images. *Environmental Advances*, 15: 100451. https://doi.org/10.1016/j.envadv.2023.100451

Garcia, R. A., Lee, Z., Barnes, B. B., Hu, C., Dierssen, H. M., & Hochberg, E. J. (2020). Benthic classification and iop retrievals in shallow water environments using meris imagery. *Remote Sensing of Environment*, 249: 112015.

Gege, P., & Dekker, A. G. (2020). Spectral and radiometric measurement requirements for inland, coastal and reef waters. *Remote Sensing*, 12: (14), 2247.

Gege, P. (1998). Characterization of the phytoplankton in lake constance for classification by remote sensing [ISBN, 0071-1128]. *Arch. Hydrobiol. Spec. Issues Advanc. Limnol.*, 53:

Gege, P. (2014). Wasi-2d: A software tool for regionally optimized analysis of imaging spectrometer data from deep and shallow waters. *Computers Geosciences*, 62: 208–215. https://doi.org/https://doi.org/10.1016/j.cageo.2013.07.022

Gendall, L., Schroeder, S., Wills, P., Hessing-Lewis, M., & Costa, M. (2023). A multi-satellite mapping framework for floating kelp. *Remote Sensing*, 15: (5), 1276.

Giardino, C., Brando, V. E., Gege, P., Pinnel, N., Hochberg, E., Knaeps, E., Dekker, A., et al. (2019). Imaging spectrometry of inland and coastal waters: State of the art, achievements and perspectives. *Surveys in Geophysics*, 40: (3), 401–429. https://doi.org/10.1007/s10712-018-9476-0

Giardino, C., Candiani, G., & Zilioli, E. (2005). Detecting chlorophyll-a in lake garda using toa meris radiances. *Photogramm Eng Rem Sens*, 71: (9), 1045–1051.

Giardino, C., Pahlevan, N., Fabbretto, A., Panizza, L., Pellegrino, A., Vandermeulen, R., Gascon, F., et al. (2025). Acix-iii aqua: Evaluation of atmospheric correction for hyperspectral prisma imagery over inland and coastal waters. *International Journal of Remote Sensing*, 1–25. https://doi.org/10.1080/01431161.2025.2574517

Giardino, C., Pellegrino, A., Fabbretto, A., Panizza, L., et al. (2025). *Acix-iii aqua: Evaluation of atmospheric correction processors for hyperspectral satellite over inland and coastal waters*. Zenodo. https://doi.org/10.5281/zenodo.17660438

Gitelson, A. A., Schalles, J. F., & Hladik, C. M. (2007). Remote chlorophyll-a retrieval in turbid, productive estuaries: Chesapeake bay case study. *Remote Sensing of Environment*, 109: 464–472.

GIZ. (2023). Advances in remote sensing of plastic waste [87 pp.]. In P. Giang & N. Ortwig (Eds.), *Deutsche gesellschaft für internationale zusammenarbeit (giz) gmbh*. https://www.giz.de/en/downloads/giz-2023-en-advances-in-remote-sensing-of-plastic-waste.pdf

Gordon, H. R. (1987). Calibration requirements and methodology for remote sensors viewing the ocean in the visible. *Rem. Sens. Environ.*, 22: 103–126.

Gordon, H. R. (1998). In-orbit calibration strategy for ocean color sensors. *Remote Sensing of Environment*, 63: 265–278.

Gordon, H. R., & Du, T. (2001). Light scattering by nonspherical particles: Application to coccoliths detached from emiliania huxleyi. *Limnol. Oceanogr.*, 46: 1438–1454. https://doi.org/10.4319/lo.2001.46.6.1438

Gordon, H. R., & McCluney, W. R. (1975). Estimation of the depth of sunlight penetration in the sea for remote sensing. *Applied Optics*, 14: (2), 413–416.

Gorroño, J., Guanter, L., Graf, L. V., & Gascon, F. (2024). A framework for the estimation of uncertainties and spectral error correlation in sentinel-2 level-2a data products. *IEEE Transactions on Geoscience and Remote Sensing*, 62: 1–13.

Graff, J. R., Westberry, T. K., Milligan, A. J., Brown, M. B., Dall'Olmo, G., van Dongen-Vogels, V., Behrenfeld, M. J., et al. (2015). Analytical phytoplankton carbon measurements spanning diverse ecosystems. *Deep Sea research part I: Oceanographic research papers*, 102: 16–25.

Guanter, L., Brell, M., Chan, J. C. W., Giardino, C., Gomez-Dans, J., Mielke, C., Yokoya, N., et al. (2019). Synergies of spaceborne imaging spectroscopy with other remote sensing approaches. *Surveys in Geophysics*, 40: 657–687.

Gupana, R. S., Odermatt, D., Cesana, I., Giardino, C., Nedbal, L., & Damm, A. (2021). Remote sensing of sun-induced chlorophyll-a fluorescence in inland and coastal waters: Current state and future prospects. *Remote Sensing of Environment*, 262: 112482.

Gupana, R. S., Damm, A., Rahaghi, A. I., Minaudo, C., & Odermatt, D. (2022). Non-photochemical quenching estimates from in situ spectroradiometer measurements: Implications on remote sensing of sun-induced chlorophyll fluorescence in lakes. *Opt. Express*, 30: (26), 46762–46781. https://doi.org/10.1364/OE.469402

Gupana, R. S., Odermatt, D., Irani Rahaghi, A., Minaudo, C., Werther, M., Giardino, C., & Damm, A. (2025). Remote sensing of sun-induced fluorescence in a deep lake: Disentangling quenching mechanisms improves relationship with chlorophyll-a concentration estimates. *IEEE Journal of Selected Topics in Applied Earth Observations and Remote Sensing*, PP: 1–20. https://doi.org/10.1109/JSTARS.2025.3528911

Hagolle, O., Dedieu, G., Mougenot, B., Debaecker, V., Duchemin, B., & Meygret, A. (2008). Correction of aerosol effects on multi-temporal images acquired with constant viewing angles: Application to formosat-2 images [Remote Sensing Data Assimilation Special Issue]. *Remote Sensing of Environment*, 112: (4), 1689–1701. https://doi.org/https://doi.org/10.1016/j.rse.2007.08.016

Han, B., Loisel, H., Vantrepotte, V., Mériaux, X., Bryère, P., Ouillon, S., Dessailly, D., Xing, Q., & Zhu., J. (2016). Development of a semi-analytical algorithm for the retrieval of suspended particulate matter from remote sensing over clear to very turbid waters. *Remote Sens.*, 8: 211. https://doi.org/10.3390/rs8030211

Hansell, D. A., & Carlson, C. A. (2002). *Biogeochemistry of marine dissolved organic matter*. Academic Press.

Harringmeyer, J. P., Ghosh, N., Weiser, M. W., Thompson, D. R., Simard, M., Lohrenz, S. E., & Fichot, C. G. (2024). A hyperspectral view of the nearshore mississippi river delta: Characterizing suspended particles in coastal wetlands using imaging spectroscopy. *Remote Sensing of Environment*, 301: 113943. https://doi.org/10.1016/j.rse.2023.113943

He, Q., Zhan, H., Cai, S., & Zhan, W. (2021). Eddy-induced nearsurface chlorophyll anomalies in the subtropical gyres: Biomass or physiology? *Geophysical Research Letters*, 48: https://doi.org/10.1029/2020GL091975

He, X., Bai, Y., Zhu, Q., & Gong, F. (2010). A vector radiative transfer model of coupled ocean–atmosphere system using matrix-operator method for rough sea-surface. *Journal of Quantitative Spectroscopy and Radiative Transfer*, 111: (10), 1426–1448.

Hedley, J. D., Mirhakak, M., Wentworth, A., & Dierssen, H. M. (2018). Influence of three-dimensional coral structures on hyperspectral benthic reflectance and water-leaving reflectance. *Applied Sciences*, 8: 2688.

Hedley, J. D., & Mobley, C. D. (2021). *Hydrolight 6.0 ecolight 6.0 technical documentation*. Numerical Optics Ltd.

Hedley, J. D., Russell, B. J., Randolph, K., Perez-Castro, M. A., Vasquez-Elizondo, R. M., Enriquez, S., & Dierssen, H. M. (2017). Remote sensing of seagrass leaf area index and species: The capability of a model inversion method assessed by sensitivity analysis and hyperspectral data of florida bay. *Frontiers in Marine Science*, 4: 362.

Heege, T., Kiselev, V., Wettle, M., & Hung, N. N. (2014). Operational multi-sensor monitoring of turbidity for the entire mekong delta. *International Journal of Remote Sensing*, 35: (8), 2910–2926. https://doi.org/10.1080/01431161.2014.890300

Helms, J. R., Stubbins, A., Ritchie, J. D., Minor, E. C., Kieber, D. J., & Mopper, K. (2008). Absorption spectral slopes and slope ratios as indicators of molecular weight, source, and photobleaching of chromophoric dissolved organic matter. *Limnology and Oceanography*, 53: 955–969. https://doi.org/10.4319/lo.2008.53.3.0955

Hestir, E. L., Brando, V. E., Bresciani, M., Giardino, C., Matta, E., Villa, P., & Dekker, A. G. (2015). Measuring freshwater aquatic ecosystems: The need for a hyperspectral global mapping satellite mission [Special

Issue on the Hyperspectral Infrared Imager (HyspIRI)]. *Remote Sensing of Environment*, 167: 181–195. https://doi.org/https://doi.org/10.1016/j.rse.2015.05.023

Hieronymi, M., Müller, D., & Doerffer, R. (2017). The olci neural network swarm (onns): A bio-geo-optical algorithm for open ocean and coastal waters [Sci]. *Front.*, 4: 140. https://doi.org/10.3389/fmars.2017.00140

Hill, V. J., Zimmerman, R. C., Bissett, W. P., Dierssen, H. M., & Kohler, D. D. (2014). Evaluating light availability, seagrass biomass, and productivity using hyperspectral airborne remote sensing in saint joseph's bay, florida. *Estuaries and Coasts*, 1–23.

Hintz, N. H., Stribel, M., & Zeising, M. (2021). Changes in spectral quality of underwater light alter phytoplankton community composition. *Limnol Oceanogr*, 66: 3327–3337. https://doi.org/10.1002/lno.11882

Hirata, T. (2020). *Derivation of the absorption coefficient of coloured dissolved organic matter (cdom), sgli standard products and algorithm theoretical basis documents (atbd).* JAXA.

Hirawake, T., Oida, J., Yamashita, Y., Waga, H., Abe, H., Nishioka, J., Nomura, D., Ueno, H., & Ooki, A. (2021). Water mass distribution in the northern bering and southern chukchi seas using light absorption of chromophoric dissolved organic matter. *Progress in Oceanography*, 197: 102641. https://doi.org/10.1016/j.pocean.2021.102641

Hirawake, T., Takao, S., Horimoto, N., Ishimaru, T., Yamaguchi, Y., & Fukuchi, M. (2011). A phytoplankton absorption-based primary productivity model for remote sensing in the southern ocean. *Polar Biol.*, 34: (2), 291–302.

Hochberg, E. J., & Atkinson, M. J. (2003). Capabilities of remote sensors to classify coral, algae, and sand as pure and mixed spectra. *Remote Sensing of Environment*, 85: 174–189.

Hoepffner, N., & Sathyendranath, S. (1991). Effect of pigment composition on absorption properties of phytoplankton. *Mar. Ecol. Prog. Ser.*, 73: l–23.

Holtrop, T., Huisman, J., Stomp, M., Biersteker, L., Aerts, J., Grébert, T., Partensky, F., Garczarek, L., & Jan van der Woerd, H. (2021). Vibrational modes of water predict spectral niches for photosynthesis in lakes and oceans. *Nature Ecology and Evolution*, 5: (1), 55–66. https://doi.org/10.1038/s41559-020-01330-x

Hong, S. M., Baek, S.-S., Yun, D., Kwon, Y.-H., Duan, H., Pyo, J., & Cho, K. H. (2021). Monitoring the vertical distribution of habs using hyperspectral imagery and deep learning models. *Science of the Total Environment*, 794: 148592.

Hu, C., et al. (2022). Global reconstruction of phytoplankton functional types from chlorophyll a fluorescence. *Remote Sensing of Environment*, 282: 113264.

Hu, C. (2022). Hyperspectral reflectance spectra of floating matters derived from hyperspectral imager for the coastal ocean (hico) observations. *Earth Syst. Sci. Data*, 14: 1183–1192. https://doi.org/10.5194/essd-14-1183-2022

Hu, C. (2024). A depth-invariant index to map floating algae: A conceptual design. *Remote Sensing Letters*, 15: (1), 1–9. https://doi.org/10.1080/2150704X.2023.2294746

Hu, C. (2025). On the logic of remote detection of plastic litter in the aquatic environments: A revisit. *Remote Sensing of Environment*, 329: 114911.

Hu, C., Barnes, B. B., Qi, L., Gower, J. F. R., Jiao, J., & Xie, Y. (2025). Monitoring pelagic sargassum in the atlantic ocean from space: Principles and practices. *Harmful Algae*, 144: 102840. https://doi.org/10.1016/j.hal.2025.102840

Hu, C., Chen, Z., Clayton, T. D., Swarzenski, P., Brock, J. C., & Muller-Karger, F. E. (2004). Assessment of estuarine water-quality indicators using modis medium-resolution bands: Initial results from tampa bay, fl. *Remote Sensing of Environment*, 93: 423–441. https://doi.org/10.1016/j.rse.2004.08.007

Hu, C., Feng, L., Lee, Z., Davis, C. O., Mannino, A., McClain, C. R., & Franz, B. A. (2012). Dynamic range and sensitivity requirements of satellite ocean color sensors: Learning from the past. *Appl. Opt.*, 51: 6045–6062.

Hu, C., Muller-Karger, F. E., Taylor, C. J., Carder, K. L., Kelble, C., Johns, E., & Heil, C. A. (2005). Red tide detection and tracing using modis fluorescence data: A regional example in sw florida coastal waters. *Remote Sensing of Environment*, 97: 311–321.

Hunter, P. D., Gilvear, D. J., Tyler, A. N., et al. (2010). Mapping macrophytic vegetation in shallow lakes using the compact airborne spectrographic imager (casi). *Aquat Conserv*, 20: 717–727. https://doi.org/10.1002/aqc.1144

Hunter, P. D., Tyler, A. N., Présing, M., Kovács, A. W., & Preston, T. (2008). Spectral discrimination of phytoplankton color groups: The effect of suspended particulate matter and sensor spectral resolution. *Remote Sensing of Environment*, 112: (4), 1527–1544.

Ibrahim, A., Franz, B., Ahmad, Z., Healy, R., Knobelspiesse, K., Gao, B. C., Zhai, P. W., et al. (2018). Atmospheric correction for hyperspectral ocean color retrieval with application to the hyperspectral imager for the coastal ocean (hico). *Remote Sensing of Environment*, 204: 60–75.

Ilić, M., Walden, S., Hammerstein, S. K., Stockenreiter, M., Stibor, H., & Fink, P. (2023). Pigment and fluorescence proxies to estimate functional diversity of phytoplankton communities. *Fundamental and Applied Limnology*, 196: (3-4), 229–249.

IOCCG. (2006). *Remote sensing of inherent optical properties: Fundamentals, tests of algorithms, and applications* (Z.-P. Lee, Ed.; Vol. No. 5). https://doi.org/10.25607/OBP-96

IOCCG. (2010). *Atmospheric correction for remotely-sensed ocean-colour products* (M. Wang, Ed.; Vol. No. 10). https://doi.org/10.25607/OBP-101

IOCCG. (2013). *In-flight calibration of satellite ocean-colour sensors* (R. Frouin, Ed.; Vol. No. 14). https://doi.org/10.25607/OBP-105

IOCCG. (2018). *Inherent optical property measurements and protocols: Absorption coefficient* (A. R. Neeley & A. Mannino, Eds.; Vol. 1.0). https://doi.org/10.25607/OBP-119

IOCCG. (2019). *Uncertainties in ocean colour remote sensing* (F. Mélin, Ed.; Vol. No. 18). https://doi.org/10.25607/OBP-696

IOC-UNESCO. (2024). *Ioc enhances research on climate change impacts on phytoplankton*. Retrieved January 29, 2024, from https://iocaribe.ioc-unesco.org/en/news-updates/ioc-enhances-research-climate-change-impacts-phytoplankton

Isada, T., Hirawake, T., Kobayashi, N., Nosaka, Y., Natsuike, M., Imai, I., Suzuki, K., & Saitoh, S.-I. (2015). Hyperspectral optical discrimination of phytoplankton community structure in funka bay and its implications for ocean-color remote sensing of diatoms. *Remote Sensing of Environment*, 159: 134–151.

Ishizaka, J., Kitaura, Y., Touke, Y., Sasaki, H., Tanaka, A., Murakami, H., Suzuki, T., Matsuoka, K., & Nakata, H. (2006). Satellite detection of red tide in ariake sound, 1998–2001. *J Oceanogr*, 62: 37–45.

Jamet, C., Loisel, H., & Dessailly, D. (2012). Retrieval of the spectral diffuse attenuation coefficient kd (□) in open and coastal ocean waters using a neural network inversion. *J. Geophys. Res. Oceans*, 117 (C10): https://doi.org/10.1029/2012JC008076

Jin, Z., Charlock, T. P., Rutledge, K., Stamnes, K., & Wang, Y. (2006). Analytical solution of radiative transfer in the coupled atmosphere-ocean system with a rough surface. *Appl. Opt.*, 45: 7443–7455.

Jin, Z., & Stamnes, K. (1994). Radiative transfer in nonuniformly refracting layered media: Atmosphere–ocean system. *Applied optics*, 33: (3), 431–442.

Johannessen, S. C., Miller, W. L., & Cullen, J. J. (2003). Calculation of uv attenuation and colored dissolved organic matter absorption spectra from measurements of ocean color. *J. Geophys. Res.*, 108: (C9), 3301.

Joiner, J., Yoshida, Y., Guanter, L., & Middleton, E. M. (2016). New methods for the retrieval of chlorophyll red fluorescence from hyperspectral satellite instruments: Simulations and application to gome-2 and sciamachy. *Atmospheric Measurement Techniques*, 9: (8), 3939–3967.

Jorge, D. S. F., Loisel, H., Jamet, C., Dessailly, D., Demaria, J., et al. (2021). A three-step semi analytical algorithm (3saa) for estimating inherent optical properties over oceanic, coastal, and inland waters from remote sensing reflectance. *Remote Sens. Environment*, 263: https://doi.org/10.1016/j.rse.2021.112537

Karthick, M., Shanmugam, P., & He, X. (2024). Enhanced polymer atmospheric correction algorithm for water-leaving radiance retrievals from hyperspectral/multispectral remote sensing data in inland and coastal waters. *Optics Express*, 32: (5), 7659–7681.

Kattawar, G. W., & Adams, C. N. (1989). Stokes vector calculations of the submarine light field in an atmosphere-ocean with scattering according to a rayleigh phase matrix: Effect of interface refractive index on radiance and polarization. *Limnology and Oceanography*, 34: (8), 1453–1472.

Kim, Y., Yoo, S., & Son, Y. B. (2016). Optical discrimination of harmful cochlodinium polykrikoides blooms in korean coastal waters. *Optics express*, 24: (22), A1471–A1488. https://doi.org/10.1364/OE.24.0A1471

Kim, Y. J., Kim, W., Im, J., Choi, J., & Lee, S. (2023). Atmospheric-correction-free red tide quantification algorithm for goci based on machine learning combined with a radiative transfer simulation. *ISPRS Journal of Photogrammetry and Remote Sensing*, 199: 197–213. https://doi.org/10.1016/j.isprsjprs.2023.04.007

Kisselev, V. B., Roberti, L., & Perona, G. (1995). Finite-element algorithm for radiative transfer in vertically inhomogeneous media: Numerical scheme and applications. *Appl. Opt.*, 34: (36), 8460–8471.

Köhler, P., Behrenfeld, M. J., Landgraf, J., Joiner, J., Magney, T. S., & Frankenberg, C. (2020). Global retrievals of solar-induced chlorophyll fluorescence at red wavelengths with tropomi. *Geophysical Research Letters*, 47: (15). https://doi.org/10.1029/2020GL087541

Konik, M., Peña, A., Hirawake, T., Hunt, B. P. V., Vishnu, P. S., Eisner, L. B., Bracher, A., Xi, H., & Costa, M. (2025). Changes in subarctic pacific phytoplankton communities over the last two decades. *Frontiers in Marine Science*, 12:

Kostadinov, T. S., Milutinovic, S., Marinov, I., & Cabre, A. (2016). Carbon-based phytoplankton size classes retrieved via ocean color estimates of the particle size distribution. *Ocean Sci.*, 12: 561–575.

Kostadinov, T. S., Robertson Lain, L., Kong, C. E., Zhang, X., Maritorena, S., Bernard, S., Loisel, H., Jorge, D. S. F., Kochetkova, E., Roy, S., Jonsson, B., Martinez-Vicente, V., & Sathyendranath, S. (2023). Ocean color

algorithm for the retrieval of the particle size distribution and carbon-based phytoplankton size classes using a two-component coated-sphere backscattering model. *Ocean Sci.*, 19: 703–727. https://doi.org/10.5194/os-19-703-2023

Kostadinov, T. S., Siegel, D. A., & Maritorena, S. (2009). Retrieval of the particle size distribution from satellite ocean color observations. *J. Geophys. Res. Oceans*, 114 (C9): https://doi.org/10.1029/2009JC005303

Kostadinov, T. S., Siegel, D. A., & Maritorena, S. (2010). Global variability of phytoplankton functional types from space: Assessment via the particle size distribution. *Biogeosciences*, 7: (3), 3239–3257. https://doi.org/10.5194/bg-7-3239-2010

Kotchenova, S. Y., Vermote, E. F., Matarrese, R., & Klemm, F. J., Jr. (2006). Validation of a vector version of the 6s radiative transfer code for atmospheric correction of satellite data. part i: Path radiance. *Appl. Opt.*, 45, (2006): 6762–6774.

Kramer, S. J., Maritorena, S., Cetinić, I., Jeremy Werdell, P., & Siegel, D. A. (2024). Phytoplankton communities quantified from hyperspectral ocean reflectance correspond to pigment-based communities. *Optics Express*, 32: (20), 34482–34491.

Kritten, L., Preusker, R., & Fischer, J. (2020). A new retrieval of sun-induced chlorophyll fluorescence in water from ocean color measurements applied on olci l-1b and l-2. *Remote Sensing*, 12: https://doi.org/10.3390/rs12233949

Kruse, F. A., Lefkoff, A. B., Boardman, J. W., Heidebrecht, K. B., Shapiro, A. T., Barloon, P. J., & Goetz, A. F. (1993). The spectral image processing system (sips)—interactive visualization and analysis of imaging spectrometer data. *Remote sensing of environment*, 44: (2-3), 145–163.

Kuhwald, K., Schneider von Deimling, J., Schubert, P., & Oppelt, N. (2022). How can sentinel-2 contribute to seagrass mapping in shallow, turbid baltic sea waters? *Remote Sensing in Ecology and Conservation*, 8: (3), 328–346. https://doi.org/10.1002/rse2.246

Kurekin, A. A., Miller, P. I., & Van der Woerd, H. J. (2014). Satellite discrimination of karenia mikimotoi and phaeocystis harmful algal blooms in european coastal waters: Merged classification of ocean color data. *Harmful Algae*, 31: 163–176.

Kutser, T., Dekker, A. G., & Skirving, W. (2003). Modeling spectral discrimination of great barrier reef benthic communities by remote sensing instruments. *Limnology and Oceanography*, 48: 497–510. https://doi.org/10.4319/lo.2003.48.1_part_2.0497

Kutser, T., Hedley, J., Giardino, C., Roelfsema, C., & Brando, V. E. (2020). Remote sensing of shallow waters–a 50 year retrospective and future directions. *Remote Sensing of Environment*, 240: 111619.

Kwon, S., Seo, W., Noh, H., & Kim, B. (2022). Hyperspectral retrievals of suspended sediment using cluster-based machine learning regression in shallow waters. *Science of The Total Environment*, 833: 155168. https://doi.org/10.1016/j.scitotenv.2022.155168

Lange, P. K., Werdell, P. J., Craig, S., Erickson, Z. K., Dall'Olmo, G., Brewin, R., Zubkov, M., Tarran, G., Bouman, H. A., Bracher, A., Poulton, N., Lomas, M., Slade, W., & Cetinić, I. (2020). Radiometric approach for the detection of picophytoplankton assemblages across oceanic fronts. *Optics Express*, 28: (18), 25682.

Lazzari, N., Becerro, M. A., Sanabria-Fernandez, J. A., & Martín-López, B. (2021). Assessing social-ecological vulnerability of coastal systems to fishing and tourism. *Science of The Total Environment*, 784: 147078. https://doi.org/10.1016/j.scitotenv.2021.147078

Lazzari, P., Álvarez, E., Terzić, E., Cossarini, G., Chernov, I., D'Ortenzio, F., & Organelli, E. (2021). Cdom spatiotemporal variability in the mediterranean sea: A modelling study. *JMSE*, 9: 176. https://doi.org/10.3390/jmse9020176

Le Quéré, C., Harrison, S. P., Colin Prentice, I., Buitenhuis, E. T., Aumont, O., Bopp, L., et al. (2005). Ecosystem dynamics based on plankton functional types for global ocean biogeochemistry models. *Glob. Chang. Biol.*, 11: 2016–2040.

Lee, Z., Carder, K., Arnone, R., & He, M. X. (2007). Determination of primary spectral bands for remote sensing of aquatic environments. *Sensors*, 7: 3428–3441. https://doi.org/10.3390/s7123428

Lee, Z., Carder, K. L., & Arnone, R. A. (2002). Deriving inherent optical properties from water color: A multiband quasi-analytical algorithm for optically deep waters. *Applied Optics*, 41: (27), 5755–5772. https://doi.org/10.1364/AO.41.005755

Lee, Z., Carder, K. L., Marra, J., Steward, R. G., & Perry, M. J. (1996). Estimating primary production at depth from remote sensing. *Appl. Opt.*, 35: 463–474.

Lee, Z., Carder, K. L., Mobley, C. D., Steward, R. G., & Patch, J. S. (1998). Hyperspectral remote sensing for shallow waters. i. a semianalytical model. *Applied optics*, 37: 6329–6338.

Lee, Z., Du, K. P., & Arnone, R. (2005). A model for the diffuse attenuation coefficient of downwelling irradiance. *J. Geophys. Res.*, 110: C02016. https://doi.org/10.1029/2004JC002275

Lee, Z., Hu, C., Shang, S., Du, K., Lewis, M., Arnone, R., & Brewin, R. (2013). Penetration of uv-visible solar radiation in the global oceans: Insights from ocean color remote sensing. *Journal of Geophysical Research: Oceans*, 118: (9), 4241–4255. https://doi.org/10.1002/jgrc.20308

Lee, Z., Lance, V. P., Shang, S., Vaillancourt, R., Freeman, S., Lubac, B., Wei, G., et al. (2011). An assessment of optical properties and primary production derived from remote sensing in the southern ocean (so gasex). *Journal of Geophysical Research: Oceans*, 116(C4):

Lee, Z., & Marra, J. (2022). The use of vgpm to estimate oceanic primary production: A "tango" difficult to dance. *Journal of Remote Sensing*. https://doi.org/10.34133/2022/9851013

Lee, Z., Marra, J., Perry, M. J., & Kahru, M. (2015). Estimating oceanic primary productivity from ocean color remote sensing: A strategic assessment. *Journal of Marine Systems*, 149: 50–59.

Lee, Z., Shang, S., Hu, C., & Zibordi, G. (2014). Spectral interdependence of remote-sensing reflectance and its implications on the design of ocean color satellite sensors. *Applied Optics/*, 53: 3301–3310.

Lee, Z., Wang, T., Zhao, L., Wang, D., Ye, X., Shang, S., & Yu, . X. (2024). Cross-satellite atmospheric correction for consistent remote sensing reflectance from multiple ocean color satellites: Concept and demonstrations. *Journal of Remote Sensing*, 4: 0302.

Legleiter, C. J., King, T. V., Carpenter, K. D., Hall, N. C., Mumford, A. C., Slonecker, E. T., Graham, J. L., Stengel, V. G., Simon, N., & Rosen, B. H. (2022). Spectral mixture analysis for surveillance of harmful algal blooms (smash): A field-, laboratory-, and satellite-based approach to identifying cyanobacteria genera from remotely sensed data. *Remote Sensing of Environment*, 279: 113089.

Lehmann, M., Gurlin, D., Pahlevan, N., Alikas, K., Conroy, T., Anstee, J., Balasubramanian, S., Barbosa, C., Binding, C., Bracher, A., & Bresciani, M. (2023). Gloria-a globally representative hyperspectral in situ dataset for optical sensing of water quality. *Scientific data*, 10: (1), 100.

Letelier, R. M., & Abbott, M. R. O. P.-N. (1996). An analysis of chlorophyll fluorescence algorithms for the moderate resolution imaging spectrometer (modis). *Remote Sensing of Environment*, 58: 215–223.

Li, M., Organelli, E., Serva, F., Bellacicco, M., Landolfi, A., Pisano, A., et al. (2024). Phytoplankton spring bloom inhibited by marine heatwaves in the north-western mediterranean sea. *Geophysical Research Letters*, 51, e2024GL109141: https://doi.org/10.1029/2024GL109141

Li, M., Shen, F., Organelli, E., Luo, W., Li, R., Sun, X., & Wei, X. (2024). Disentangling particle composition to improve space-based quantification of poc in optically complex estuarine and coastal waters. *IEEE Transactions on Geoscience and Remote Sensing*, 62: 1–15.

Li, X., Lee, Z., Wang, D., & Shang, S. (2025). Atmospheric correction of coastal waters based on satellite-aeronet-oc matchups via neural networks. *Journal of Remote Sensing*, 5: 0886.

Li, X., Shang, S., Lee, Z., Lin, G., Zhang, Y., Wu, J., Kang, Z., Liu, X., Yin, C., & Gao, Y. (2021). Detection and biomass estimation of phaeocystis globosa blooms off southern China from uav-based hyperspectral measurements. *IEEE Transactions on Geoscience and Remote Sensing*. https://doi.org/10.1109/TGRS.2021.3051466

Lian, D. M. X. L., Laws, E. A., Liu, T., Wang, J., Shang, S., & Lee, Z. (2024). A trapezoidal relationship between solar radiation and chlorophyll concentrations at the center of the south pacific gyre. *Progress in Oceanography*, 225: (2024), 103281.

Liu, R., Xiao, Y., Ma, Y., Cui, T., & An, J. (2022). Red tide detection based on high spatial resolution broad band satellite data using a pseudo hue angle (pha-ri). *ISPRS Journal of Photogrammetry and Remote Sensing*, 184: 131–147.

Loisel, H., Nicolas, J. M., Sciandra, A., Stramski, D., & Poteau, A. (2006). Spectral dependency of optical backscattering by marine particles from satellite remote sensing of the global ocean. *J. Geophys. Res. Oceans*, 111 (C9):

Loisel, H., Stramski, D., Dessailly, D., Jamet, C., Li, L., & Reynolds, R. A. (2018). An inverse model for estimating the optical absorption and backscattering coefficients of seawater from remote-sensing reflectance over a broad range of oceanic and coastal marine environments. *J. Geophys. Res. Oceans*, 123: 2141–2171. https://doi.org/10.1002/2017JC013632

Lomas, M. W., Neeley, A. R., Vandermeulen, R., Mannino, A., Thomas, C., Novak, M. G., & Freeman, S. A. (2024). Phytoplankton optical fingerprint libraries for development of phytoplankton ocean-colour satellite products. *Scientific Data*, 11: 168.

Losa, S., Soppa, M. A., Dinter, T., Wolanin, A., Brewin, R. J. W., Bricaud, A., Oelker, J., Peeken, I., Gentili, B., Rozanov, V. V., & Bracher, A. (2017). Synergistic exploitation of hyper- and multispectral precursor sentinel measurements to determine phytoplankton functional types at best spatial and temporal resolution (synsenpft). *Frontiers in Marine Science*, 4: 203. https://doi.org/10.3389/fmars.2017.00203

Lubac, B., Loisel, H., Guiselin, N., Astoreca, R., Artigas, L. F., & Mériaux, X. (2008). Hyperspectral and multispectral ocean color inversions to detect phaeocystis globosa blooms in coastal waters. *J. Geophys. Res.*, 113: (6), 1–17.

Mannino, A., Russ, M. E., & Hooker, S. B. (2008). Algorithm development and validation for satellite-derived distributions of doc and cdom in the u. s. middle atlantic bight. *J. Geophys. Res.*, 113: C07051. https://doi.org/10.1029/2007JC004493

Maranon, E., Cermeno, P., Huete-Ortega, M., Lopez-Sandoval, D. C., Mourino Carballido, B., & Rodríguez-Ramos, T. (2014). Resource supply overrides temperature as a controlling factor of marine phytoplankton growth. *PLoS One*, 9: e99312.

Marie, L., Gege, P., Damm, A., & Odermatt, D. (2025). Differentiating phytoplankton taxa in lakes using hyperspectral in situ reflectance and imaging microscopy. *Science of the Total Environment*, 1003: 180718.

Markelin, L., Simis, S. G., Hunter, P. D., Spyrakos, E., Tyler, A. N., Clewley, D., & Groom, S. (2016). Atmospheric correc- tion performance of hyperspectral airborne imagery over a small eutrophic lake under changing cloud cover. *Remote Sens*, 9: (1), 2.

Martínez-Vicente, V., Dall'Olmo, G., Tarran, G., Boss, E., & Sathyendranath, S. (2013). Optical backscattering is correlated with phytoplankton carbon across the atlantic ocean. *Geophys. Res. Lett.*, 40: 1154–1158.

Martínez-Vicente, V., Evers-King, H., Roy, S., Kostadinov, T. S., Tarran, G. A., Graff, J. R., Brewin, R. J. W., Dall'Olmo, G., Jackson, T., Hickman, A. E., Rottgers, R., Krasemann, H., Maranon, E., Platt, T., & Sathyendranath, S. (2017). Intercomparison of ocean color algorithms for picophytoplankton carbon in the ocean [Sci]. *Front.*, 4: 378.

Matsuoka, A., Hooker, S. B., Bricaud, A., Gentili, B., & Babin, M. (2013). Estimating absorption coefficients of colored dissolved organic matter (cdom) using a semi-analytical algorithm for southern beaufort sea waters: Application to deriving concentrations of dissolved organic carbon from space. *Biogeosciences*, 10: 917–927. https://doi.org/10.5194/bg-10-917-2013

McKinna, L. I. W. (2010). Optical detection and quantification of trichodesmium spp. within the great barrier reef [Doctoral dissertation, James Cook University].

McKinna, L. I. W., Cetinić, I., Chase, A. P., & Werdell, P. J. (2019). Approach for propagating radiometric data uncertainties through nasa ocean color algorithms. *Frontiers in Earth Science*, 7: 176. https://doi.org/10.3389/feart.2019.00176

McKinna, L. I. W., Cetinić, I., & Werdell, P. J. (2021). Development and validation of an empirical ocean color algorithm with uncertainties: A case study with the particulate backscattering coefficient [Article e2021JC017231]. *Journal of Geophysical Research: Oceans*, 126: (5).

McKinna, L. I. W., & Werdell, P. J. (2024a). *Inherent optical properties, version 1.0*. NASA EarthDATA Algorithm Publication Tool. https://doi.org/10.5067/ZGBW3QECROJ2

McKinna, L. I. W., & Werdell, P. J. (2024b). *Spectral diffuse attenuation coefficient, version 1.0*. NASA EarthDATA Algorithm Publication Tool. https://doi.org/10.5067/E6JP5Z1CGRFT

McKinna, L. I. W., Werdell, P. J., & Proctor, C. W. (2016). Implementation of an analytical raman scattering correction for satellite ocean-color processing. *Optics Express*, 24: (14), A1123–A1137. https://doi.org/10.1364/OE.24.0A1123

Mélin, F., & Vantrepotte, V. (2015). How optically diverse is the coastal ocean? *Remote Sensing of Environment*, 160: 235–251. https://doi.org/10.1016/j.rse.2015.01.023

Mélin, F., & Zibordi, G. (2010). Vicarious calibration of satellite ocean color sensors at two coastal sites. *Applied optics*, 49: (5), 798–810.

Mikkelsen, O. A., Slade, W. H., Leeuw, T., Dana, D. R., & Pottsmith, C. (2020). American geophysical union, ocean sciences meeting. *A new submersible instrument for measuring hyperspectral backscattering in natural waters (hyper-bb)*, (3198).

Miller, R. L., & McKee, B. A. (2004). Using modis terra 250 m imagery to map concentrations of total suspended matter in coastal waters. *Remote Sensing of Environment*, 93: 259–266. https://doi.org/10.1016/j.rse.2004.07.012

Mishra, S., & Mishra, D. R. (2012). Normalized difference chlorophyll index: A novel model for remote estimation of chlorophyll-a concentration in turbid productive waters. *Remote Sensing of Environment*, 117: 394–406.

Mitchell, C., Hu, C., Bowler, B., Drapeau, D., & Balch, W. M. (2017). Estimating particulate inorganic carbon concentrations of the global ocean from ocean color measurements using a reflectance difference approach. *Journal of Geophysical Research: Oceans*, 122: (11), 2017. https://doi.org/10.1002/2017JC013146

Mobley, C. D., Sundman, L. K., Davis, C. O., Bowles, J. H., Downes, T. V., Leathers, R. A., Gleason, A., et al. (2005). Interpretation of hyperspectral remote-sensing imagery by spectrum matching and look-up tables. *Applied Optics*, 44: (17), 3576–3592.

Mora-Soto, A., Schroeder, S., Gendall, L., Wachmann, A., Narayan, G. R., Read, S., Pearsall, I., Rubidge, E., Lessard, J., Martell, K., Wills, P., & Costa, M. (2024). Kelp dynamics and environmental drivers in the southern salish sea, british columbia, canada [Article 1323448. Sci]. *Front.*, 11: https://doi.org/10.3389/fmars.2024.1323448

Morel, A., & Antoine, D. (1994). Heating rate within the upper ocean in relation to its bio-optical state. *Journal of Physical Oceanography*, 24: (7), 1652–1665.

Morel, A., & Gentili, B. (2009). A simple band ratio technique to quantify the colored dissolved and detrital organic material from ocean color remotely sensed data. *Remote Sensing of Environment*, 113: 998–1011. https://doi.org/10.1016/j.rse.2009.01.008

Morel, A., & Maritorena, S. (2001). Bio-optical properties of oceanic waters: A reappraisal. *J. Geophys. Res.*, 106: (C4), 7163–7180.

Morel, A., Antoine, D., & Gentili, B. (2002). Bidirectional reflectance of oceanic waters: Accounting for raman emission and varying particle scattering phase function. *Appl. Opt.*, 41: (30), 6289–6306. https://doi.org/10.1364/AO.41.006289

Morrison, J. R. (2003). In situ determination of the quantum yield of phytoplankton chlorophyll a fluorescence: A simple algorithm, observations, and a model. *Limnology and Oceanography*, 48: (2), 618–631. https://doi.org/10.4319/lo.2003.48.2.0618

Mouw, C. B., Greb, S., Aurin, D., DiGiacomo, P. M., Lee, Z. P., et al. (2015). Aquatic color radiometry remote sensing of coastal and inland waters: Challenges and recommendations for future satellite missions. *Remote Sensing of Environment*, 160: 15–30. https://doi.org/10.1016/j.rse.2015.02.001

Mouw, C. B., Hardman-Mountford, N. J., Alvain, S., Bracher, A., Brewin, R. J., Bricaud, A., Uitz, J., et al. (2017). A consumer's guide to satellite remote sensing of multiple phytoplankton groups in the global ocean. *Frontiers in Marine Science*, 4: 41. https://doi.org/10.3389/fmars.2017.00041

Muller-Karger, F. E., Hestir, E., Ade, C., Turpie, K., Roberts, D., Siegel, D., Miller, R., Humm, D., Izenberg, N., Keller, M., Morgan, F., Frouin, R., Dekker, A., Gardner, R., Goodman, J., Schaeffer, B., Franz, B., Pahlevan, N., Mannino, A. G., … Appeltans, W. (2018). Satellite sensor requirements for monitoring essential biodiversity variables of coastal ecosystems. *Ecol Appl*, 28: (3), 749–760.

Nasiha, H. J., Shanmugam, P., & Sundaravadivelu, R. (2019). Estimation of sediment settling velocity in estuarine and coastal waters using optical remote sensing data. *Adv. Space Res.*, 2019: (63), 3473–3488.

Nasiha, H. J., Wang, Z., Giannini, F., & Costa, M. (2022). Spatial variability of in situ above-water reflectance in coastal dynamic waters: Implications for satellite match-up analysis. *Front. Remote Sens.*, 3: 876748. https://doi.org/10.3389/frsen.2022.876748

Nechad, B., Ruddick, K. G., & Park, Y. (2010). Calibration and validation of a generic multisensor algorithm for mapping of total suspended matter in turbid waters. *Remote Sensing of the Environment*, 114: 854–866. https://doi.org/10.1016/j.rse.2009.11.022

Nelson, N. B., & Siegel, D. A. (2013). The global distribution and dynamics of chromophoric dissolved organic matter. *Annual Review of Marine Science*, 5: 447–476. https://doi.org/10.1146/annurev-marine-120710-100751

Neville, R. A., & Gower, J. F. R. (1977). Passive remote sensing of phytoplankton via chlorophyll □ fluorescence [–3493]. *Journal of Geophysical Research*, 82: (3487), 1896–1977. https://doi.org/10.1029/JC082i024p03487

Noh, J. H., Kim, W., Son, S., Ahn, J.-H., & Park, Y. (2018). Remote quantification of cochlodinium polykrikoides blooms occurring in the east sea using geostationary ocean color imager (goci). *Harmful algae*, 73: 129–137.

Novak, M. G., Burmeister, H., & Röttgers, R. (2024). Hyperspectral measurements of light backscattering by particles in water with a fixed angle setup: Proof of concept and instrument calibration. *Opt. Express*, 32: 23722–23735.

Novoa, S., Doxaran, D., Ody, A., Vanhellemont, Q., Lafon, V., Lubac, B., & Gernez, P. (2017). Atmospheric corrections and multi-conditional algorithm for multi-sensor remote sensing of suspended particulate matter in low-to-high turbidity levels coastal waters. *Remote Sens.*, 9: 61. https://doi.org/10.3390/rs9010061

Oelker, J., Losa, S. N., Richter, A., & Bracher, A. (2022). Tropomi-retrieved underwater light attenuation in three spectral regions in the ultraviolet to blue. *Frontiers in Marine Science*, 9: 787992. https://doi.org/10.3389/fmars.2022.787992

Oelker, J., Richter, A., Dinter, T., Rozanov, V. V., Burrows, J. P., & Bracher, A. (2019). Global diffuse attenuation coefficient derived from vibrational raman scattering detected in hyperspectral backscattered satellite spectra. *Optics Express*, 27: (12), A829–A855. https://doi.org/10.1364/OE.27.00A829

Ohall, A., Bisson, K., Garaba, S. P., & Rivero-Calle, S. (2025). The marine debris hyperspectral reference library collection (madlib). *Earth System Science Data*, 17: 7293–7311. https://doi.org/10.5194/essd-17-7293-2025

Ohlmann, J. C., Siegel, D. A., & Gautier, C. (1996). Ocean mixed layer radiant heating and solar penetration: A global analysis. *Journal of Climate*, 9: (10), 226–2280.

Oida, J., Hirawake, T., Yamashita, Y., Abe, H., Nishioka, J., Waga, H., Nomura, D., & Kakehi, S. (2024). Classification of optical water groups in the subarctic pacific and adjacent seas using satellite-derived light absorption spectra of chromophoric dissolved organic matter. *Deep Sea Research Part I: Oceanographic Research Papers*, 208: 104313. https://doi.org/10.1016/j.dsr.2024.104313

Olmanson, L. G., Brezonik, P. L., & Bauer, M. E. (2015). Remote sensing for regional lake water quality assessment: Capabilities and limitations of current and upcoming satellite systems. In T. Younos & T. E. Parece (Eds.), *Advances in watershed science and assessment* (pp. 111–140). Springer.

Ondrusek, M., Stengel, E., Kinkade, C. S., Vogel, R. L., Keegstra, P., Hunter, C., & Kim, C. (2012). The development of a new optical total suspended matter algorithm for the chesapeake bay. *Remote Sensing of Environment*, 119: 243–254. https://doi.org/10.1016/j.rse.2011.12.018

O'Neill, J., & Costa, M. (2013). Mapping eelgrass (zostera marina) in the gulf islands national park reserve of canada using high spatial resolution satellite and airborne imagery. *Remote Sensing of Environment*, 133: 152–167.

Orenstein, E. C., Ayata, S. D., Maps, F., Becker, É. C., Benedetti, F., Biard, T., et al. (2022). Machine learning techniques to characterize functional traits of plankton from image data. *Limnology and Oceanography*, 67: (11), 2496–2513.

Organelli, E., Bricaud, A., Antoine, D., & Matsuoka, A. (2014). Seasonal dynamics of light absorption by chromophoric dissolved organic matter (cdom) in the nw mediterranean sea (boussole site). *Deep Sea Research Part I: Oceanographic Research Papers*, 91: 72–85. https://doi.org/10.1016/j.dsr.2014.05.003

Organelli, E., & Claustre, H. (2019). Small phytoplankton shapes colored dissolved organic matter dynamics in the north atlantic subtropical gyre. *Geophysical Research Letters*, 46: 12183–12191. https://doi.org/10.1029/2019GL084699

Organelli, E., Dall'Olmo, G., Brewin, R. J. W., Nencioli, F., & Tarran, G. A. (2020). Drivers of spectral optical scattering by particles in the upper 500 m of the atlantic ocean. *Opt. Express*, 28: 34147–34166.

Organelli, E., Dall'Olmo, G., Brewin, R. J. W., Tarran, G. A., Boss, E., & Bricaud, A. (2018). The open-ocean missing backscattering is in the structural complexity of particles. *Nat. Commun.*, 9: (5439), 1–11.

Organelli, E., Nuccio, C., Lazzara, L., Uitz, J., Bricaud, A., & Massi, L. (2017). On the discrimination of multiple phytoplankton groups from light absorption spectra of assemblages with mixed taxonomic composition and variable light conditions. *Applied Optics*, 56: (14), 3952–3968.

O'Shea, R. E., Pahlevan, N., Smith, B., Bresciani, M., Egerton, T., Giardino, C., Li, L., Moore, T., Ruiz-Verdú, A., Ruberg, S., Simis, S. G. H., Stumpf, R., & Vaičiūtė, D. (2021). Advancing cyanobacteria biomass estimation from hyperspectral observations: Demonstrations with hico and prisma imagery. *Remote Sensing of Environment*, 266: 112693.

Ouillon, S., Douillet, P., Petrenko, A., Neveux, J., Dupouy, C., Froidefond, J.-M., et al. (2008). Optical algorithms at satellite wavelengths for total suspended matter in tropical coastal waters. *Sensors*, 8: (7), 4165–4185. https://doi.org/10.3390/s8074165

Ozesmi, S. L., & Bauer, M. E. (2002). Satellite remote sensing of wetlands. *Wetl Ecol Manag*, 10: (5), 381–402.

Pahlevan, N., Mangin, A., Balasubramanian, S. V., Smith, B., Alikas, K., Barbosa, C., Bélanger, S., Binding, C., Bresciani, M., Giardino, C., Gurlin, D., Fan, Y., Harmel, T., Lehmann, M., Ma, R., Olmanson, L., Oppelt, N., Reynaud, N., Sander de Carvalho, L., … Warren, M. A. (2021). Acix-aqua: Global assessment of atmospheric correction methods for studying lakes, rivers, and nearshore coastal waters using landsat-8 and sentinel-2 missions. *Remote Sensing of Environment*, 258: 112366.

Park, Y., Garaba, S. P., & Sainte-Rose, B. (2021). Detecting the great pacific garbage patch floating plastic litter using worldview-3 satellite imagery. *Optics Express*, 29: (22), 35288–35298. https://doi.org/10.1364/OE.440380

Phinn, S. R., Roelfsema, C. M., & Mumby, P. J. (2012). Multi-scale, object-based image analysis for mapping geomorphic and ecological zones on coral reefs. *International Journal of Remote Sensing*, 33: (12), 3768–3797. https://doi.org/10.1080/01431161.2011.633122

Poulin, C., Zhang, X., Yang, P., & Huot, Y. (2018). Diel variations of the attenuation, backscattering and absorption coefficients of four phytoplankton species and comparison with spherical, coated spherical and hexahedral particle optical models. *J. Quant. Spectrosc. Radiat. Transf.*, 217: 288–304.

Qi, L., & Hu, C. (2021). To what extent can ulva and sargassum be detected and separated in satellite imagery? *Harmful Algae*, 103: 102001. https://doi.org/10.1016/j.hal.2021.102001

Qi, L., Hu, C., Mikelsons, K., et al. (2020). In search of floating algae and other organisms in global oceans and lakes. *Remote Sens. Environ.*, 239: 111659. https://doi.org/10.1016/j.rse.2020.111659

Qi, L., Lee, Z., Hu, C., & Wang, M. (2017). Requirement of minimal signal-to-noise ratios of ocean color sensors and uncertainties of ocean color products. *J. Geophys. Res. Oceans*, 122: 2595–2611. https://doi.org/10.1002/2016JC012558

Qi, L., Wang, M., & Hu, C. (2023). Uncertainties in modis-derived ulva prolifera amounts in the yellow sea: A systematic evaluation using sentinel-2/msi observations. [Article 1501805]. *IEEE Geosciences and Remote Sensing Letters*, 20: https://doi.org/10.1109/LGRS.2023.3272889

Qi, L., Wang, M., Hu, C., & Holt, B. (2022). On the capacity of sentinel-1 synthetic aperture radar in detecting floating macroalgae and other floating matters. *Remote Sens. Environ.*, 280: 113188. https://doi.org/10.1016/j.rse.2022.113188

Qing, S., Zhang, J., Cui, T., & Bao, Y. (2014). Remote sensing retrieval of inorganic suspended particle size in the bohai sea. *Continental Shelf Research*, 73: 64–71. https://doi.org/10.1016/j.csr.2013.11.020

Ramon, D., Steinmetz, F., Jolivet, D., Compiègne, M., & Frouin, R. (2019). Modeling polarized radiative transfer in the ocean-atmosphere system with the gpu-accelerated smart-g monte carlo code. *Journal of Quantitative Spectroscopy and Radiative Transfer*, 222: 89–107.

Reynolds, R. A., & Stramski, D. (2019). Optical characterization of marine phytoplankton assemblages within surface waters of the western arctic ocean. *Limnology and Oceanography*, 64: (6), 2478–2496.

Reynolds, R. A., Stramski, D., & Neukermans, G. (2016). Optical backscattering of particles in arctic seawater and relationships to particle mass concentration, size distribution, and bulk composition. *Limnology and Oceanography*, 61: 1869–1890. https://doi.org/10.1002/lno.10341

Roithmayr, C. M., Lukashin, C., Speth, P. W., Young, D. F., Wielicki, B. A., Thome, K. J., & Kopp, G. (2014). Opportunities to intercalibrate radiometric sensors from international space station. *Journal of Atmospheric and Oceanic Technology*, 31: (4), 890–902.

Roy, S., Sathyendranath, S., Bouman, H., & Platt, T. (2013). The global distribution of phytoplankton size spectrum and size classes from their light-absorption spectra derived from satellite data. *Remote Sens. Environ.*, 139: 185–197.

Roy, S., Sathyendranath, S., & Platt, T. (2017). Size-partitioned phytoplankton carbon and carbon-to-chlorophyll ratio from ocean color by an absorption-based bio-optical algorithm. *Remote Sens. Environ.*, 194: 177–189.

Rozanov, V. V., Dinter, T., Rozanov, A. V., Wolanin, A., Bracher, A., & Burrows, J. P. (2017). Radiative transfer modeling through terrestrial atmosphere and ocean accounting for inelastic scattering processes: Software package sciatran. *J. Quant. Spectrosc. Rad. Transfer*, 194: 65–85. https://doi.org/10.1016/j.jqsrt.2017.03.009

Rozanov, V. V., Rozanov, A. V., Kokhanovsky, A. A., & Burrows, J. P. (2014). Radiative transfer through terrestrial atmosphere and ocean: Software package sciatran. *Journal of Quantitative Spectroscopy and Radiative Transfer*, 133: 13–71.

Ruddick, K., Lacroix, G., Lancelot, C., Nechad, B., Park, Y., Peters, S., & Van Mol, B. (2008). Optical remote sensing of the north sea. In V. Barale & M. Gade (Eds.), *Remote sensing of the european seas* (pp. 79–90). Springer Netherlands. https://doi.org/10.1007/978-1-4020-6772-3_6

Russell, B. J., Dierssen, H. M., & Hochberg, E. J. (2019). Water column optical properties of pacific coral reefs across geomorphic zones and in comparison to offshore waters. *Remote Sensing*, 11(15): 1757.

Sadeghi, A., Dinter, T., Vountas, M., Taylor, B., Peeken, I., Altenburg Soppa, M., & Bracher, A. (2012). Improvements to the phytodoas method for identification of coccolithophores using hyper-spectral satellite data. *Ocean Sciences*, 8: 1055–1070. https://doi.org/10.5194/os-8-1055-2012

Sathyendranath, S., et al. (2020). Ocean productivity from space: Commentary on the series of annual reviews. *Remote Sensing of Environment*, 239: 111668.

Sathyendranath, S., Stuart, V., Nair, A., Oka, K., Nakane, T., Bouman, H., Forget, H.-M., Maass, H., & Platt, T. (2009). Carbon-to-chlorophyll ratio and growth rate of phytoplankton in the sea. *Mar. Ecol. Prog. Ser.*, 383: 73–84.

Sathyendranath, S., Longhurst, A., Caverhill, C. M., & Platt, T. (1995). Regionally and seasonally differentiated primary production in the north atlantic. *Deep Sea Research Part I: Oceanographic Research Papers*, 42: (10), 1773–1802. https://doi.org/10.1016/0967-0637(95)00059-F

Schiller, H., & Doerffer, R. (1999). Neural network for emulation of an inverse model operational derivation of case ii water properties from meris data. *International Journal of Remote Sensing*, 20: 1735–1746.

Schuch, A. P., Yagura, T., Makita, K., Yamamoto, H., et al. (2012). Dna damage profiles induced by sunlight at different latitudes. *Environ Mol Mutagen*, 53: (3), 198–206. https://doi.org/10.1002/em.21678

Seegers, B. N., Stumpf, R. P., Schaeffer, B. A., Loftin, K. A., & Werdell, P. J. (2018). Performance metrics for the assessment of satellite data products: An ocean color case study. *Optics express*, 26: (6), 7404–7422.

Shang, S., Wu, J., Huang, B., Lin, G., Lee, Z., Liu, J., & Shang, S. (2014). A new approach to discriminate dinoflagellate from diatom blooms from space in the east China sea. *Journal of Geophysical Research: Oceans*, 119: (7), 4653–4668.

Shin, J., Khim, B.-K., Jang, L.-H., Lim, J., & Jo, Y.-H. (2022). Convolutional neural network model for discrimination of harmful algal bloom (hab) from non-habs using sentinel-3 olci imagery. *ISPRS Journal of Photogrammetry and Remote Sensing*, 191: 250–262.

Smith, G., & Garaba, S. P. (2025). Insights from monitoring abundances and characteristics of plastic leakage in city waterways and tourist beaches of cambodia. *Environmental Challenges*, 19: 101121. https://doi.org/10.1016/j.envc.2025.101121

Smyth, T. J. (2011). Penetration of uv irradiance into the global ocean. *J. Geophys. Res.*, 116(C11), 2011JC007183:

Song, L. P., Lee, Z., Shang, S., Huang, B., Wu, J., Wu, Z., Lu, W., & Liu, X. (2023). On the spatial and temporal variations of primary production in the south China sea. *IEEE Transactions on Geoscience and Remote Sensing*, 61: 1–14.

Song, L. P., Lee, Z., Shang, S., & Wu, J. (2024). Sensitivity of a carbon-based primary production model on satellite ocean color products. *Remote Sensing of Environment*, 311: (2024), 114304.

Song, Q., Chen, S., Xue, C., Lin, M., Du, K., Li, S., Huang, X., et al. (2019). Vicarious calibration of cocts-hy1c at visible and near-infrared bands for ocean color application. *Optics Express*, 27: (20), A1615–A1626.

Soppa, M. A., Brell, M., Chabrillat, S., Alvarado L. M. A. Gege, P., Plattner, S., Somlai-Schweiger, I., Schroeder, T., Steinmetz, F., Scheffler, D., Giardino, C., Colella, S., Vansteenwegen, D., Langheinrich, M., Carmona, E., Bachmann, M., Pato, M., Fischer, S., & Bracher, A. (2024). First full mission evaluation of enmap normalized water leaving reflectance products using three atmospheric correction processors. *Optics Express*, 31: (16), 28215–28230. https://doi.org/10.1364/OE.523813

Soppa, M. A., Silva, B., Steinmetz, F., Keith, D., Scheffler, D., Bohn, N., & Bracher, A. (2021). Assessment of polymer atmospheric correction algorithm for hyperspectral remote sensing imagery over coastal waters. *Sensors*, 21: (12), 4125.

Soppa, M. A., Völker, C., & Bracher, A. (2016). Diatom phenology in the southern ocean: Mean patterns, trends and the role of climate oscillations. *Remote Sensing*, 8: 420. https://doi.org/10.3390/rs8050420

Soppa, M., Peeken, I., & Bracher, A. (2017). Global chlorophyll a concentrations for diatoms, haptophytes and prokaryotes obtained with the diagnostic pigment analysis of hplc data compiled from several databases and individual cruises. In *In supplement to: Losa, svetlana n; soppa, mariana a; dinter, tilman; wolanin, aleksandra; brewin, robert j w; bricaud, annick; oelker, julia; peeken, ilka; gentili, bernard; rozanov, vladimir v; bracher, astrid (2017): Synergistic exploitation of hyper- and multi-spectral precursor sentinel measurements to determine phytoplankton functional types (synsenpft). frontiers in marine science, 4(203), 22 pp, https://doi.org/10.3389/fmars.2017.00203*. PANGAEA. https://doi.org/10.1594/PANGAEA.875879

Stamnes, K., Tsay, S. C., Wiscombe, W., & Jayaweera, K. (1988). Numerically stable algorithm for discrete-ordinate-method radiative transfer in multiple scattering and emitting layered media. *Appl. Opt.*, 27: (12), 2502–2509.

Sterckx, S., Knaeps, E., Bollen, M., Trouw, K., & Houthuys, R. (2007). Retrieval of suspended sediment from advanced hyperspectral sensor data in the scheldt estuary at different stages in the tidal cycle. *Marine Geodesy*, 30: (1-2), 97–108. https://doi.org/10.1080/01490410701296341

Stramski, D., et al. (2008). Relationships between the surface concentration of particulate organic carbon and optical properties in the eastern south pacific and eastern atlantic oceans. *Biogeosciences*, 5: 171–201.

Stramski, D., Boss, E., Bogucki, D., & Voss, K. J. (2004). The role of seawater constituents in light backscattering in the ocean. *Prog. Oceanogr.*, 61: (1), 27–56.

Stramski, D., Bricaud, A., & Morel, A. (2001). Modeling the inherent optical properties of the ocean based on the detailed composition of planktonic community. *Applied Optics*, 40: 2929–2945. https://doi.org/10.1364/ao.40.002929

Stumpf, R. P. (2001). Applications of satellite ocean color sensors for monitoring and predicting harmful algal blooms. *Human and Ecological Risk Assessment: An International Journal*, 7: 1363–1368.

Stumpf, R. P., & Werdell, P. J. (2010). Adjustment of ocean color sensor calibration through multi-band statistics. *Optics Express*, 18: (2), 401–412.

Sun, D., Hu, C., Qiu, Z., & Wang, S. (2015). Reconstruction of hyperspectral reflectance for optically complex turbid inland lakes: Test of a new scheme and implications for inversion algorithms. *Optics Express*, 23: A718–A740. https://doi.org/10.1364/OE.23.00A718

Tao, Z., Wang, Y., Ma, S., Lv, T., & Zhou, X. (2017). A phytoplankton class-specific marine primary productivity model using modis data. *IEEE Journal of Selected Topics in Applied Earth Observations and Remote Sensing*, 10: (12), 5519–5528.

Taramelli, A., Tornato, A., Magliozzi, M. L., Mariani, S., Valentini, E., Zavagli, M., Rast, M., et al. (2020). An interaction methodology to collect and assess user-driven requirements to define potential opportunities of future hyperspectral imaging sentinel mission. *Remote Sensing*, 12: (8), 1286.

Taylor, B., Taylor, M., Dinter, T., & Bracher, A. (2013). Estimation of relative phycoerythrin concentrations from hyperspectral underwater radiance measurements - a statistical approach. *Journal of Geophysical Research - Oceans*, 118: 2948–2960. https://doi.org/10.1002/jgrc.20201

Teague, J., Day, J. C., Allen, M. J., Scott, T. B., Hochberg, E. J., & Megson-Smith, D. (2023). A demonstration of the capability of low-cost hyperspectral imaging for the characterisation of coral reefs. *Oceans*, 4: (3), 286–300. https://doi.org/10.3390/oceans4030020

Terzić, E., Miró, A., Organelli, E., Kowalczuk, P., D'Ortenzio, F., & Lazzari, P. (2021). Radiative transfer modeling with biogeochemical-argo float data in the mediterranean sea. *Journal of Geophysical Research: Oceans*, 126: e2021JC017690: https://doi.org/10.1029/2021JC017690

Thome, K. J. (2001). Absolute radiometric calibration of landsat 7 etm+ using the reflectance-based method [Landsat 7]. *Remote Sensing of Environment*, 78: (1), 27–38. https://doi.org/https://doi.org/10.1016/S0034-4257(01)00247-4

Thompson, D., Guanter, L., Berk, A., Gao, B.-C., Richter, R., Schläpfer, D., & Thome, K. J. (2019). Retrieval of atmospheric parameters and surface reflectance from visible and shortwave infrared imaging spectroscopy data. *Surv Geophys*, 40: 333–360. https://doi.org/10.1007/s10712-018-9488-9

Timmer, B., Reshitnyk, L. Y., Hessing-Lewis, M., Juanes, F., & Costa, M. (2022). Comparing the use of red-edge and near-infraredwavelength ranges for detecting submerged kelp canopy [rs14092241]. *Remote Sens.*, 14: 2241. https://doi.org/10.3390

Torrecilla, E., Stramski, D., Reynolds, R. A., Millán-Núñez, E., & Piera, J. (2011). Cluster analysis of hyperspectral optical data for discriminating phytoplankton pigment assemblages in the open ocean. *Remote Sensing of Environment*, 115: 2578–2593.

Vahtmäe, E., Paavel, P., & Kutser, T. (2020). How much benthic information can be retrieved with hyperspectral sensor from the optically complex coastal waters? *J. Appl. Remote Sens.*, 14: (1), 016504. https://doi.org/10.1117/1.JRS.14.016504

Valente, A., Sathyendranath, S., Brotas, V., Groom, S., Grant, M., Jackson, T., Chuprin, A., Taberner, M., Airs, R., Antoine, D., Arnone, R., Balch, W., Barker, K., Barlow, R., Bélanger, S., Berthon, J.-F., Beşiktepe, S., Borsheim, Y., Bracher, A., … Zibordi, G. (2022). A compilation of global bio-optical in situ data for ocean-color satellite applications – version three. *Earth Syst. Sci. Data*. https://doi.org/10.5194/essd-14-5737-2022

Vandermeulen, R. A., Mannino, A., Craig, S. E., & Werdell, P. J. (2020). 150 shades of green: Using the full spectrum of remote sensing reflectance to elucidate color shifts in the ocean. *Remote Sensing of Environment*, 247: 111900.

Vandermeulen, R. A., Mannino, A., Neeley, A. R., Werdell, P. J., & Arnone, R. (2017). Determining the optimal spectral sampling frequency and uncertainty thresholds for hyperspectral remote sensing of ocean color. *Opt. Express*, 25: A785–A797. https://doi.org/10.1364/OE.25.00A785

Vasilkov, A., Krotkov, N., Herman, J., McClain, C., Arrigo, K., & Robinson, W. (2001). Global mapping of underwater uv irradiances and dna-weighted exposures using total ozone mapping spectrometer and sea-viewing wide field-of-view sensor data products. *J. Geophys. Res.*, 106: (C11), 27205–27219.

Vishnu, P. S., Belluz, J. D. B., Xi, H., Hussain, M. S., Bracher, A., & Costa, M. (2025). Highly resolved surface phytoplankton community composition on the west coast of canada derived from in situ hyperspectral radiometry. *Journal of Geophysical Research: Biogeosciences*, 130: (10), e2025JG008956. https://doi.org/10.1029/2025JG008956

Volta, C., Bellacicco, M., Xing, X., Yang, G., & Marullo, S. (2025). Phytoplankton dynamics in subtropical gyres: New insights into biomass and physiology from 25 years of satellite observations. *Geophysical Research Letters*, 52: (12), e2024GL111817. https://doi.org/10.1029/2024GL111817

Vountas, M., Dinter, T., Bracher, A., Burrows, J. P., & Sierk, B. (2007). Spectral studies of ocean water with space-borne sensor sciamachy using differential optical absorption spectroscopy (doas). *Ocean Science*, 3: 429–440.

Walcutt, N. L., Knörlein, B., Cetinić, I., Ljubesic, Z., Bosak, S., Sgouros, T., Omand, M. M., et al. (2020). Assessment of holographic microscopy for quantifying marine particle size and concentration. *Limnology and Oceanography: Methods*, 18: (9), 516–530.

Wang, G. Q., Lee, Z. P., Mishra, D. R., & Ma, R. H. (2016). Retrieving absorption coefficients of multiple phytoplankton pigments from hyperspectral remote sensing reflectance measured over cyanobacteria bloom waters. *Limnology and Oceanography-Methods*, 14: 432–447.

Wang, Y., Lee, Z., Ondrusek, M., Li, X., Zhang, S., & Wu, J. (2022). An evaluation of remote sensing algorithms for the estimation of diffuse attenuation coefficients in the ultraviolet bands. *Opt. Express*, 30: 6640–6655.

Werdell, P. J., & Bailey, S. W. (2005). An improved in-situ bio-optical data set for ocean color algorithm development and satellite data product validation. *Remote Sensing of Environment*, 98: (1), 122–140.

Werdell, P. J., Bailey, S. W., Franz, B. A., Morel, A., & McClain, C. R. (2007). On-orbit vicarious calibration of ocean color sensors using an ocean surface reflectance model. *Appl Opt*, 46: (23), 5649–5666.

Werdell, P. J., Franz, B. A., Bailey, S. W., Feldman, G. C., Boss, E., Brando, V. E., Dowell, M., Hirata, T., Lavender, S. J., Lee, Z., Loisel, H., Maritorena, S., Mélin, F., Moore, T. S., Smyth, T. J., Antoine, D., Devred, E., D'Andon, O. H. F., & Mangin, A. (2013). Generalized ocean color inversion model for retrieving marine inherent optical properties. *Applied optics*, 52: 2019–2037. https://doi.org/10.1364/AO.52.002019

Werdell, P. J., McKinna, L. I. W., Boss, E., Ackleson, S. G., Craig, S. E., Gregg, W. W., et al. (2018). An overview of approaches and challenges for retrieving marine inherent optical properties from ocean color remote sensing. *Prog. Oceanogr.*, 160: 186–212. https://doi.org/10.1016/j.pocean.2018.01.00

Werther, M., Burggraaff, O., Gurlin, D., Saranathan, A. M., Balasubramanian, S. V., Giardino, C., Odermatt, D., et al. (2025). On the generalization ability of probabilistic neural networks for hyperspectral remote sensing of absorption properties across optically complex waters. *Remote Sensing of Environment*, 328: 114820.

Westberry, T., Behrenfeld, M. J., Siegel, D. A., & Boss, E. (2008). Carbon-based primary productivity modeling with vertically resolved photoacclimation. *Global Biogeochem. Cycles*, 22: (2), 1–18. https://doi.org/10.1029/2007GB003078

Westberry, T. K., Silsbe, G. M., & Behrenfeld, M. J. (2023). Gross and net primary production in the global ocean: An ocean color remote sensing perspective. *Earth-Science Reviews*, 237: 104322. https://doi.org/10.1016/j.earscirev.2023.104322

Wolanin, A., Rozanov, V. V., Noel, S., Dinter, T., Vountas, M., Burrows, J. P., & Bracher, A. (2015). Global retrieval of marine and terrestrial chlorophyll fluorescence at its red peak using hyperspectral top of atmosphere radiance measurements: Feasibility study and first results. *Remote Sensing of Environment*, 166: 243–261. https://doi.org/10.1016/j.rse.2015.05.018

Wolanin, A., Soppa, M. A., & Bracher, A. (2016). Investigation of spectral band requirements for improving retrievals of phytoplankton functional types. *Remote Sensing*, 8: 871. https://doi.org/10.3390/rs8100871

Wozniak, B., Dera, J., Ficek, D., Ostrowska, M., & Majchrowski, R. (2002). Dependence of the photosynthesis quantum yield in oceans on environmental factors. *Oceanologia*, 44: (4).

Wozniak, S. B., & Stramski, D. (2004). Modeling the optical properties of mineral particles suspended in seawater and their influence on ocean reflectance and chlorophyll estimation from remote sensing algorithms. *Appl. Opt.*, 43: (17), 3489–3503.

Xi, H., Hieronymi, M., Röttgers, R., Krasemann, H., & Qiu, Z. F. (2015). Hyperspectral differentiation of phytoplankton taxonomic groups: A comparison between using remote sensing reflectance and absorption spectra. *Remote Sensing*, 7: 14781–14805. https://doi.org/10.3390/rs71114781

Xi, H., Larouche, P., Tang, S., & Michel, C. (2014). Characterization and variability of particle size distributions in hudson bay, canada. *J. Geophys. Res. Oceans*, 2014: (119), 3392–3406.

Xie, Y., Huang, B., Lin, L., Laws, E. A., Wang, L., Shang, S., Dai, M., et al. (2015). Photosynthetic parameters in the northern south China sea in relation to phytoplankton community structure. *Journal of Geophysical Research: Oceans*, 120: (6), 4187–4204.

Yamashita, Y., Nosaka, Y., Suzuki, K., Ogawa, H., Takahashi, K., & Saito, H. (2013). Photobleaching as a factor controlling spectral characteristics of chromophoric dissolved organic matter in open ocean. *Biogeosciences*, 10: 7207–7217. https://doi.org/10.5194/bg-10-7207-2013

Yang, G., Bellacicco, M., Organelli, E., & Xing, X. (2024). Global variability of phytoplankton carbon and non-algal particles from ocean colordata based on a photoacclimation model [Article e2023JC019922]. *Journal of Geophysical Research: Oceans*, 129: (1).

Ye, H., Liao, X., Li, T., Shen, Q., Zhang, F., Jianhua, Z., & Li, J. (2019). Gaussian decomposition and component pigment spectral analysis of phytoplankton absorption spectra. *Chinese Journal of Oceanology and Limnology*, 37: 1542–1554. https://doi.org/10.1007/s00343-019-8079-z

Zhai, P. W., Hu, Y., Chowdhary, J., Trepte, C. R., Lucker, P. L., & Josset, D. B. (2010). A vector radiative transfer model for coupled atmosphere and ocean systems with a rough interface. *Journal of Quantitative Spectroscopy and Radiative Transfer*, 111: (7-8), 1025–1040.

Zhang, M., Hu, C., & Barnes, B. B. (2019). Performance of polymer atmospheric correction of ocean color imagery in the presence of absorbing aerosols. *IEEE Transactions on Geoscience and Remote Sensing*, 57: (9), 6666–6674.

Zhang, M., Hu, C., Cannizzaro, J., Kowalewski, M. G., & Janz, S. J. (2018). Diurnal changes of remote sensing reflectance over chesapeake bay: Observations from the airborne compact atmospheric mapper. estuarine. *Coastal and Shelf Science*, 200: 181–193. https://doi.org/10.1016/j.ecss.2017.10.021

Zhang, M., Hu, C., English, D., Carlson, P., Muller-Karger, F. E., Toro-Farmer, G., & Herwitz, S. R. (2015). Atmospheric correction of aisa measurements over the florida keys optically shallow waters: Challenges in radiometric calibration and aerosol selection. *IEEE J. of Selected Topics in Applied Earth Observations and Remote Sensing (JSTARS)*, 8: 4189–4196.

Zhang, X., Hu, L., & He, M. (2009). Scattering by pure seawater: Effect of salinity. *Optics Express*, 17: (7), 5698–5710. https://doi.org/10.1364/OE.17.005698

Zhang, X., Huot, Y., Bricaud, A., & Sosik, H. M. (2015). Inversion of spectral absorption coefficients to infer phytoplankton size classes, chlorophyll concentration, and detrital matter. *Appl. Opt.*, 54: (18), 5805–5816.

Zhao, H., Cao, W., Deng, L., Liao, J., Zeng, K., Zheng, W., Zhang, Y., Xu, J., & Zhou, W. (2023). Estimation of primary production from the light absorption of phytoplankton and photosynthetically active radiation in the south China sea [Article 1249802. Sci]. *Front.*, 10: https://doi.org/10.3389/fmars.2023.1249802

Zheng, G., & Stramski, D. (2013). A model based on stacked-constraints approach for partitioning the light absorption coefficient of seawater into phytoplankton and non-phytoplankton components. *J. Geophys. Res. Oceans*, 118: (4), 2155–2174.

Zheng, G., Stramski, D., & DiGiacomo, P. M. (2015). A model for partitioning the light absorption coefficient of natural waters into phytoplankton, nonalgal particulate, and colored dissolved organic components: A case study for the chesapeake bay. *Journal of Geophysical Research: Oceans*, 120: 2601–2621. https://doi.org/10.1002/2014JC010604

Zheng, L., Lee, Z., Wang, Y., Yu, . X., Lai, W., & Shang, S. (2025). Evaluation of near-blue uv remote sensing reflectance over the global ocean from snpp viirs, pace oci. *and GCOM-C SGLI. Optics Express*, 33: (19), 40465–40488. https://doi.org/10.1364/OE.568441

Zhu, Q., Shen, F., Shang, P., Pan, Y. Q., & Li, M. Y. (2020). Hyperspectral remote sensing of phytoplankton species composition based on transfer learning [2019). Remote Sensing, 12]. *2001*, 11:

Zibordi, G., Johnson, B. C., Kwiatkowska, E., Voss, K. J., Antoine, D., Barnard, A., Chen, S., et al. (2025). System vicarious calibration for climate and global long-term operational ocean color applications. *Bulletin of the American Meteorological Society*, 106: (2), E394–E407. https://doi.org/10.1175/BAMS-D-24-0085.1

Zoffoli, M., Lee, Z., & Marra, J. (2018). Regionalization and dynamic parameterization of quantum yield of photosynthesis to improve the ocean primary production estimates from remote sensing. *Frontiers in Marine Science*, 2018: 5.